The Pro-Apoptotic Function of CED-9 Requires CED-9-CED-4 Interaction

By

Nolan T. Tucker
B.S. Genetics University of Georgia, 2018

Submitted to the Department of Biology
In partial fulfillment of the requirements for the degree of

DOCTOR OF PHILOSOPHY IN BIOLOGY
at the
MASSACHUSETTS INSTITUTE OF TECHNOLOGY

February 2024

Signature of the Author: _____
Nolan T. Tucker
Department of Biology
January 19th, 2024

Certified by: _____
H. Robert Horvitz
Professor of Biology
Thesis Supervisor

Accepted by: _____
Mary Gehring
Professor of Biology
Member, Whitehead Institute
Co-Director, Biology Graduate Committee

The Pro-Apoptotic Function of CED-9 Requires CED-9-CED-4 Interaction

By Nolan T. Tucker

Submitted to the Department of Biology on January 19th, 2024 in Partial Fulfillment of the Requirements for the Degree of Doctor of Philosophy in Biology

Abstract

Apoptosis is a fundamental, conserved process of cell death required for animal development and tissue homeostasis.

In *Caenorhabditis elegans* apoptosis is inhibited by the BCL-2 homolog CED-9. In addition to its canonical anti-apoptotic role, CED-9 possesses an apparent pro-apoptotic function, because reduction in CED-9 function can result in decreased cell death – e.g., a *ced-9(lf)* allele enhances the partial cell-death defect of animals with a weak loss-of-function mutation in the pro-apoptotic caspase gene *ced-3.* This pro-apoptotic function of *ced-9* is poorly understood. CED-9 has been thought to inhibit apoptosis by binding to and inhibiting the pro-apoptotic protein CED-4, the *C. elegans* homolog of APAF-1. In this work we show that mutations in either CED-9 or CED-4 located in their CED-9-CED-4 binding regions as defined by X-ray crystallography cause a defect in executing apoptosis without affecting the anti-apoptotic function of *ced-9*. We further show that these mutant CED-9 and CED-4 proteins are defective in a CED-9-CED-4 interaction *in vivo*. These data indicate that the known *in vivo* CED-9-CED-4 interaction is required for the pro-apoptotic function of *ced-9* but is dispensable for its anti-apoptotic function.

While caspase-mediated apoptosis is the best characterized form of programmed cell elimination, other conserved mechanisms, such as cell extrusion, also exist. In *C. elegans,* at least eight cells that normally die by apoptosis are eliminated by cell extrusion in the absence of apoptosis. From an EMS mutagenesis screen, performed on worms lacking caspase activity, searching for survival of an extruded cell (ABplpappap), I isolated a nonsense mutation in the GMP reductase gene, *gmpr-1.* Interestingly, this allele *(n6457)* also allows ABplpappap to escape caspase-mediated apoptosis. Additionally, I found that RNAi against genes that affect either pyrimidine metabolism (*pyr-1*) or purine metabolism *(gmpr-1* and *adss-1*) similarly allows ABplpappap to survive but that RNAi against *R151.2,* which affects both purine and pyrimidine metabolism, does not. *gmpr-1(n6457)* is suppressed by RNAi against *R151.2* or *pyr-1* but not by RNAi against the purine metabolism gene *adss-1*. These results suggest that the ability to maintain a normal physiologic ratio of purines and pyrimidines plays a role in cell extrusion and possibly in apoptosis as well.

Given the highly conserved nature of cell-death genes and processes, interactions between human CED-9/BCL-2 family members and APAF-1 as well as nucleotide imbalance might play important roles in human diseases that involve disruptions in apoptosis, such as certain neurodegenerative disorders and cancers.

Acknowledgments

Throughout my time as a graduate student, I have been fortunate to have the support of many colleagues, friends, and family members to rely upon, without them this work would surely not have been possible.

First, I thank my advisor, Bob Horvitz. Having majored in genetics as an undergraduate I found Bob's 7.52 Genetics lectures to be the most interesting and engaging lectures that I had attended throughout my academic experience. These lectures demonstrated his deep insights into genetic concepts and personal connection to the subject matter and are what first prompted me to rotate in the Horvitz lab. Bob's genuine love and excitement for science was apparent and unwavering, each time we sat down to talk I found myself reenergized and more engaged in my work. These opportunities to talk about science with someone so knowledgeable and enthusiastic were invaluable to me. I am incredibly grateful for the time and guidance that Bob provided.

Next, I would like to thank my committee members. I thank Matthew Vander Heiden for making himself available and volunteering his time to provide me with advice. I also thank Peter Reddien whose work as a graduate student laid the foundation for my Ph.D. work. I also thank Peter for the many opportunities that he gave me to meet, both formally and informally following 7.03 Genetics lectures, to discuss career matters and matters related to science.

I must also thank the many members of the Horvitz lab who made my time more enjoyable by helping to create a friendly and productive lab environment. First, I thank our wonderful lab manager, Na An. Na was always available to help solve any problem no matter how large or small. Without her support in these matters, my work truly would not have been possible. I also thank Rita Droste who, along with her assistance with many things, undertook the job of helping me to search for the lost and unlabeled antiserum crucial to my work in the depths of the lab's freezers that, to our dismay, we discovered had accumulated many such vials over a period of 40 years to sift through. Rita's help in finding this antiserum was essential to the completion of this work. I also thank Sally Shin for her help with all administrate issues both for myself and to the lab in general to ensure its ability to function. I also thank postdocs Kirk Burkhart and Akiko Doi for guidance in my first years in the lab. Steve Sando is also deserving of my thanks for his advice and guidance early on and for always being able to provide a piece of strange or interesting science to be discussed over coffee in the lunchroom. I thank Wenhan Chang for brightening the occasional weekend with the presence of his dog, Pudding. I thank Iliana Kesisova and Ji Na Kong for their help and guidance in teaching me many biochemical techniques. I thank Dipon Ghosh, Eugene Lee, and UROP Vin Armelin for many discussions centered around life as a fan of a disappointing NFL franchise. I also owe thanks to Dongyeop Lee who was always able to solve any lab problem imaginable. I thank Vivek Dwivedi for his mentorship during my first years in the lab. I would also like to thank Josh Saul and Calista Diehl who shared a lab room with me for many years. Josh's unbelievable organization skills allowed me to rely on him to provide a wide variety of materials and templates and Calista was always available to talk to about life, science, and the oddity of the ever-fluctuating temperature and Wi-Fi status of room 68-433.

I thank my undergraduate advisor Janet Westpheling for her support and encouragement. Working in Jan's lab was my first exposure to bench work, and I am grateful to her for allowing me the space to work independently on my own project despite my lack of experience. Since I first joined her lab Jan has been unbelievably supportive and I thank her for pushing me to apply to MIT.

I must thank my friends from the University of Georgia whose love for fun and knack for creating good times regardless of circumstance were able to provide me with much needed breaks from graduate school whenever we could get together. First, I thank Harrison Brock for always being willing to get outdoors for the hunting or fishing trips that got me through UGA as an undergrad. Harrison's ability to entertain the rest of us and to be the life of the party wherever he goes has never failed to be anything short of electrifying. I also thank Jay Keen for invaluable talks over the years about everything from life to work to girlfriends. I am always delighted to get a call from Jay to discuss why next year looks promising for our beloved Falcons. I thank Henry Cross for reliably providing me with excuses to leave the bars early during our undergraduate years. I am thankful to Roney Walters for his fierce love of his friends, and outgoingness. I would also like to thank Jacob Deal who ensures that I will never feel bad for being late to any function under any circumstances. I am grateful to Ilia Dichev for his inspiring love for new experiences and whose propensity to escalate a situation – whether it be for better or worse – I will always appreciate. I thank Robert Hines and Nathan Haskell for their knack for devastating "roasts" that friends on the receiving end of can never hope to emotionally recover from. These instances are always hilarious when not directed at oneself. I am thankful to Quill Yates for providing me with a surefire fantasy football victory every year. I thank Eric Ingstar for enhancing any activity he's involved in even when that activity is sitting in hours of Houston traffic. I also want to thank Bhaskar Lokanathan for always seeking out fun times, his son Rishi is well positioned to carry on our legacy to the next generation.

I thank David Schofield for his support and friendship. It was rare for me to come home from Boston to visit my family and not see David already there as soon as I walked in the door. I wish him the best of luck in his own Ph.D. studies where he will surely accomplish great things.

I must also thank my family without whom this work would not have been possible. I thank my brother Luke and sister Autumn for their support and my brother Nick for his support and willingness to pick me up from the airport multiple times a year knowing that we will surely endure hours of traffic. I thank my parents for their assurance that I have a loving home and stocked fridge to come home to on holidays. I also thank my parents for their years of guidance and support that made my pursuit of a Ph.D. possible.

Lastly, I thank my girlfriend, Noor Sohal. Noor was there for me throughout the entirety of my graduate school experience to celebrate successes and help me through stressful times. I was ecstatic when she was able to join me in Cambridge for two years between her undergrad and medical school. Since we met Noor has been a source of joy with an incredible ability to bring fun with her whenever she goes. I am overwhelmingly grateful for Noor's support and, whether through conversations on the phone or weekend trips to New Hampshire, her companionship always made me happy to be where I was and for that I am truly grateful.

Table of Contents

Chapter One

Introduction

I. Introduction

The programmed elimination of unwanted or unneeded cells by apoptosis during animal development is an evolutionarily conserved process essential for proper development and tissue homeostasis. Insufficient or excessive cell elimination can result in diseases such as cancer and neurodegenerative disorders, respectively. The conserved molecular genetic pathway of apoptosis was discovered largely from analyses of the nematode *Caenorhabditis elegans.* I have discovered that in *C. elegans* the pro-apoptotic function of the canonically anti-apoptotic cell-death gene *ced-9* depends on an interaction with the pro-apoptotic gene *ced-4*.

In this chapter I briefly review the functions of the core regulators of apoptosis in *C. elegans* (Section II.) I also discuss the pro-apoptotic function of *ced-9* and the pro-apoptotic functions of the mammalian homologs of *ced-9*, the canonically anti-apoptotic BCL-2 family members (Section III.).

While caspase-mediated apoptosis is the best characterized form of programmed cell elimination, other mechanisms, such as cell extrusion, also exist. I have also discovered that the apparent perturbation of purine-pyrimidine metabolism disrupts both cell extrusion and apoptosis of the extruded cell ABplpappap. In the final section of this Introduction, I discuss cell extrusion in *C. elegans* and its regulation by replication stress (Section IV.).

II. Genetic regulation of apoptosis in *C. elegans*

Programmed Cell Death

The phenomenon of naturally occurring cell elimination was initially documented by Carl Vogt in 1842 when he observed dying cells in the notochord and in cartilage of toads undergoing metamorphosis. Early instances of naturally occurring cell death were also recorded across various organisms and tissues, including fly larvae, chondrocytes during skeletal development, muscle cells in developing toads, and neurons in developing chick embryos (Clarke and Clarke, 1996).

The term "apoptosis," has its roots in the Greek word meaning "falling off," -- historically used to describe the shedding of petals or leaves from trees. The term was later adopted to describe a distinct process of cell death that differs from "necrosis," which results from damage or trauma and displays certain characteristics (Kerr, Wyllie, and Currie, 1972; Wyllie, 1980). Kerr, Wylie, and Currie gathered examples from various tissues, including tumor specimens and healthy tissue, containing cells that appeared to progress through two stages the authors defined to be characteristics of apoptosis. The first was the condensation of cells as they shrink to form highly refractile “apoptotic” bodies, undergo membrane blebbing, nuclear and cytoplasmic condensation, and DNA fragmentation. The second stage was the engulfment

and removal of the condensed cell by another cell through phagocytosis, the process by which one cell is internalized by another.

The presence of distinct features that are characteristic of cells undergoing programmed cell death as well as their occurrence in healthy tissue during embryogenesis (Glücksmann, 1951; Saunders, 1966; Lockshin and Williams, 1964) indicated that cell death was an inherent process controlled by a programmed, genetic mechanism.

C. elegans as an animal for the study of development

C. elegans was first purposed by Sydney Brenner to be an animal well-suited for the study of the genetics of nervous system function (Brenner, 1973) as well as certain aspects of developmental biology (Brenner, 1974). The transparency of the organism allows for easy observation of internal cells, *C. elegans* have a short generation time (going from embryo to fertile adult in about three days), and most *C. elegans* are hermaphroditic, simplifying genetic experiments by eliminating the necessity of genetic crosses to create homozygotes. Males are also present at a low frequency and can be induced in larger numbers to allow for crossing. These factors make *C. elegans* an excellent model to study diverse aspects of developmental biology. Additionally, using Nomarski optics, the cell lineage of *C. elegans* was found to be invariant, making *C. elegans* an appealing animal to study cell fate (Sulston and Horvitz, 1977). Hermaphrodites produce 1090 somatic cells, 131 of which undergo cell death; that specific cells in the cell

lineage invariably die provided further evidence that apoptosis is a "programmed," genetic phenomenon. Among these 131 cell deaths 113 occur during embryogenesis while the remaining 18 deaths take place during the first three stages of larval development. Notably, dying cells in the embryo were typically found to be the smaller of two cells produced by asymmetric cell division and were often engulfed by the larger sister cell produced by this division (Sulston *et al.,* 1983). A screen for mutations in genes involved in the cell death in the nematode produced mutations in the nuclease *nuc-1,* and the phagocytosis genes *ced-1* and *ced-2;* the first cell death abnormal (Ced) mutants identified (Hedgecock, Sulston, and Thomson, 1983). These mutants were isolated by screening EMS mutagenized worms using Nomarski optics to identify mutants with abnormalities in cell deaths resulting in cell corpses – dead cells that had not been cleared from the animal, i.e. cells capable of initiating apoptosis but unable to undergo the process completely. The isolation of these mutants proved significant not only because they defined genes involved in a key step of the apoptotic pathway but also because they empowered a screen for mutations in genes involved in the initiation of apoptosis (Ellis and Horvitz, 1986). This screen searched for *ced-1* mutants that also carried a mutation that altered the pattern or the presence of these corpses and lead to the identification of mutations preventing the initiation of apoptosis.

Apoptosis is regulated by *egl-1*, *ced-9*, *ced-4*, and *ced-3*

The presence of “undead” corpses indicate that *ced-1* and *ced-2* mutants are unable to clear dead cells but are capable of initiating and executing apoptosis and progressing through the first morphological stage described by Kerr, Wylie, and Currie, giving them their characteristic, highly refractile state. To identify additional genes involved in apoptosis, an EMS screen was performed by mutagenizing *ced-1* animals and looking for mutants in which cell corpses were not visible. This screen proved to be of great significance, as it produced the first mutations in genes responsible for the execution of apoptosis, *ced-3* and *ced-4* (Ellis and Horvitz, 1986). By using genetic mosaic animals, *ced-3* and *ced-4* were found to function cell autonomously (Yuan and Horvitz 1990). It was also found that in the absence of *ced-3* or *ced-4* cells normally fated to die did not undergo apoptosis but instead survived and differentiated. In the absence of apoptosis, these ectopically surviving cells have sometimes been shown to be of similar morphologies to and capable of performing the same function as their lineal sister or aunt cells (Avery and Horvitz, 1987). For example, the M4 sister cell, a cell fated to die, not only survives in *ced-3* mutants but also assumes the function in pharyngeal pumping typically performed by the M4 cell, without which the animal cannot survive, following the laser ablation of the M4 cell (Avery and Horvitz, 1987).

A screen for mutations causing the ectopic survival of sister cells of the two NSM neurons isolated two cell-death specification (Ces) genes that control the cell-death decision of specific cells, *ces-1,* an inhibitor of apoptosis, and *ces-2,* a promoter of apoptosis, (Ellis and Horvitz, 1991). This

screen also isolated a mutation causing a dominant cell-killing defect; this mutation proved to be a gain-of-function mutation in the first anti-apoptotic gene identified, *ced-9* (Hengartner, Ellis, and Horvitz, 1992).

The fourth and final gene regulating the core apoptotic pathway in *C. elegans* was discovered as a gain-of-function mutation that caused an egg laying defective (Egl) phenotype by dominantly causing the ectopic death of the HSNs neurons, the hermaphrodite specific neurons that regulate egg laying and are eliminated via apoptosis in the male (Trent, Tsuing, and Horvitz 1983; Ellis and Horvitz 1986).

The discovery of the genes *egl-1, ced-9, ced-3,* and *ced-4,* which control the process of apoptosis, marked a significant advancement in the field of cell death and demonstrated directly that cell death can occur as a programmed, genetic process rather than only as a result of damaged to the cell but also identified the key genes involved in this process.

The canonical apoptosis pathway

The discovery of cell death genes prompted investigation into the order by which the genes act in the cell death pathway. To analyze the gene *ced-9,* which was defined by a gain-of-function mutation that prevents apoptotic cell death, a screen was performed to identify *cis*-dominant suppressors of the gain-of-function allele *n1950*, e.g., seeking an additional mutation in the *ced-9* gene suppressing the cell-killing defect caused by the first (Hengartner, Ellis, and Horvitz, 1992). The intragenic *ced-9* loss-of-function mutations isolated

from this screen were found to cause ectopic cell death, which was presumed to be the cause of the maternal-effect lethality and sterility of these mutants. It was further observed that the maternal-effect lethal phenotype caused by loss-of *ced-9* function could be rescued by a loss-of-function mutation in either *ced-4* or *ced-3*, indicating that *ced-9* acts upstream of these two genes in the apoptotic pathway.

Overexpression studies were used to determine whether *ced-3* acted downstream of *ced-4* or vice versa or whether they acted in parallel. *ced-3* was found to act downstream of *ced-4,* as overexpression of *ced-3* by a transgene is sufficient to cause ectopic death in the ALM neurons in the absence of *ced-4* while *ced-4* overexpression is insufficient to execute apoptosis in the absence of *ced-3* (Shaham and Horvitz, 1996).

ced-4 and *ced-3* loss-of-function mutations suppress the ectopic death of the HSN neuron caused by an *egl-1* gain-of-function allele (Ellis and Horvitz, 1986), and overexpression of *egl-1* in the ALM neurons by a transgene was found to be insufficient to induce ectopic death without *ced-4* and *ced-3* (Conradt and Horvitz 1998)*;* these observation placed *egl-1* upstream of *ced-4* and *ced-3* in the apoptosis pathway. Unlike *ced-4* and *ced-3*, *egl-1* loss-of-function mutations were found to be insufficient to rescue the maternal-effect lethal phenotype caused by loss-of *ced-9* function (Conradt and Horvitz 1998), indicating that *egl-1* acts upstream of *ced-9*.

From this genetic evidence *egl-1* was ascertained to function upstream of *ced-9,* which functioned upstream of *ced-4,* which functioned upstream of

ced-3. Based on the effect that loss-of function mutations in these had on cell death it was determined that *egl-1* must inhibit *ced-9,* which inhibits *ced-4* which activates *ced-3,* which promotes apoptosis. These fundamental discoveries defined the first genetic, apoptosis pathway (Fig. 1A). A current understanding of the mechanistic contributions from each of the molecular players will be described below in order, starting from the most upstream gene.

EGL-1 is expressed in response to apoptotic stimuli

egl-1 is a BH3-only (BCL-2 Homology domain 3) protein, similar to mammalian BAD, BID, BIM, BIK, NOXA, and PUMA among others (reviewed in Lomonosova and Chinnadurai, 2008). BH3-only genes, such as *egl-1*, are known to be expressed in response to apoptotic stimuli initiating the apoptotic cascade and are thought to inhibit the anti-apoptotic BCL-2 proteins (Fletcher and Huang, 2006; Nehme *et al.*, 2010).

Through yeast two-hybrid and co-immunoprecipitation experiments using GST-tagged *ced-9, egl-1* was found to physically interact with *ced-9* (the homolog of mammalian BCL-2) through its BH3-only domain (Conradt and Horvitz 1998). The binding of EGL-1 protein to CED-9 causes a conformational change in CED-9 and likely an inhibition of its anti-apoptotic function (Yan *et al.*, 2004). This is orthologous to the function of mammalian BH3-only proteins, which bind to and inhibit anti-apoptotic BCL-2 proteins, causing a conformational change in the protein which results in the release of

its pro-apoptotic binding partner (reviewed in Lomonosova and Chinnadurai, 2008). The transcription of EGL-1 in response to apoptotic stimuli is the first step in the initiation of apoptosis.

CED-9 binds CED-4 at mitochondria

ced-9 is a homolog of mammalian BCL-2 (Hengartner and Horvitz, 1994). It has been proposed through protein interaction and localization studies that CED-9 acts to prevent cell death by physically interacting with and sequestering the pro-apoptotic protein CED-4 (APAF-1 in mammals) to mitochondria (Chen *et al.,* 2000; Chinnaiyan *et al.,* 1997; Spector *et al.,* 1997). *In vitro* and yeast two-hybrid binding assays showed that CED-9 is capable of binding CED-4. Physical interaction between CED-9 and CED-4 *in vivo* was confirmed by a CED-4 localization study using a polyclonal antibody generated against CED-4 protein (Chen *et al.,* 2000). This study showed that in wild-type embryos CED-4 is sequestered to mitochondria in a CED-9-dependent manner and was translocated to the perinuclear membrane in the absence of CED-9. Crystal structures showing EGL-1-CED-9 and CED-9-CED-4 complexes provided further evidence that EGL-1 acts to displace CED-4 from CED-9 (Yan *et al.,* 2004; 2005).

These prior studies led to the canonical model for the mechanism by which CED-9 regulates apoptosis. In this model, in living cells, CED-9 functions to prevent apoptosis by sequestering CED-4 to mitochondria, inhibiting its function; cells fated to die express EGL-1 (a BH3-only protein)

that then binds CED-9 (Conradt and Horvitz, 1998; Yan *et al.,* 2004), this interaction causes a conformational change in CED-9 that results in the dissociation of CED-4 from CED-9 (Yan *et al.,* 2005). In this thesis, I present data that this model, in which the sequestration of CED-4 by CED-9 is anti-apoptotic, is incomplete (Chapter Two). Specifically, I found that mutations made in CED-9 and CED-4 that prevent CED-9-CED-4 interaction disrupt a pro-apoptotic function of CED-9 resulting in less cell death, not more as the canonical model would predict in the absence of CED-9-CED-4 interaction.

CED-4 release activates CED-3

Human APAF-1 was defined as a protein capable of activating the caspases caspase-3 and caspase-9 *in vitro* and by sequence was found to be similar to the already known CED-4 (Zou *et al.,* 1997; Li *et al.,* 1997). Both CED-4 and the human gene APAF-1 as the N terminal of both proteins possess a caspase recruitment (CARD) domain (Zou *et al.,* 1997). This CARD domain is essential to the binding of CED-4/APAF-1 to their caspase binding partner.

In the absence of EGL-1, CED-4 binds CED-9 as a dimer on the surface of mitochondria (Yan, Xu, and Shi, 2006). Upon induction of apoptosis, EGL-1 associates with CED-9, displacing CED-4. CED-4 then translocates to the perinuclear membrane (Chen *et al.,* 2000) and forms an octameric apoptosome, facilitating the auto activation of the caspase CED-3 (Qi *et al.,* 2010).

Based on these studies, it was proposed that the pro-apoptotic function of CED-4 is activated by EGL-1 through an EGL-1-CED-9 interaction that results in the release of CED-4 (Conradt and Horvitz, 1998) and its translocation to the perinuclear membrane possibly facilitated by the inner nuclear membrane protein SUN-1, which might act as the nuclear envelope receptor for CED-4 binding (Tzur *et al.,* 2006).

Apoptosis is executed by the caspase CED-3 in *C. elegans*

CED-3 was found to be similar to the mammalian Interleukin-1β-Converting Enzyme (ICE) gene and is defining member of the caspase family, a family of proteases named for the presence of a catalytic cysteine which cleaves aspartate residues (Cysteine ASPartate proteASE) (Duan *et al.*, 1996; Xue, Shaham, and Horvitz, 1996; Alnemri *et al.,* 1996; Yuan *et al.,* 1993). Loss-of *ced-3* function prevents almost all cells fated to die from undergoing apoptosis.

Caspases are expressed as inactive proteins, containing an inhibitory pro-domain that must be auto cleaved or cleaved by another caspase. Similar to human caspase-9, CED-3 is inactive until it interacts with octameric CED-4 (APAF-1 in humans), which brings inactive caspases together, facilitating auto cleavage of the pro-domain and forming an active apoptosome (Wu *et al.*, 1997; Huang *et al.*, 2013)**.** Following the cleavage of its pro-domain, activated CED-3 protein then cleaves its target proteins to execute apoptosis. Approximately 3% of the *C. elegans* proteome appears to be made up of

target substates of CED-3. These targets comprise proteins across many different families including cytoskeletal components like actin, light chain myosin, and tubulin as well as chaperone proteins and proteins involved in metabolic processes, to name a few (Taylor *et al.*, 2007).

Taken together, the discoveries outlined above led to the canonical, molecular model of apoptosis: EGL-1 is expressed in response to apoptotic stimuli, EGL-1 protein binds to and inhibits CED-9 at mitochondria facilitating the release of dimeric CED-4, which then forms an octamer capable of binding to CED-3 and promoting autocleavage of the pro-domain, generating active CED-3 that then cleaves its target proteins to carry out apoptosis (Fig. 1B).

Phagocytosis

Phagocytosis (or engulfment) was named for the actin-dependent process by which one cell engulfs another. Phagocytosis is crucial to the removal of dead cells or cell “corpses”. Following the discovery of the involvement of the genes *ced-1* and *ced-2* in engulfment, an additional screen was conducted to identify mutations in more genes involved in the regulation of this process (Ellis, Jacobson, and Horvitz, 1991). In this screen, Nomarski optics were used to identify embryos from mutagenized worms that contained highly refractile cells, i.e. uncleared cell corpses. This screen isolated mutations in five new genes involved in the engulfment process, *ced-5, ced-6, ced-7, ced-8,* and *ced-10.* The expressivity of uncleared corpses in double mutants

involving these genes separated these genes into two groups, the first consisting of *ced-1, ced-6, ced-7,* and *ced-8* and the second containing *ced-2, ced-5,* and *ced-10*: this work suggested the presence of two distinct, parallel engulfment pathways, since mutations in genes in the first group can enhance the prevalence of cell corpses caused by mutations in genes in the second group but not each other and *vice versa*. The engulfment gene *ced-12* was later identified and found to function as a member of the *ced-2/5/10* group of engulfment genes (Chung *et al.,* 2000). The discovery of these engulfment genes formed the basis of further research into the genetic regulation of apoptosis and phagocytosis (Chen *et al.,* 2013; Suzuki *et al.,* 2013; Fadok *et al.,* 2001; Zhou, Hartwieg, and Horvitz, 2001).

ced-8 regulates phosphatidylserine presentation

Phosphatidylserine (PS) is normally found in the inner leaflet of healthy cells and is translocated to the surface of apoptotic cells (Fadok *et al*., 1998). PS presentation in apoptotic cells is a highly conserved process that is suppressible by BCL-2 overexpression – suggesting that this phenomenon occurs downstream of apoptosis. It was also found that PS presentation occurs in dying cells regardless of the apoptotic stimuli (Van Den Eijnde *et al.,* 1998; Martin *et al.,* 1995). The presentation of PS on the surface of dying cells is recognized as an “eat me” signal to engulfing cells (Fadok *et al.,* 2001). Further, PS presentation is an important feature used in the study of apoptosis, as annexin V staining for PS is a common method of detecting

apoptotic cells in diverse systems, including both *C. elegans* and mammalian systems (Vermes *et al.,* 1995).

CED-8 (Akr8 in mammals) is a substrate of CED-3 and its cleavage by CED-3 following the activation of apoptosis promotes the externalization of PS to the surface of the plasma membrane (Chen *et al.,* 2013; Suzuki *et al,.* 2013). Therefore, CED-8 serves an important purpose, functioning in a cell actively undergoing apoptosis to coordinate cell death with cell corpse removal.

The *ced-7, ced-1, ced-6* pathway

Through double mutant studies *ced-7* was found to function in a pathway with *ced-1* and *ced-6*, and functions in both the apoptotic cell and the engulfing cell, a feature unique to *ced-7* (Ellis, Jacobson, and Horvitz, 1991). *ced-7* is a homolog of human ATP-binding cassette (ABC) transporter ABC-1 (Wu and Horvitz, 1998b). *ced-7* and *ced-1* both appear to regulate PS externalization (Mapes *et al.,* 2012). *ced-1* is a transmembrane protein with homology to human scavenger receptor from endothelial cells (SREC) proteins. *ced-7* functions in somatic cells to regulate the clustering of CED-1 protein on the membrane of engulfing cells that neighbor cell corpses (Zhou, Hartwieg, and Horvitz, 2001). Since CED-1 clustering is dependent on CED-7, CED-1 acts downstream of CED-7 to promote engulfment.

ced-6 was cloned and found to contain a phosphotyrosine-binding domain and is similar in sequence to the human adaptor genes SHC, NUMB, and

DAB (Liu and Hengartner, 1998). Like *ced-1, ced-6* is expressed in engulfing cells rather than dead cells. Through *in vitro* binding and yeast two-hybrid assays CED-6 and CED-1, as well as their mammalian homologs the adaptor protein GULP and the receptor-related protein CD91/LRP, respectively, were found to be capable of forming a physical interaction (Su *et al.,* 2002). This interaction provided additional evidence that CED-6 and CED-1 function in the same pathway.

ced-6 acts downstream of *ced-7* and *ced-1* as overexpression of *ced-6* suppresses the engulfment defects caused by either *ced-7* or *ced-1* mutations (Liu and Hengartner 1998). Additionally, CED-1 clustering occurs in the absence of *ced-6* (Zhou, Hartwieg, and Horvitz, 2001). *ced-7* is believed to function upstream of *ced-1* by allowing CED-1 protein to recognize cell corpses.

The *ced-2, ced-5, ced-12, ced-10* pathway

ced-2, ced-5, ced-10, and *ced-12* regulate a second engulfment pathway. In addition to mutations in these genes enhancing the engulfment defect caused by *ced-7, ced-1,* and *ced-6* mutations but not each other these genes also cause a defect in the migration of the distal tip cells (DTC), a migration that determines the shape of the gonad in hermaphrodites, while mutations in the parallel pathway do not. (Wu and Horvitz 1998a; Zhou *et al.* 2001; Ellis, Jacobson, and Horvitz 1991). This provided further evidence of the existence of a distinct pathway where *ced-2, ced-5, ced-10,* and *ced-12* act together.

ced-5 was shown to be similar to human DOCK180 and although DOCK180 was unable to rescue the engulfment defect caused by loss-of *ced-5* function it was capable of rescuing the DTC migration defect, showing at there is at least some functional relation between the proteins (Wu and Horvitz 1998a).

ced-2 was found to share homology with the human adaptor protein CrkII (Reddien and Horvitz, 2000). Interestingly, CrkII forms foci on the cell surface with DOCK180 (Kiyokawa, Hashimoto, Kurata, et al. 1998). Additionally, *in vitro* binding and yeast two-hybrid assays showed that CED-2/CrkII and CED-5/DOCK180 were capable of forming a physical interaction (Reddien and Horvitz, 2000).

In the same study characterizing *ced-2, ced-10* was mapped to the same position as the previously identified gene *rac-1* (Reddien and Horvitz, 2000). Furthermore, *rac-1* cDNA, expressed by a heat-shock promoter, was shown to rescue both the DTC migration and engulfment defects caused by a *ced-10* mutation. Therefore, it was determined that *ced-10* is *rac-1*, a gene with high sequence similarity to human Rac. Rac is a GTPase known to function in signal transduction, cell migration, and phagocytosis (Van Aelst and D'Souza-Schorey 1997; Caron and Hall 1998; Massol *et al.* 1998). Interestingly, other studies observed that the Rac signaling pathway is activated by DOCK180 in *Drosophila* embryogenesis and in actin remodeling in fibroblasts (Nolan et al. 1998; Kiyokawa, Hashimoto, Kobayashi, et al. 1998).

In a later study, another screen searching for mutations that induced cell corpses identified mutations in the gene *ced-12,* shown to be a novel member of the engulfment pathway defined by *ced-2, ced-5,* and *ced-10* through the creation of double mutants (Chung *et al.,* 2000). *ced-12*, is a homolog of mammalian ELMO1 and ELMO2 (genes involved in engulfment and cell motility) (Gumienny *et al.*, 2001). Similar to CrkII, ELMO can physically interact with DOCK180 *in vitro* (Gumienny *et al.,* 2001).

Like *ced-1* and *ced-6*, transgenic studies suggest that *ced-2, ced-5, ced-10,* and *ced-12* function in engulfment, since none of these genes is expressed in cell corpses but all are expressed in engulfing cells, making *ced-7* the only one of these genes that is expressed in the dying cell (Wu and Horvitz, 1998a; Gumienny *et al.*, 2001). To determine the ordering of these genes in a genetic pathway, overexpression studies were performed that showed that *ced-10* over-expression rescues the DTC migration and engulfment defects caused by *ced-2, ced-5,* and *ced-12* mutants; however, the overexpression of *ced-2, ced-5,* or *ced-12* cannot rescue either defect caused by mutations in any other gene in this pathway (Gumienny *et al.,* 2001; Reddien and Horvitz, 2000). This evidence suggests that *ced-2, ced-5, and ced-12* might act together and upstream of *ced-10.*

Asymmetric cell division

Asymmetric cell division is a process crucial to the determination of cell fate, including the creation of a diversity of cell types and the decision of

certain cells to undergo apoptosis (reviewed in Horvitz and Herskowitz, 1992). Generally, cells that are fated to be eliminated by apoptosis are the smaller daughters of a mother cell that has undergone an asymmetric cell division (Sulston and Horvitz, 1977; Sulston *et al.*, 1983). Efforts to identify the genetic basis for asymmetric cell division in *C. elegans* were focused on the asymmetric cell divisions of the cells Q.a and Q.p and their daughters, Q.aa and Q.pp, respectively, as well as other neuroblast cells (Guenther and Garriga, 1996; Frank *et al.*, 2005; Cordes, Frank, and Garriga, 2006; Singhvi *et al.*, 2011; Chien *et al.*, 2013; Gurling, Talavera, and Garriga, 2014; Teuliere *et al.*, 2014). The findings of these studies demonstrated a genetic basis for asymmetric cell division driving the production of diverse cell types including an apoptotic fate generally taken by a smaller daughter cell.

The *pig-1* pathway is the first of three distinct parallel pathways regulating asymmetric cell divisions in *C. elegans. pig-1* is the *C. elegans* homolog of the mammalian AMPK-like kinase MELK. The *pig-1* pathway is activated when PIG-1 protein is phosphorylated by a cascade including the genes *par-4, strd-1, and mop-25.1/25.2* – homologs of the mammalian proteins LKB1, STRAD, and MO25, respectively (Cordes, Frank, and Garriga, 2006; Chien *et al.*, 2013). This pathway is conserved and likely functions to regulate cell polarity, a feature crucial to the ability of cells to unequally distribute cellular components among its daughters following cell division (Chien *et al.* 2013).

The second pathway is the *arf* pathway, regulated by ADP-ribosylation factors (ARFs), small membrane-bound guanosine-binding proteins that are

inactive when bound to GDP and active when bound to GTP; these proteins are conserved in all eukaryotes (reviewed in Donaldson and Jackson, 2000). In *C. elegans* this pathway comprises five genes, *arf-1, arf-5, arf-6*, *cnt-2,* and *grp-1* (Teuliere *et al.*, 2014). *arf-1,5, and 6* are homologs of mammalian ARFs. *cnt-2* encodes an ARF-GTPase activating protein (GAP) (Singhvi *et al.*, 2011). *grp-1* is a cytohesin (a family of proteins involved in the regulation of vesicle trafficking and cell signaling) and encodes an ARF-guanosine nucleotide exchange factor (Teuliere *et al.*, 2014). ARF proteins are known to function in diverse processes related to vesicular trafficking; this known function might relate to the mechanism by which this pathway controls asymmetric cell division (Donaldson and Jackson, 2000).

The gene *toe-2* defines the third and final pathway. TOE-2 is a DEP (domain found in Dishevelled, EGL-10, and Pleckstrin) domain-containing protein (Gurling, Talavera, and Garriga, 2014). Interestingly, *toe-2* is required for the Q.a but not the Q.p asymmetric cell division (Gurling, Talavera, and Garriga, 2014). Since the Q.a asymmetric cell division relies on a spindle-independent mechanism and the Q.p division relies on a spindle-dependent mechanism *toe-2* likely regulates asymmetric cell division through a mechanism that is spindle-independent (Ou *et al.* 2010).

Apoptosis in development

As Carl Vogt noted based on studies of morphogenic toads in 1842, dying cells must be cleared for proper animal development. Cell proliferation is

rapid during embryogenesis and development, and the creation of new cells must be balanced with cell death to maintain tissue homeostasis (Hipfner and Cohen, 2004).

One striking example of programmed cell death shaping animal morphology during development occurs during amphibian tadpole morphogenesis. Apoptosis occurs in the tail of the tadpole to remove unneeded cells (Jacobson, Weil, and Raff, 1997). Programmed cell death also plays a role in proper development of the embryo, such as in the removal of interdigital tissue in mouse and other mammalian fetuses (Glücksmann, 1951; Saunders, 1966; Mori *et al.*, 1995). Apoptosis in the interdigital tissue similarly occurs in the developing chick embryo (Garcia-Martinez *et al.* 1993). Cell death is also required for the morphological characteristics of the early stages of embryogenesis such as gastrulation (Coucouvanis and Martin 1995; Glücksmann 1951; Saunders 1966).

Tissue homeostasis is another major process that is controlled by programmed cell death (Fuchs and Steller 2011). As cells divide animals must be able to balance cellular proliferation with cell death to maintain a proper number of cells, e.g., as observed for epithelial cells in the hydra *Hydra attenuate* to regulate growth rate (Bosch and David 1984). Programmed cell death also functions to remove superfluous neurons during animal development (Hamburger, Brunso-Bechtold, and Yip, 1981; Xia *et al.*, 1995).

Apoptosis is an important regulatory process during times of high cellular proliferation. During embryogenesis cells are proliferating rapid and the removal of these cells is crucial to achieve proper morphology and to clear superfluous cells. Following development, cell division still occurs, and the creation of new cells must be balanced to maintain tissue homeostasis (Bosch and David 1984; Henson and Hume 2006).

Apoptosis in disease

In humans, either excessive or insufficient cell death can result in diseases, including cancers and certain neurodegenerative and autoimmune disorders (Hyman and Yuan 2012; Hipfner and Cohen 2004; Takeuchi et al. 2005). In addition to the essential role of apoptosis in development and maintaining tissue homeostasis, apoptosis is also required for the removal of potentially damaged cells, such as cells that have undergone DNA damage. Inability to remove these damaged cells can result in the accumulation of mutations from DNA damage leading to cancer (reviewed in Wong, 2011).

Overexpression of the anti-apoptotic protein BCL-2 can prevent apoptosis and cause cancer; one such example of BCL-2 overexpression occurs as a result of the chromosomal translocation t(14:18) – which leads to constitutive expression of BCL-2 by creating a transgene wherein BCL-2 is expressed by an immunoglobin heavy chain enhancer – a common characteristic of follicular lymphoma and other non-Hodgkin lymphomas (Vaux, Cory, and Adams, 1988; Rabkin *et al.*, 2008). Apoptosis typically clears damaged,

potentially cancerous cells through the intrinsic pathway – an apoptosis pathway controlled by BCL-2 family proteins – in a manner dependent on the tumor-suppressor protein, p53; overexpression of BCL-2 prevents activation of this pathway (Nagata, 1997). Dysregulation of apoptosis can also lead to autoimmune disorders; one example is caused by a deficiency in the pro-apoptotic BCL-2 proteins BAX and BAK. BAX and BAK normally function to prevent autoimmune disease by maintaining homeostasis of B cells and removing autoreactive B cells (Takeuchi *et al.* 2005; Mason *et al*. 2013).

Excessive apoptosis can also lead to disease in many neurodegenerative disorders in which otherwise healthy neurons undergo apoptosis (reviewed in Hyman and Yuan, 2012). For example, ectopic caspase activation has been suggested to contribute to Alzheimer's disease (AD) pathology, since caspases have been shown to be upregulated in the brains of AD patients (Matsui et al. 2006). Additionally, caspases cleave and activate multiple targets believed to be involved in AD pathology, including tau protein, and TUNEL (Terminal deoxynucleotidyl transferase dUTP Nick End Labeling) staining – an assay used to mark apoptotic cells by recognizing DNA fragmentation – shows that TUNEL-positive neurons often present in AD, indicating the presence of apoptotic neurons (Matsui *et al*., 2006; Allen *et al.,* 2001; Chan, Griffin, and Mattson, 1999; Cotman *et al.,* 2005; Cribbs *et al.,* 2004; Gastard, Troncoso, and Koliatsos, 2003).

Apoptosis must be tightly regulated to prevent disease progression in humans. The dysregulation of apoptosis in either direction – causing ectopic

survival of damaged cells or ectopic death in healthy cells – can result in cancer, autoimmune disorders, or neurodegenerative disorders.

III. The pro-apoptotic function of CED-9 and BCL-2 family members

Apoptosis in mammals

Unlike *C. elegans*, which has only one BCL-2 family member (*ced-9)*, mammals possess many of these genes, some anti-apoptotic, such as BCL-2 BCL-XL and MCL1, and some pro-apoptotic, such as BAX and BAK (reviewed in Youle and Strasser, 2008). Mammalian cell death can occur either cell intrinsically as a result of damage to the cell (e.g., DNA damage) or cell extrinsically as a result of stimulation of receptors on the cell surface by extracellular stimuli.

The intrinsic pathway of apoptosis in mammals is most similar to that of *C. elegans*. Following the activation of this pathway, for example by p53-induced transcription of BH3-only proteins like NOXA, BIK, and PUMA following DNA damage (Villunger *et al.,* 2003; Mathai *et al.*, 2002), BH3-only proteins directly bind to and inhibit anti-apoptotic BCL-2 family members the function of which in mammals is to sequester pro-apoptotic BCL-2 family members such as BAX and BAK; once released the pro-apoptotic BCL-2 proteins form pores in mitochondria to release mitochondria-bound proteins in a process called mitochondrial outer membrane permeabilization (MOMP) (reviewed in Kale, Osterlund, and Andrews, 2018). Through MOMP, the pro-apoptotic BCL-2

family members release cytochrome c, which activates APAF-1; active APAF-1 then activates the functional homolog of CED-3, capsase-9, to initiate apoptosis through the activation of other caspases (Liu *et al.,* 1996; Kluck *et al*., 1997; Zou *et al.,* 1997; Yang *et al.,* 1997; Li *et al.,* 1997). Caspases that function mainly in the activation of other caspases, such as caspase-9, are called initiator caspases, while those that function downstream of initiator caspases to cleave other proteins are called effector caspases, such as caspase-3, -6, and -7 (Wang and Lenardo, 2000).

The extrinsic pathway of apoptosis (also called the death-receptor pathway) is activated following the stimulation of death receptors on the surface of the dying cell by intercellular signals such as the type 1 TNF receptor (TNFR1) and the Fas receptor (FasR also called CD95) that are stimulated by the cytokines TNF and Fas-ligand (FasL), respectively; once stimulated the adaptor proteins TRADD (TNF receptor-associated death domain) and FADD (Fas-associated death domain protein) recruit caspase-8, activating it via autocleavage (Hengartner, 2000). Like caspase-9 in the intrinsic pathway, capsase-8 is the main effector caspase in the extrinsic pathway.

In both mammals and *C. elegans* anti-apoptotic BCL-2 proteins function at the mitochondria to prevent cell death. In models for both of these processes, BH3-only proteins function in a pro-apoptotic manner to change the binding affinity of anti-apoptotic BCL-2 proteins for their pro-apoptotic binding partner, CED-4 in *C. elegans* and pro-apoptotic BCL-2 family members such as BAX

and BAK in mammals. Though in both *C. elegans* and mammals inhibition of CED-9/BCL-2 by BH3-only proteins leads to the activation of CED-4/APAF-1, in mammals APAF-1 is activated through MOMP facilitated by pro-apoptotic BCL-2 proteins and the sequential release of cytochrome c from mitochondrial intermembrane space, while the canonical apoptotic pathway for *C. elegans* has CED-4 as active once released from a direct CED-9-CED-4 interaction. Once active, CED-4/APAF-1 allows for caspase activation in mammals and *C. elegans,* and in both mammalian pathways (intrinsic and extrinsic) and the *C. elegans* pathway apoptosis is initiated following induced proximity of caspases that results in the autocleavage of the inhibitory pro-domain.

CED-9 possess an apparent pro-apoptotic function

In addition to its canonical anti-apoptotic role, *ced-9* appears to have a pro-apoptotic function. For example, *ced-9(lf)* mutations can enhance the partial cell-death defect observed in worms with a weak loss-of-function mutation in the pro-apoptotic caspase gene *ced-3* (Hengartner and Horvitz, 1994). The existence of a pro-apoptotic function of CED-9 implies that the canonical model for *C. elegans* cell death, in which CED-9 functions only as an anti-apoptotic protein, is incomplete.

Additionally, the canonical model proposes that in living cells cell death is blocked by the CED-9-dependent sequestration of CED-4 to mitochondria. However, in *ced-9(n1653ts)* mutant animals – which carry a temperature-

sensitive allele that (like *ced-9(0)* alleles) causes lethality at non-permissive temperatures but (like *ced-9(+)* alleles) at permissive temperatures allows viability – at permissive temperature some CED-4 protein is localized to the perinuclear membrane, as assayed by anti-CED-4 polyclonal antibody localization, though (like *ced-9(+)* alleles) these animals are still viable (Chen *et al.,* 2000). This observation suggests that CED-4 localization at the perinuclear membrane is not sufficient to drive apoptosis. In addition, despite the ability of *ced-9(lf)* alleles to enhance ectopic cell-survival caused by weak-loss-of function alleles in the cell-death promoting *ced-3* gene, loss-of *ced-9* function in the presence of a weak *ced-3* loss-of-function mutation results in CED-4 localization to the perinuclear membrane (Chen *et al.,* 2000), again uncoupling CED-4 localization at the perinuclear membrane from the activation of apoptotic death.

The presumptive pro-apoptotic role of *ced-9* was previously poorly understood. Since *C. elegans* cell-death genes show striking homology to mammalian cell-death genes, the finding that CED-9 possess a pro-apoptotic function has implications for our understanding of the functions of mammalian BCL-2 family members in cell death and how perturbation of their functions can affect human diseases, including certain neurogenerative disorders and cancers. Interestingly, canonically anti-apoptotic BCL-2-family proteins have also been shown to possess poorly understood pro-apoptotic functions (addressed below) (Lin *et al*., 2004; Cheng *et al.*, 1997; Basañez *et al*., 2001; Flores-Romero *et al*., 2019).

The pro-apoptotic function of CED-9 is the primary focus of this thesis – I conclude that this pro-apoptotic function depends on CED-9-CED-4 interaction. This finding is opposite to the prediction made by the canonical model of apoptosis in *C. elegans,* which predicts that a loss-of CED-9-CED-4 interaction would result in excessive apoptosis. This thesis describes the creation of seven *ced-9* and one *ced-4* allele with mutations in the presumptive CED-9-CED-4 binding region as described by a crystal structure of the complex (Yan *et al.,* 2005). Surprisingly, these alleles not only disrupt the pro-apoptotic function of CED-9 but they also appear to have no effect on the anti-apoptotic function of CED-9. Additionally, I show that all of these alleles disrupt CED-9-CED-4 interaction *in vivo.* This finding fundamentally changes our understanding of the core apoptotic pathway of *C. elegans* and might have important implications for the understanding of apoptosis in other organisms, including humans.

The pro-apoptotic function of anti-apoptotic BCL-2 proteins

Since *C. elegans* has no known pore-forming BCL-2 proteins – such as BAX/BAK in mammals – it is possible that *ced-9,* the mammalian BCL-2 homolog, must assume both a pro- and anti-apoptotic role while mammalian BCL-2 proteins are able to separate the two functions into distinct proteins that play separate, opposite roles in the apoptotic process. However, like CED-9, anti-apoptotic BCL-2 family members can assume a pro-apoptotic function.

For example, it has been observed that BCL-2 can become pro-apoptotic in the presence of the nuclear hormone receptor NUR77 (Lin *et al.,* 2004). Additionally, expression of NUR77 correlates with induction of apoptosis in certain cell types (Woronicz *et al.,* 1994; Liu *et al.,* 1994), these findings suggest that NUR77 might promote apoptosis through BCL-2. An *in vitro* study showed that over-expression of caspase-3 can cause the cleavage of BCL-2 following the induction of apoptosis and that mutants of BCL-2 resistant to capsase-3 cleavage provided cells protection from apoptosis; suggesting that a truncated BCL-2 protein (following cleavage by caspases) might activated apoptosis, further suggesting that the induction of a pro-apoptotic state of BCL-2 is possible (Cheng *et al.,* 1997). This cleavage by caspase-3 occurs at residue D34, an amino acid that is C-terminal of the BH4 (BCL-2 Homology domain 4) domain of BCL-2, removing the BH4 domain, which resides at the N-terminus of the 239 amino-acid BCL-2 protein (Cheng *et al.,* 1997). This study also shows that, when expressed by a transgene, truncated BCL-2 proteins (lacking amino acids 1-34) causes reduced viability in baby hamster kidney fibroblast (BHK) cells. Though this study uses *in vitro* systems to determine that BCL-2 can be cleaved by overexpressed caspase-3 and transgenic expression of proteins often result in protein overexpression, these findings show that it is possible to transform BCL-2 into a pro-apoptotic state. Interestingly, CED-3 is capable of cleaving CED-9 *in vitro* at both residues D47 and D67 (Xue and Horvitz, 1997). I found that mutations made in a CED-4 binding region of CED-9 D67-E81 (as defined by X-ray

crystallography (Yan *et al.,* 2005) are sufficient to prevent CED-9-CED-4 interaction *in vivo* (Chapter Two). Since this CED-4 binding region is N-terminal of the BH4 domain in *C. elegans* (D76-A102), a similar cleavage of CED-9 at an amino acid C-terminal of its BH4 domain by CED-3 would release a 178 amino acid CED-9 protein. This C-terminal fragment of CED-9 could promote apoptosis by ensuring that, following the release of CED-4 from CED-9 by EGL-1, activated CED-4 remains free from CED-9, allowing the apoptosome to remain intact. It is also possible that CED-9 possesses an unknown anti-apoptotic function that is dependent on the N-terminus of CED-9 but not on CED-9-CED-4 interaction. Supporting the later hypothesis is the discovery that CED-3 cleaves CED-9 *in vitro* at amino acids D47 and D67 and that a recombinant CED-9 protein excluding this cleaved region (CED-9(68-260)) provides less protection relative to CED-9(+) and remains sufficient for CED-4 interaction *in vitro* (Xue and Horvitz, 1997). Therefore, it is possible that CED-9(1-67) mediates an anti-apoptotic function of CED-9 that is independent of CED-9-CED-4 interaction and that the removal of CED-9(1-67) by active CED-3 promotes apoptosis. To test this hypothesis, I propose first confirming that *in vitro* CED-9(68-260) interacts with CED-4. Then CED-9(68-260) should be made at the endogenous CED-9 locus by CRISPR-Cas9 in a *ced-3(lf)* background. If CED-9(1-67) is anti-apoptotic then CED-9(68-260) might be inviable on its own, similar to *ced-9(0)* alleles. However, CED-9(68-260) can be tested for its ability to interact with CED-4 *in vivo* in a *ced-3(lf)* background by using antibody staining with an anti-CED-4 polyclonal

antibody or an endogenously tagged CED-4::GFP allele to assess CED-4 localization. If CED-9(68-260) causes maternal-effect lethality but retains CED-4 binding capability (CED-4 localized to mitochondria), then CED-9(1-67) mediates an anti-apoptotic function of CED-9 that is independent of CED-4 interaction. If CED-9(1-67) is found to mediate an anti-apoptotic function of CED-9 then it should be determined whether this peptide has any binding partners, the sequestration of which by CED-9(1-67) might explain the apparently CED-4-sequestration independent anti-apoptotic function of CED-9 (Chapter Two). To do this CED-9(1-67) should be expressed with an epitope tag and incubated with *C. elegans* protein extracts. The peptide and any binding partners should then be purified by pulling-down the epitope tag and LC-MS/MS should be used to identify any peptide that is bound to CED-9(1-67).

Interestingly, canonically pro-apoptotic BCL-2 family members, such as Bax and Bak, contain three BH domains (BH1-3), while their anti-apoptotic counterparts, such as BCL-2 and CED-9, contain four (BH1-4) – the BH4 domain is N-terminal in all of these cases (reviwed in Levine, Sinha, and Kroemer, 2008). Perhaps caspase-mediated cleavage of the BH4 domain at the N-terminus of anti-apoptotic BCL-2 proteins causes them to switch into a pro-apoptotic state, similar to how the cleavage of the N-terminal pro-domain of caspases (either by themselves or other caspases) is required to activate their pro-apoptotic function.

In a separate study caspase-3 also appeared capable of transforming BCL-XL into a pro-apoptotic state. In this study, two recombinant and short BCL-XL proteins (lacking the first 61 and 74 amino acids, respectively – both lack the BH4 domain of BCL-XL) and BCL-XL cleaved by caspase-3 showed an ability to form pores, inducing cytochrome c release form mitochondria in BHK cells (Basañez *et al.,* 2001). It has also been suggested that outer mitochondrial membrane lipid composition can influence the typically anti-apoptotic BCL-2 protein BFL-1, causing the protein to switch from an anti- to pro-apoptotic state (Flores-Romero *et al.,* 2019).

Thus, while the lack of pro-apoptotic pore-forming BCL-2 proteins such as BAX/BAK might necessitate the bifunctionality of *ced-9,* it appears that anti-apoptotic, mammalian BCL-2 proteins have retained at least some pro-apoptotic function. This apparent conservation of bifunctionality suggests that the pro-apoptotic function of canonically anti-apoptotic BCL-2 proteins has remained physiologically relevant and capable of contributing to cell death in the organism. Despite extensive research spanning decades, the pro-apoptotic mechanism(s) of these bifunctional proteins and how such mechanisms might influence the progression of diseases resulting from a disruption in the cell-death process remains poorly understood.

IV. Cell extrusion

The evolutionarily conserved process of caspase-mediated apoptosis is the most extensively studied form of cell death. Nonetheless, other

conserved mechanisms of cell elimination, such as cell extrusion, also exist (Denning, Hatch, and Horvitz, 2012; Eisenhoffer *et al.*, 2012; Dwivedi *et al.*, 2021).

Cell extrusion is a process of cell elimination by which a cell is removed from layer of tissue without compromising the integrity of the layer (Rosenblatt, Raff, and Cramer, 2001). Cell extrusion occurs in a wide range of metazoans, including sponges, mammals, fish, insects and nematodes (Ellis and Horvitz, 1986; Degoeij *et al.*, 2009; Denning, Hatch, and Horvitz, 2012; Eisenhoffer *et al.*, 2012; Eisenhoffer and Rosenblatt, 2013). In mammals, cell extrusion is used in epithelial cells to remove apoptotic cells without disrupting the integrity of the barrier created by the epithelial layer (Rosenblatt, Raff, and Cramer, 2001). In *C. elegans,* cell extrusion appears to be used as a "back-up" mechanism of cell elimination; in the absence of apoptosis eight cells in the *C. elegans* embryo – all fated to die by apoptosis under normal conditions – are instead eliminated via cell extrusion (Denning, Hatch, and Horvitz, 2012; Ellis and Horvitz, 1986).

Cell extrusion in tissue homeostasis

The epithelium forms a protective barrier of tissue that is continually being replaced via cell division and apoptosis. A large number of cells undergo apoptosis in epithelial tissue, and the cell corpses left behind must be removed to maintain tissue homeostasis. During the process of removing cell corpses, the integrity of this barrier must be maintained to preserve the

protective function of the tissue. To do so, apoptotic cells (cells exhibiting apoptotic markers such as reactivity to TUNEL staining) in the epithelium are removed by cell extrusion (Potten 1998; Watson *et al.,* 2009; Rosenblatt, Raff, and Cramer, 2001). This method of cell extrusion to remove apoptotic cells was observed in the epithelium of both chicken and mice embryos as well as *in vitro* in Madin Darby canine kidney (MDCK) cells following UV-induced apoptosis (Potten, 1998; Slattum, McGee, and Rosenblatt, 2009; Watson *et al.*, 2009). In these experiments, actin and myosin antibodies detected the formation of a contractile actomyosin ring that formed around apoptotic cells (identified by the presence of condensed nuclei). Drug-induced inhibition of actin polymerization, myosin contraction, and Rho-kinase activity, which is a key GTPase regulating actomyosin contractility, all prevent cell extrusion, indicating that an intact and contractile actomyosin rings is required for cell extrusion. Specifically, the protein p115 RhoGEF was found to regulate the constriction of actomyosin and the apical extrusion of these apoptotic epithelial cells (Slattum, McGee, and Rosenblatt, 2009). Interestingly, the addition of fluorescently labelled, apoptotic MDCK cells to a healthy monolayer of cells triggered the formation of this ring in the cells that contacted the apoptotic cell, indicating that the ring is formed is response to signal by the apoptotic cell (Rosenblatt, Raff, and Cramer, 2001).

To identify the signal that initiates cell extrusion, the fragments of dead cells were added to an MDCK cell monolayer and assessed for their ability to stimulate actin accumulation in surrounding cells (Gu *et al*. 2011). In this

study actin accumulation was stimulated by the addition of cell fragments following the treatment of the fragments with trypsin; therefore, it was unlikely that a protein was required to activate formation of the ring. Treatment with candidate bio-reactive lipids showed that the addition of sphingosine-1-phosphate (S1P) was sufficient to induce actin accumulation in the monolayer while total lipid extract from S1P-deficient *E. coli* was not, suggesting that S1P is required for ring formation and apoptotic cell extrusion. Treatment with S1P receptor-specific antagonists revealed that the cell surface S1P receptor $S1P_2$ is required in surrounding cells but not the apoptotic cell itself to promote extrusion (Gu *et al,.* 2011). Since p115 RhoGEF is required for this process it was hypothesized that S1P is trafficked to the surface of apoptotic cells by p115 RhoGEF where it signals surrounding cells through $S1P_2$ to activate formation of the actomyosin ring (Rosenblatt, Raff and Cramer, 2001; Slattum, McGee, and Rosenblatt, 2009; Gu *et al.*, 2011).

In addition to the removal of apoptotic cells in the epithelium, cell extrusion also removes cells in response to overcrowding both *in vivo* in both human and zebrafish tissues at sites containing the highest concentration of cells and *in vitro* following the induction of cellular proliferation in MDCK cells (Eisenhoffer *et al.,* 2012). This study also found that cell extrusion requires Rho Kinase and $S1P_2$ signaling as well as the mechanosensitive ion channel Piezo-1 to remove cells in response to overcrowding and apoptosis in the epithelium (Eisenhoffer *et al,.* 2012). Somatic cells, especially those in the epithelium, are constantly proliferating, and this proliferation must be

balanced by the elimination of cells to maintain proper cell number; cell extrusion functions to maintain this homeostasis by removing apoptotic cells and excessive cells in areas of overcrowding.

The dysregulation of cell extrusion has also been shown to contribute to human disease progression (Gu *et al.,* 2015). Specifically, tumors lacking $S1P_2$ signaling become resistant to apoptosis and the absence of proper cell extrusion regulation promotes the basal invasion of these cells that would otherwise be apically extruded (Gu *et al.,* 2015). These factors promote chemotherapy resistance and metastasis.

Cell extrusion in *C. elegans*

Cell extrusion of as many as eight cells (and six on average) occurs in *C. elegans* embryos that lack caspase activity. All eight of these extruded cells are eliminated via caspase-mediated apoptosis in wild-type embryos. Extrusion of these cells occurs in *C. elegans* embryos carrying loss-of-function mutations in *egl-1, ced-4,* or *ced-3* or a gain-of-function mutation of *ced-9* (Denning, Hatch, and Horvitz, 2012).

To identify genes involved in cell extrusion, an F_3 EMS mutagenesis screen was conducted that sought mutants defective in the extrusion of cells from *ced-3(lf)* caspase-deficient embryos (Denning, Hatch, and Horvitz, 2012). This screen identified mutants in which a commonly extruded cell, ABplpappap, fails to be extruded and instead survives (Ellis and Horvitz, 1986; Denning, Hatch, and Horvitz, 2012). In these mutants, ABplpappap

often generates an extra excretory cell (a cell associated with the excretory system) by adopting the fate of its lineal aunt cell. The excretory cell in *C. elegans* is involved in osmoregulation (Buechner, 2002), and mutations blocking cell extrusion of ABplpappap in the absence of *ced-3* activity caused a large cyst to appear to the head of the animal, suggesting a disruption in osmoregulation in animals exhibiting the Two Excretory cell (Tex) phenotype (Denning, Hatch, and Horvitz, 2012). This study showed that undead cells fated to be extruded in the absence of apoptosis can survive in the presence of an extrusion mutation and differentiate to the fate of a closely related cell; these results also show a function for cell extrusion in *C. elegans* as a back-up mechanism of cell elimination that removes at least one cell that would otherwise disturb an important physiological process.

Interestingly, this screen identified mutations in *pig-1,* a gene involved in asymmetric cell division (Cordes, Frank, and Garriga, 2006). Further, RNAi knockdown of *pig-1* as well as *par-4* and *strd-1* – other members of the *pig-1* asymmetric cell division pathway – were sufficient to block ABplpappap extrusion in *ced-3(lf)* animals; the other members of the *pig-1* pathway, *mop-25.1* and *mop-25.2,* had to be knocked down simultaneously (Denning, Hatch, and Horvitz, 2012). This study also found that RNAi knockdown of members of a second asymmetric *cell* division pathway – *arf-1, arf-5*, and *grp-1* – were similarly sufficient to block cell extrusion. These experiments provided compelling evidence for the involvement of asymmetric cell division in cell extrusion.

Replication stress induces cell extrusion

A more extensive screen for genes involved in cell extrusion was conducted using RNAi, which showed that cell-cycle genes have a role in cell extrusion (Dwivedi *et al.,* 2021). This screen used an RNAi library containing 11,511 clones; bacteria from this library expressing RNAi against *C. elegans* genes were fed to L4-staged *ced-3(lf)* animals, and their offspring were examined for the Tex phenotype. 27 genes were identified from screen, 10 of which had known roles in cell cycle regulation – mostly a role in regulating S-phase. Upon further investigation using cell biological techniques, this work found that cell extrusion is driven by S-phase arrest, a phenomenon that is prevented when cell cycle or asymmetric cell division genes are mutated. This work also found that S-phase arrest similarly drives cell extrusion in mammalian cell culture, using hydroxyurea to induce replication stress in MDCK cells (Koç *et al.*, 2004).

Additionally, the role of asymmetric cell division genes *pig-1* and *grp-1* were examined for their ability to affect the unequal cell division that creates the small cell ABplpappap and a potential role in its extrusion in the absence of caspase activity. RNAi knockdown of either of these genes resulted in the formation of a much larger ABplpappap and blocked its extrusion, suggesting that asymmetric cell division promotes S-phase arrest in extruded cells (Dwivedi *et al.*, 2021). Interestingly, RNAi against *gmpr-1* and *pyr-1* genes required for purine nucleotide balance and pyrimidine synthesis, respectively,

not only prevented cell extrusion in *ced-3(lf)* embryos but also caused the ectopic survival of ABplpappap in wild-type embryos and the ectopic extrusion of some cells in these embryos. This result suggests that an insufficient supply of resources such as nucleotides for DNA synthesis might promote S-phase arrest which in turn promotes cell extrusion.

These findings form the basis of a model for programmed cell extrusion in which asymmetric cell division generates a small cell lacking the sufficient resources for DNA synthesis such as nucleotides, causing replication stress and S-phase arrest and thereby driving the extrusion of the small cell (Dwivedi *et al.,* 2021) (Fig. 2).

In this thesis I describe my findings that loss-of *gmpr-1* function – either through RNAi knockdown or mutation – causes a defect in cell extrusion as well as a defect in apoptosis. I performed a targeted RNAi screen that showed that RNAi knockdown of *adss-1* (involved in purine nucleotide balance) and *pyr-1* similarly blocked extrusion and apoptosis of ABplpappap. In addition to identifying new nucleotide metabolism genes involved in ABplpappap survival I also searched for genes that when knocked down by RNAi either suppressed or enhanced the effects of a *gmpr-1* mutation. Interestingly, I found that the effects of a *gmpr-1* mutation are suppressed by RNAi knockdown of *pyr-1* but not *adss-1,* and that RNAi knockdown of *R151.2,* a gene involved in both purine and pyrimidine synthesis did not produce the Tex phenotype on its own but did suppress ABplpappap survival caused by the *gmpr-1* mutant. This result suggests that it is an imbalance

between purine and pyrimidine levels and not a scarcity of either that prevents ABplpappap death.

The mechanism by which an apparent inability to regulate balance between purines and pyrimidines is not known. Future studies might reveal an important method of cell elimination regulating both apoptosis and cell extrusion. The elucidation of such a mechanism could have implications for our understanding of the development of cancers caused by the dysregulation of apoptosis (Rabkin *et al.,* 2008), and the progression of metastasis, which could develop because dysregulation in cell extrusion (Gu *et al.,* 2015), in these cancers.

Concluding remarks

Apoptosis is a naturally occurring form of cell death essential for development and tissue homeostasis. In Chapter Two of this thesis, I report that interaction between the BCL-2 homolog CED-9 and its pro-apoptotic binding partner, the APAF-1 homolog CED-4 promotes apoptosis in *C. elegans*. Like CED-9, anti-apoptotic BCL-2 family members can also be pro-apoptotic in certain conditions, suggesting a conserved, and poorly understood pro-apoptotic function of these proteins.

Cell extrusion is a form of cell death that occurs in the absence of apoptosis in *C. elegans* embryos to eliminate certain cells normally fated to die by apoptosis. Chapter Three of this thesis describes how replication stress drives cell extrusion in both *C. elegans* embryos and MDCK cells. In

this chapter I report that the loss-of-function of certain nucleotide metabolism genes (*gmpr-1* and *pyr-1*) blocks extrusion of the cell ABplpappap in *ced-3(lf)* embryos, causes ectopic extrusion of some cells in *ced-3(+)* embryos, and blocks apoptosis in the cell ABplpappap in *ced-3(+)* embryos – suggesting an unknown role for purine/pyrimidine balance in regulating cell elimination through cell extrusion and apoptosis.

The final chapter of this thesis focuses on future experimentation aimed at addressing the anti-apoptotic function of CED-9, the mechanism underlying the pro-apoptotic nature of CED-9-CED-4 interaction, and further investigation into the apparent role of purine/pyrimidine balance in regulating both cell extrusion and apoptosis. Finally, this chapter includes unpublished data concerning the long-isoform of CED-4 and the role of nucleotide metabolism genes in cell elimination.

Acknowledgments

I thank Calista Diehl, Iliana Kesisova, and Eugene Lee for comments about this chapter.

Figure 1. The canonical model of caspase-mediated apoptosis in *C. elegans* in which A) EGL-1 promotes apoptosis by inhibiting CED-9, which inhibits CED-4. CED-4 activates CED-3 that then promotes cell death – mammalian homologs in parentheses. Molecularly B) Dimerized CED-4 is sequestered to mitochondria by CED-9. Upon induction of apoptosis through *egl-1* expression, EGL-1 protein binds to CED-9, changing the conformation of CED-9 and releasing CED-4. Released CED-4 forms an octamer that binds to dimerized pro-CED-3 forming the apoptosome. The apoptosome promotes autocleavage of pro-CED-3 activating the caspase and promoting cell death.

A

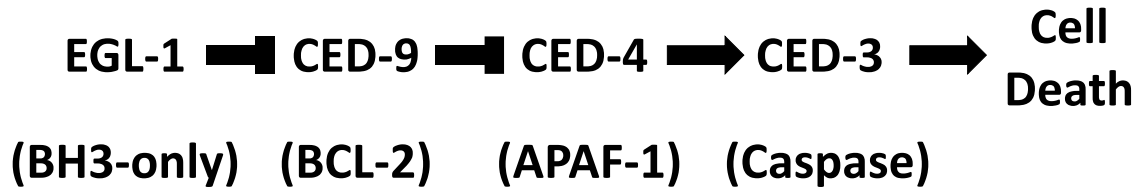
EGL-1
CED-9
CED-4
CED-3
Cell Death
(BH3-only)
(BCL-2)
(APAF-1)
(Caspase)

B

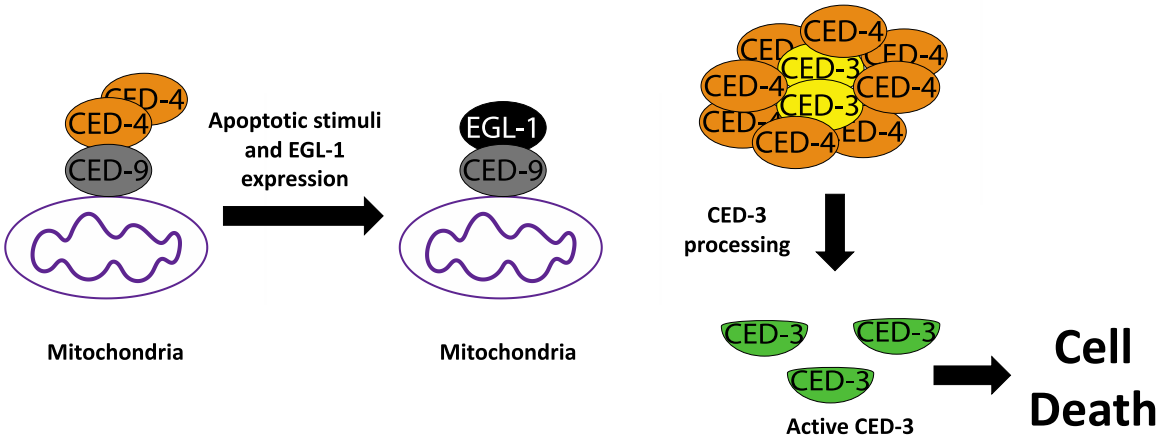
CED-4
CED-4
CED-9
Apoptotic stimuli and EGL-1 expression
EGL-1
CED-9
Mitochondria
Mitochondria
CED-4
CED-3
CED-3
CED-4
CED-4
CED-4
CED-3
CED-4
CED-4
CED-3 processing
CED-3
CED-3
CED-3
Active CED-3
Cell Death

Figure 2. Replication stress induced cell extrusion is promoted in *C. elegans* by an asymmetric cell division event, creating a small eventually extruded cell with insufficient resources for DNA replication. This cell enters S-phase and the eventually extruded experiences replication stress and S-phase arrest in both *C. elegans* and mammals. Replication stress experienced by this cell promotes cell extrusion. Figure adapted from Dwivedi *et al.,* (Dwivedi et al. 2021).

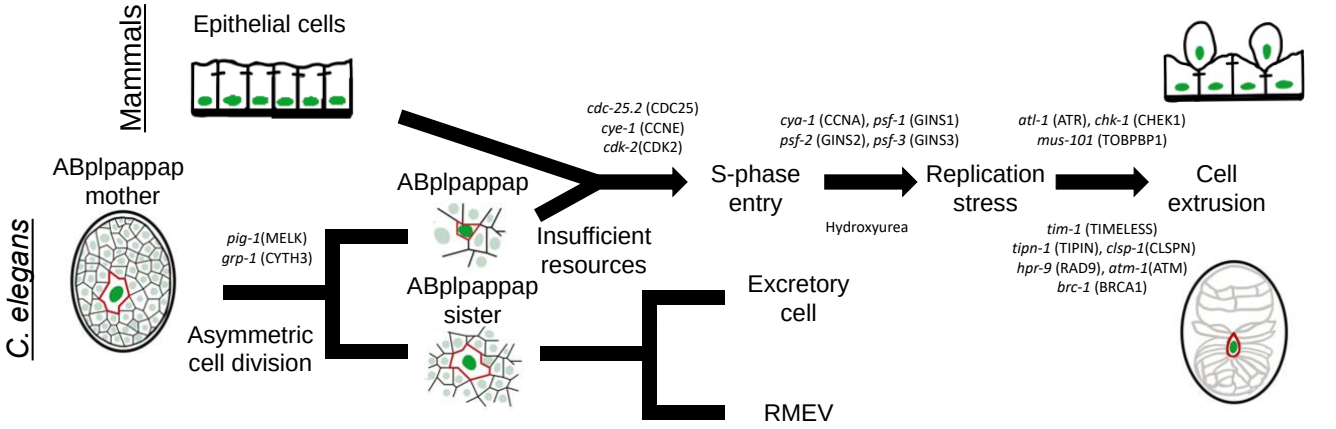

Adapted from Dwivedi *et al* 2021

References

Aelst, L. V., and D'Souza-Schorey, C. (1997). Rho GTPases and Signaling Networks. *Genes and Development*. **11**, 2295-2322. https://doi.org/10.1101/gad.11.18.2295.

Allen, J. W., Eldadah,, B.A., Huang, X., Knoblach, S.M., and Faden, A.I. (2001). Multiple Caspases Are Involved in β-Amyloid-Induced Neuronal Apoptosis. *Journal of Neuroscience Research* **65**, 45-53. https://doi.org/10.1002/jnr.1126.

Alnemri, E.S., Livingston, D.J., Nicholson, D.W., Salvesen, G., Thornberry, N.A., Wong, W.W., and Yuan, J. (1996). Human ICE/CED-3 Protease Nomenclature. *Cell*. 87, 171. https://doi.org/10.1016/S0092-8674(00)81334-3.

Avery, L., and Horvitz, R.H. (1987). A Cell That Dies during Wild-Type *C. elegans* Development Can Function as a Neuron in a *ced-3* Mutant. *Cell* **51**, 1071-1078. https://doi.org/10.1016/0092-8674(87)90593-9.

Basañez, G., Zhang, J., Chau, B.N., Maksaev, G.I., Frolov, V.A., Brandt, T.A., Burch, J., Hardwick, J.M., and Zimmerberg, J. 2001. Pro-Apoptotic Cleavage Products of Bcl-XL Form Cytochrome c-Conducting Pores in Pure Lipid Membranes*." *Journal of Biological Chemistry* **276**, 31083–91. https://doi.org/https://doi.org/10.1074/jbc.M103879200.

Bosch, T.C.G. and David, C.N. (1984). Growth Regulation in Hydra: Relationship between Epithelial Cell Cycle Length and Growth Rate. *Developmental Biology* **104**, 161-171. https://doi.org/10.1016/0012-1606(84)90045-9.

Brenner, S. (1973). The Genetics of Behaviour. *British Medical Bulletin* **29**, 269–71. https://doi.org/10.1093/oxfordjournals.bmb.a071019.

Brenner, S. 1974. The Genetics of *Caenorhabditis elegans. Genetics* **77**, 71–94. https://doi.org/10.1093/genetics/77.1.71.

Brière, J.J., Schlemmer, D., Chretien, D., and Rustin, P. (2004). Quinone Analogues Regulate Mitochondrial Substrate Competitive Oxidation. *Biochemical and Biophysical Research Communications* **316**, 1138–42. https://doi.org/10.1016/j.bbrc.2004.03.002.

Buechner, M. (2002). Tubes and the Single *C. elegans* Excretory Cell. *Trends in Cell Biology* **12**, 479-484. https://doi.org/10.1016/S0962-8924(02)02364-4.

Caron, E., and Hall, A. (1998). Identification of Two Distinct Mechanisms of Phagocytosis Controlled by Different Rho GTPases. *Science* **282,** 1717-1721. https://doi.org/10.1126/science.282.5394.1717.

Chan, S.L., Sue, W., Griffin, T., and Mattson, M.P. (1999). Evidence for Caspase-Mediated Cleavage of AMPA Receptor Subunits in Neuronal Apoptosis and Alzheimer's Disease. *Journal of Neuroscience Research* **57**, 315-323.

https://doi.org/10.1002/(sici)1097-4547(19990801)57:3<315::aid-jnr3>3.0.co;2-%23.

Chen, F., Hersh, B.M., Conradt, B., Zhou, Z., Riemer, D., Gruenbaum, Y., and Horvitz, H.R. (2000). Translocation of *C. elegans* CED-4 to Nuclear Membranes during Programmed Cell Death. *Science* **287**, 1485–89. https://doi.org/10.1126/science.287.5457.1485.

Chen, Y.Z, Mapes, J., Lee, E.S, Skeen-Gaar, R.R., and Xue, D. (2013). Caspase-Mediated Activation of Caenorhabditis ElegansCED-8 Promotes Apoptosis and Phosphatidylserine Externalization. *Nature Communications* **4,** 2726. https://doi.org/10.1038/ncomms3726

Cheng, E.H.Y., Kirsch, D.G., Clem, R.J., Ravi, R., Kastan, M.B., Bedi, A., Ueno, K., and Hardwick., J.M. (1997). Conversion of Bcl-2 to a Bax-like Death Effector by Caspases. *Science* **278**, 1966-1968. https://doi.org/10.1126/science.278.5345.1966.

Chien, S.C., Brinkmann, E.M., Teuliere, J., and Garriga, G. (2013). *Caenorhabditis elegans* PIG-1/MELK Acts in a Conserved PAR-4/LKB1 Polarity Pathway to Promote Asymmetric Neuroblast Divisions. *Genetics* **193,** 897-909. https://doi.org/10.1534/genetics.112.148106.

Chinnaiyan, A.M., O'Rourke, K., Lane, B.R., and Dixit, V.M. (1997). Interaction of CED-4 with CED-3 and CED-9: A Molecular Framework for Cell Death. *Science* **275,** 1122–26. https://doi.org/10.1126/science.275.5303.1122.

Chung, S., Gumienny, T.L., Hengartner, M.O., and Driscoll, M. (2000). A Common Set of Engulfment Genes Mediates Removal of Both Apoptotic and Necrotic Cell Corpses in *C. elegans*. *Nature Cell Biology* **2**, 931-937. https://doi.org/10.1038/35046585.

Clarke, P.G.H. and Clarke, S. (1996). Nineteenth Century Research on Naturally Occurring Cell Death and Related Phenomena. *Anatomy and Embryology* **193**, 81–99. https://doi.org/10.1007/BF00214700.

Conradt, B., and Horvitz, H.R. (1998). The *C. elegans* Protein EGL-1 Is Required for Programmed Cell Death and Interacts with the Bcl-2-like Protein CED-9. *Cell* **93**, 519–29. https://doi.org/10.1016/s0092-8674(00)81182-4.

Cordes, S., C. Frank, C.A., and Garriga, G. (2006). The *C. elegans* MELK Ortholog PIG-1 Regulates Cell Size Asymmetry and Daughter Cell Fate in Asymmetric Neuroblast Divisions. *Development* **133**, 2747-2756. https://doi.org/10.1242/dev.02447.

Cotman, C.W., Poon, W.W., Rissman, R.A., and Blurton-Jones, M. (2005). The Role of Caspase Cleavage of Tau in Alzheimer Disease Neuropathology **64**, 104-112. *Journal of Neuropathology and Experimental Neurology*. https://doi.org/10.1093/jnen/64.2.104.

Coucouvanis, E., and Martin, G.R. (1995). Signals for Death and Survival: A Two-Step

Mechanism for Cavitation in the Vertebrate Embryo. *Cell* **83**, 279-287. https://doi.org/10.1016/0092-8674(95)90169-8.

Cribbs, D.H., Poon, W.W., Rissman, R.A., and Blurton-Jones, M. 2004. Caspase-Mediated Degeneration in Alzheimer's Disease. *American Journal of Pathology* **165**, 353-355 https://doi.org/10.1016/S0002-9440(10)63302-0.

Degoeij, J.M., De Kluijver, A., Van Duyl, F.C., Vacelet, J., Wijffels, R.H., De Goeij, A.F., Cleutjens, J.P.M., and Schutte, B. (2009). Cell Kinetics of the Marine Sponge Halisarca Caerulea Reveal Rapid Cell Turnover and Shedding. *Journal of Experimental Biology* **212**, 3892-3900. https://doi.org/10.1242/jeb.034561.

Denning, D.P., Hatch, V., and Horvitz, H.R. (2012). Programmed Elimination of Cells by Caspase-Independent Cell Extrusion in *C. elegans*. *Nature* **488**, 226–30. https://doi.org/10.1038/nature11240.

Donaldson, J.G., and Jackson, C.L. (2000). Regulators and Effectors of the ARF GTPases. *Current Opinion in Cell Biology* **12**, 475-482. https://doi.org/10.1016/S0955-0674(00)00119-8.

Duan, H., Chinnaiyan, A.M., Hudson, P.L., Wing, J.P., He, W.W., and Dixit, V.M. (1996). ICE-LAP3, a Novel Mammalian Homologue of the *Caenorhabditis elegans* Cell Death Protein Ced-3 Is Activated during Fas- and Tumor Necrosis Factor-Induced Apoptosis. *Journal of Biological Chemistry* **271**, 1621–25. https://doi.org/10.1074/jbc.271.3.1621.

Dwivedi, V.K., Pardo-Pastor, C., Droste, R., Kong, J.N., Tucker, N., Denning, D.P., Rosenblatt, J., and Horvitz, H.R. (2021). Replication Stress Promotes Cell Elimination by Extrusion. *Nature* **593**, 591–96. https://doi.org/10.1038/s41586-021-03526-y.

Eijnde, S. M., Van Den, L., Boshart, E. H., Baehrecke, C. I., De Zeeuw, C., Reutelingsperger, P.M., and Vermeij-Keers, C. (1998). Cell Surface Exposure of Phosphatidylserine during Apoptosis Is Phylogenetically Conserved. *Apoptosis* **3**, 9-16. https://doi.org/10.1023/A:1009650917818.

Eisenhoffer, G.T., Loftus, P.D., Yoshigi, M., Otsuna, H., Chien, C.B., Morcos, P.A.,. and Rosenblatt, J. (2012). Crowding Induces Live Cell Extrusion to Maintain Homeostatic Cell Numbers in Epithelia. *Nature* **484**, 546–49. https://doi.org/10.1038/nature10999.

Eisenhoffer, G.T., and Rosenblatt, J. (2013). Bringing Balance by Force: Live Cell Extrusion Controls Epithelial Cell Numbers. *Trends in Cell Biology* 23, 185-192 https://doi.org/10.1016/j.tcb.2012.11.006.

Ellis, H.M., and Horvitz, H.R. (1986). Genetic Control of Programmed Cell Death in the Nematode *C. elegans*. *Cell* **44,** 817–29. https://doi.org/https://doi.org/10.1016/0092-8674(86)90004-8.

Ellis, R.E., and Horvitz, H.R. (1991). Two *C. elegans* Genes Control the Programmed Deaths of Specific Cells in the Pharynx. *Development* **112**, 591–603. https://doi.org/10.1242/dev.112.2.591.

Ellis, R.E., Jacobson, D.M., and Horvitz, H.R. (1991). Genes Required for the Engulfment of Cell Corpses during Programmed Cell Death in *Caenorhabditis elegans*. *Genetics* **129**, 79-94. https://doi.org/10.1093/genetics/129.1.79.

Fadok, V.A., Bratton, D.L., Frasch, S.C., Warner, M.L., and Henson, P.M. (1998). The Role of Phosphatidylserine in Recognition of Apoptotic Cells by Phagocytes. *Cell* **5**, 551-562. *Death and Differentiation*. https://doi.org/10.1038/sj.cdd.4400404.

Fadok, V.A., De Cathelineau, A., Daleke, D.L., Henson, P.M., and Bratton, D.L. (2001). Loss of Phospholipid Asymmetry and Surface Exposure of Phosphatidylserine Is Required for Phagocytosis of Apoptotic Cells by Macrophages and Fibroblasts. *Journal of Biological Chemistry* **276**, 1071-1077. https://doi.org/10.1074/jbc.M003649200.

Fletcher, J. I., and Huang, D.C.S. (2006). BH3-Only Proteins: Orchestrating Cell Death. *Cell Death and Differentiation* **13**, 1268-1271. https://doi.org/10.1038/sj.cdd.4401995.

Flores-Romero, H., Landeta, O., Ugarte-Uribe, B., Cosentino, K., García-Porras, M., García-Sáez, A.J., and Basañez, G. (2019). BFL1 Modulates Apoptosis at the Membrane Level through a Bifunctional and Multimodal Mechanism Showing Key Differences with BCLXL. *Cell Death and Differentiation* 26, 1880–94. https://doi.org/10.1038/s41418-018-0258-5.

Frank, C. A., Hawkins, N.C., Guenther, C., Horvitz, H.R., and Garriga, G. (2005). *C. elegans* HAM-1 Positions the Cleavage Plane and Regulates Apoptosis in Asymmetric Neuroblast Divisions. *Developmental Biology* **284**, 301-310. https://doi.org/10.1016/j.ydbio.2005.05.026.

Fuchs, Y., and Steller, H. (2011). Programmed Cell Death in Animal Development and Disease. *Cell* **147**, 742-758. https://doi.org/10.1016/j.cell.2011.10.033.

Garcia-Martinez, V.,Macias, C., Ganan, Y., Garcia-Lobo, J.M., Francia, M.V., Fernandez-Teran, M.A., and Hurle, J.M. (1993). Internucleosomal DNA Fragmentation and Programmed Cell Death (Apoptosis) in the Interdigital Tissue of the Embryonic Chick Leg Bud. *Journal of Cell Science* **106**, 201-208. https://doi.org/10.1242/jcs.106.1.201.

Gastard, M.C., Troncoso, J.C., and Koliatsos, V.E. (2003). Caspase Activation in the Limbic Cortex of Subjects with Early Alzheimer's Disease. *Annals of Neurology* **54**, 393-398. https://doi.org/10.1002/ana.10680.

Glücksmann, A. (1951). Cell Deaths in Normal Vertebrate Ontology. *Biological Reviews* **26**, 59-86. https://doi.org/10.1111/j.1469-185X.1951.tb00774.x.

Gu, Y., Forostyan, T., Sabbadini, R., and Rosenblatt, J. (2011). Epithelial Cell Extrusion Requires the Sphingosine-1-Phosphate Receptor 2 Pathway. *Journal of Cell Biology* **193**, 667-676. https://doi.org/10.1083/jcb.201010075.

Gu, Y., Shea, J., Slattum, G., Firpo, M.A., Alexander, M., Golubovskaya, V.M., and Rosenblatt, J. (2015). Defective Apical Extrusion Signaling Contributes to Aggressive Tumor Hallmarks. *ELife* **4**. https://doi.org/10.7554/eLife.04069.

Guenther, C., and Garriga, G. (1996). Asymmetric Distribution of the *C. elegans* HAM-1 Protein in Neuroblasts Enables Daughter Cells to Adopt Distinct Fates. *Development* **122**, 3509–18. https://doi.org/10.1242/dev.122.11.3509.

Gumienny, T.L., Brugnera, E., Tosello-Trampont, A.C., Kinchen, J.M., Haney, L.B., Nishiwaki, K., Walk, S.F., Nemergut, M.E., Macara, I.G., Francis, R., Schedl, T., Qin, Y., Van Aelst, L., Hengartner, M.O., and Ravichandran, K.S. (2001). CED-12/ELMO, a Novel Member of the CrkII/Dock180/Rac Pathway, Is Required for Phagocytosis and Cell Migration. *Cell* **107**, 27-41. https://doi.org/10.1016/S0092-8674(01)00520-7.

Gurling, M., Talavera, K., and Garriga, G. (2014). The DEP Domain-Containing Protein TOE-2 Promotes Apoptosis in the Q Lineage of *C. elegans* through Two Distinct Mechanisms. *Development* **141**, 2724–34. https://doi.org/10.1242/dev.110486.

Hamburger, V., Brunso-Bechtold, J.K., and Yip, J.W. (1981). Neuronal Death in the Spinal Ganglia of the Chick Embryo and Its Reduction by Nerve Growth Factor. *Journal of Neuroscience* **1**, 60-71. https://doi.org/10.1523/jneurosci.01-01-00060.1981.

Hedgecock, E.M., Sulston, J.E., and Thomson, J.N. (1983). Mutations Affecting Programmed Cell Deaths in the Nematode *Caenorhabditis elegans. Science* **220**, 1277–79. https://doi.org/10.1126/science.6857247.

Hengartner, M.O. (2000). The Biochemistry of Apoptosis. *Nature* **407**, 770–776. https://doi.org/10.1038/35037710.

Hengartner, M.O., Ellis, R.E., and Horvitz, H.R. (1992). *Caenorhabditis elegans* Gene *ced-9* Protects Cells from Programmed Cell Death. *Nature* **356**, 494-499. https://doi.org/10.1038/356494a0

Hengartner, M.O., and Horvitz, H.R. (1994). *C. elegans* Cell Survival Gene *ced-9* Encodes a Functional Homolog of the Mammalian Proto-Oncogene Bcl-2. *Cell* **76**, 665-676. https://doi.org/10.1016/0092-8674(94)90506-1.

Henson, P.M, and Hume, D.A. (2006). Apoptotic Cell Removal in Development and Tissue Homeostasis. *Trends in Immunology* **27**, 244-250. https://doi.org/10.1016/j.it.2006.03.005.

Hipfner, D.R., and Cohen, S.M. (2004). Connecting Proliferation and Apoptosis in Development and Disease. *Nature Reviews Molecular Cell Biology* **5**, 805–815. https://doi.org/10.1038/nrm1491.

Robert, H.R. and Herskowitz, I. (1992). Mechanisms of Asymmetric Cell Division: Two Bs or Not Two Bs, That Is the Question. *Cell* **68**, 237-255. https://doi.org/10.1016/0092-8674(92)90468-R.

Huang, W., Jiang, T., Choi, W., Qi, S., Pang, Y., Hu, Q., Xu, Y., Gong, X., Jeffrey, P.D., Wang, J., Shi, Y. (2013). Mechanistic Insights into CED-4-Mediated Activation of CED-3. *Genes and Development* **27**, 2039-2048. https://doi.org/10.1101/gad.224428.113.

Hyman, B.T., and Yuan, J. (2012). Apoptotic and Non-Apoptotic Roles of Caspases in Neuronal Physiology and Pathophysiology. *Nature Reviews Neuroscience* **13,** 395-406. https://doi.org/10.1038/nrn3228.

Jacobson, M.D., Weil, M., and Raff, M.C. (1997). Programmed Cell Death in Animal Development. *Cell* 88, 347–54. https://doi.org/10.1016/s0092-8674(00)81873-5.

Kale, J., Osterlund, E.J., and Andrews, D.W. (2018). BCL-2 Family Proteins: Changing Partners in the Dance towards Death. *Cell Death and Differentiation* **25**, 65–80. https://doi.org/10.1038/cdd.2017.186.

Kerr, J.F.R., Wyllie, A.H., and Currie, A.R. (1972). Apoptosis: A Basic Biological Phenomenon with Wide-Ranging Implications in Tissue Kinetics. *British Journal of Cancer* **26**, 239-257. https://doi.org/10.1038/bjc.1972.33.

Kiyokawa, E., Hashimoto, Y., Kobayashi, S., Sugimura, H., Kurata, T., and Matsuda, M. (1998). Activation of Rac1 by a Crk SH3-Binding Protein, DOCK180. *Genes and Development* **12**, 3331-3336. https://doi.org/10.1101/gad.12.21.3331.

Kiyokawa, E., Hashimoto, Y., Kurata, T., Sugimura, H., and Matsuda, M. (1998). Evidence That DOCK180 Up-Regulates Signals from the CrkII-P130(Cas) Complex. *Journal of Biological Chemistry* **273**, 24479-24484. https://doi.org/10.1074/jbc.273.38.24479.

Kluck, R.M., Bossy-Wetzel, E., Green, D.R., and Newmeyer, D.D. (1997). The Release of Cytochrome c from Mitochondria: A Primary Site for Bcl- 2 Regulation of Apoptosis. *Science* **275**, 1132–36. https://doi.org/10.1126/science.275.5303.1132.

Koç, A., Wheeler, L.J., Mathews, C.K., and Merrill, G.F. (2004). Hydroxyurea Arrests DNA Replication by a Mechanism That Preserves Basal DNTP Pools. *Journal of Biological Chemistry* **279**, 223-230. https://doi.org/10.1074/jbc.M303952200.

Li, P., Nijhawan, D., Budihardjo, I., Srinivasula, S.M., Ahmad, M., Alnemri, E.S., and Wang, X. (1997). Cytochrome c and DATP-Dependent Formation of Apaf-1/Caspase-9

Complex Initiates an Apoptotic Protease Cascade. *Cell* **91**, 479-489. https://doi.org/10.1016/S0092-8674(00)80434-1.

Lin, B., Kolluri, S.K., Lin, F., Liu, W., Han, Y., Cao, X., Dawson, M.I., Reed, J.C., and Zhang, X. (2004). Conversion of Bcl-2 from Protector to Killer by Interaction with Nuclear Orphan Receptor Nur77/TR3. *Cell* **116**, 527–40. https://doi.org/https://doi.org/10.1016/S0092-8674(04)00162-X.

Liu, Q.A., and Hengartner, M.O. (1998). Candidate Adaptor Protein CED-6 Promotes the Engulfment of Apoptotic Cells in *C. elegans*. *Cell* **93**, 961-972. https://doi.org/10.1016/S0092-8674(00)81202-7.

Liu, X., Kim, C.N, Yang, J., Jemmerson, R., and Wang, X. (1996). Induction of Apoptotic Program in Cell-Free Extracts: Requirement for dATP and Cytochrome c. *Cell* **86**, 147-157. https://doi.org/10.1016/S0092-8674(00)80085-9.

Liu, Z.G, Smith, S.W., McLaughlin, K.A., Schwartz, L.M., and Osborne, B.A. (1994). Apoptotic Signals Delivered through the T-Cell Receptor of a T-Cell Hybrid Require the Immediate-Early Gene Nur77. *Nature* **367**, 281–284. https://doi.org/10.1038/367281a0.

Levine, B., Sinha, S., and Kroemer, G. (2008). BCL-2 family members. *Autophagy* **4**, 600–606 https://doi: 10.4161/auto.6260.

Lockshin, R.A., and Williams, C.M. (1964). Programmed Cell Death-II. Endocrine Potentiation of the Breakdown of the Intersegmental Muscles of Silkmoths. *Journal of Insect Physiology* **10**, 643-649. https://doi.org/10.1016/0022-1910(64)90034-4.

Lomonosova, E., and Chinnadurai, G. (2008). BH3-Only Proteins in Apoptosis and beyond: An Overview. *Oncogene* **27**, 2-19. https://doi.org/10.1038/onc.2009.39.

Mapes, J., Chen, Y.Z., Kim, A., Mitani, S., Kang, B.H., and Xue, D. (2012). CED-1, CED-7, and TTR-52 Regulate Surface Phosphatidylserine Expression on Apoptotic and Phagocytic Cells. *Current Biology* **22**, 1267-1275. https://doi.org/10.1016/j.cub.2012.05.052.

Martin, S.J., Reutelingsperger, C.P.M., McGahon, A.J., Rader, J.A., Van Schie, R.C.A.A., LaFace, D.M., and Green, D.R. (1995). Early Redistribution of Plasma Membrane Phosphatidylserine Is a General Feature of Apoptosis Regardless of the Initiating Stimulus: Inhibition by Overexpression of BCL-2 and Abl. *Journal of Experimental Medicine* **182**, 1545-1556. https://doi.org/10.1084/jem.182.5.1545.

Mason, K.D., Lin, A., Robb, L., Josefsson, E.C., Henley, K.J., Gray, D.H.D., Kile, B.T., Roberts, A.W., Strasser, A., Huang, D.C.S., Waring, P., and O'Reilly, L.A. (2013). Proapoptotic Bak and Bax Guard against Fatal Systemic and Organ-Specific Autoimmune Disease. *Proceedings of the National Academy of Sciences* **110**, 2599-

2604. https://doi.org/10.1073/pnas.1215097110.

Massol, P., Montcourrier, P., Guillemot, J.C., and Chavrier, P. (1998). Fc Receptor-Mediated Phagocytosis Requires CDC42 and Rac1. *EMBO Journal* **17,** 6219-6229. https://doi.org/10.1093/emboj/17.21.6219.

Mathai, J.P., Germain, M., Marcellus, R.C., and Shore, G.C. (2002). Induction and Endoplasmic Reticulum Location of Bik/Nbk in Response to Apoptotic Signaling by E1a and P53. *Oncogene* **21**, pages 2534–2544. https://doi.org/10.1038/sj.onc.1205340.

Matsui, T., Ramasamy, K., Ingelsson, M., Fukumoto, H., Conrad, C., Frosch, M.P., Irizarry, M.C., Yuan, J., and Hyman, B.T. (2006). Coordinated Expression of Caspase 8, 3 and 7 MRNA in Temporal Cortex of Alzheimer Disease: Relationship to Formic Acid Extractable Aβ42 Levels. *Journal of Neuropathology and Experimental Neurology* **65**, 508-515. https://doi.org/10.1097/01.jnen.0000229238.05748.12.

Mori, C., Nakamura, N., Kimura, S., Irie, H., Takigawa, T., and Shiota, K. (1995). Programmed Cell Death in the Interdigital Tissue of the Fetal Mouse Limb Is Apoptosis with DNA Fragmentation. *The Anatomical Record* **242**, 103-110. https://doi.org/10.1002/ar.1092420114.

Nagata, S. (1997). Apoptosis by Death Factor. *Cell* **88**, 355-365. https://doi.org/10.1016/S0092-8674(00)81874-7.

Nehme, R., Grote, P., Tomasi, T., Löser, S., Holzkamp,H., Schnabel, R., and Conradt, B. (2010). Transcriptional Upregulation of Both *egl-1* BH3-Only and *ced-3* Caspase Is Required for the Death of the Male-Specific CEM Neurons. *Cell Death and Differentiation* **17**, 1266-1276. https://doi.org/10.1038/cdd.2010.3.

Nolan, K.M., Barrett, K., Lu, Y., Hu, K.Q., Vincent, S., and Settleman, J. (1998). Myoblast City, the Drosophila Homolog of DOCK180/CED-5, Is Required in a Rac Signaling Pathway Utilized for Multiple Developmental Processes. *Genes and Development* **12**, 3337-3342. https://doi.org/10.1101/gad.12.21.3337.

Ou, G., Stuurman, N., D'Ambrosio, M., and Vale, R.D. (2010). Polarized Myosin Produces Unequal-Size Daughters During Asymmetric Cell Division. *Science* **330,** 673–77. https://doi.org/10.1126/science.1193220.

Potten, C.S. (1998). Stem Cells in Gastrointestinal Epithelium: Numbers, Characteristics and Death. *Philosophical Transactions of the Royal Society B: Biological Sciences* **353**, 1151-1162. https://doi.org/10.1098/rstb.1998.0246.

Qi, S., Pang, Y., Hu, Q., Liu, Q., Li, H., Zhou, Y., He, T., Liang, Q., Liu, Y., Yuan, X., Luo, G., Li, H., Wang, J., Yan, N., and Shi, Y. (2010) Crystal Structure of the *Caenorhabditis elegans* Apoptosome Reveals an Octameric Assembly of CED-4. *Cell* **141,** 446–57. https://doi.org/10.1016/j.cell.2010.03.017.

Rabkin, C.S., Hirt, C., Janz, S., and Dölken, G. (2008). T(14;18) Translocations and Risk of Follicular Lymphoma. *British Journal of Hematology* **194**, 810-821. https://doi.org/10.1093/jncimonographs/lgn002.

Reddien, P.W., and Horvitz, H.R. (2000). CED-2/CrkII and CED-10/Rac Control Phagocytosis and Cell Migration in *Caenorhabditis elegans*. *Nature Cell Biology* **2**, 131-136. https://doi.org/10.1038/35004000.

Rosenblatt, J., Raff, M.C., and Cramer, L.P. (2001). An Epithelial Cell Destined for Apoptosis Signals Its Neighbors to Extrude It by an Actin- and Myosin-Dependent Mechanism. *Current Biology* **11**, 1847-1857. https://doi.org/10.1016/S0960-9822(01)00587-5.

Saunders, J.W. (1966). Death in Embryonic Systems. *Science* **154**, 604-612. https://doi.org/10.1126/science.154.3749.604.

Shaham, S., and Horvitz, H.R. (1996). Developing *Caenorhabditis elegans* Neurons May Contain Both Cell-Death Protective and Killer Activities. *Genes and Development* **10**, 578-591. https://doi.org/10.1101/gad.10.5.578.

Singhvi, A., Teuliere, J., Talavera, K., Cordes, S., Ou, G., Vale, R.D., Prasad, B.C., Clark, S.G., and Garriga, G. (2011). The Arf GAP CNT-2 Regulates the Apoptotic Fate in *C. elegans* Asymmetric Neuroblast Divisions. *Current Biology* **21**, 948-954. https://doi.org/10.1016/j.cub.2011.04.025

Slattum, G., McGee, K.M., and Rosenblatt, J. (2009). P115 RhoGEF and Microtubules Decide the Direction Apoptotic Cells Extrude from an Epithelium. *Journal of Cell Biology* 186, 693-702. https://doi.org/10.1083/jcb.200903079.

Spector, M.S., Desnoyers, S., Hoeppner, D.J., and Hengartner, M.O. (1997). Interaction between the *C. elegans* Cell-Death Regulators CED-9 and CED-4. *Nature* **385**, 653–56. https://doi.org/10.1038/385653a0.

Su, H.P., Nakada-Tsukui, K., Tosello-Trampont, A.C., Li, Y., Bu, G., Henson, P.M., and Ravichandran, K.S. (2002). Interaction of CED-6/GULP, an Adapter Protein Involved in Engulfment of Apoptotic Cells with CED-1 and CD91/Low Density Lipoprotein Receptor-Related Protein (LRP). *Journal of Biological Chemistry* **277**, 11772-11779. https://doi.org/10.1074/jbc.M109336200.

Sulston, J.E., Schierenberg, E., White, J.G., and Thomson, J.N. (1983). The Embryonic Cell Lineage of the Nematode *Caenorhabditis elegans*. *Developmental Biology* 100, 64-119. https://doi.org/10.1016/0012-1606(83)90201-4.

Sulston, J.E., and Horvitz, H.R. (1977). Post-Embryonic Cell Lineages of the Nematode, *Caenorhabditis elegans*. *Developmental Biology* **56,** 110–56.

https://doi.org/10.1016/0012-1606(77)90158-0.

Suzuki, J., Denning, D.P., Imanishi, E., Horvitz, H.R., and Nagata, S. (2013). Xk-Related Protein 8 and CED-8 Promote Phosphatidylserine Exposure in Apoptotic Cells. *Science* **341**, 403-406. https://doi.org/10.1126/science.1236758.

Takeuchi, O., Fisher, J., Suh, H., Harada, H., Malynn, B.A., and Korsmeyer, S.J. (2005). Essential Role of BAX, BAK in B Cell Homeostasis and Prevention of Autoimmune Disease. *Proceedings of the National Academy of Sciences of the United States of America* **102**, 11272-11277. https://doi.org/10.1073/pnas.0504783102.

Taylor, R.C., Brumatti, G., Ito, S., Hengartner, M.O., Derry, W.B., and Martin, S.J. (2007). Establishing a Blueprint for CED-3-Dependent Killing through Identification of Multiple Substrates for This Protease. *Journal of Biological Chemistry* **282**, 15011-15021. https://doi.org/10.1074/jbc.M611051200.

Teuliere, J., Cordes, S., Singhvi, A., Talavera, K., and Garriga, G. (2014). Asymmetric Neuroblast Divisions Producing Apoptotic Cells Require the Cytohesin GRP-1 in *Caenorhabditis elegans*. *Genetics* 198, 229–47. https://doi.org/10.1534/genetics.114.167189.

Trent, C., Tsuing, N., and Horvitz, H.R. (1983). Egg-Laying Defective Mutants of the Nematode *Caenorhabditis elegans*. *Genetics* **104**, 619-647. https://doi.org/10.1093/genetics/104.4.619.

Tzur, Y.B., Margalit, A., Melamed-Book, N., and Gruenbaum, Y. (2006). Matefin/SUN-1 Is a Nuclear Envelope Receptor for CED-4 during *Caenorhabditis elegans* Apoptosis. *Proceedings of the National Academy of Sciences of the United States of America* **103**, 13397-13402. https://doi.org/10.1073/pnas.0604224103.

Vaux, D.L., Cory, S., and Adams, J.M. (1988). Bcl-2 Gene Promotes Haemopoietic Cell Survival and Cooperates with c-Myc to Immortalize Pre-B Cells. *Nature* 335, 440-442 https://doi.org/10.1038/335440a0.

Vermes, I., Haanen, C., Steffens-Nakken, H., and Reutellingsperger, C. (1995). A Novel Assay for Apoptosis Flow Cytometric Detection of Phosphatidylserine Expression on Early Apoptotic Cells Using Fluorescein Labelled Annexin V. *Journal of Immunological Methods* **184**, 39-51. https://doi.org/10.1016/0022-1759(95)00072-I.

Villunger, A., Michalak, E.M., Coultas, L., Müllauer, F., Böck, G., Ausserlechner, M.J., Adams, J.M., and Strasser, A. (2003). p53- and Drug-Induced Apoptotic Responses Mediated by BH3-Only Proteins Puma and Noxa. *Science* **302**, 1036-1038. https://doi.org/10.1126/science.1090072.

Wang, J., and Lenardo, M.J. (2000). Roles of Caspases in Apoptosis, Development, and Cytokine Maturation Revealed by Homozygous Gene Deficiencies. *Journal of Cell*

Science **113**, 753-757. https://doi.org/10.1242/jcs.113.5.753.

Watson, A.J.M., Duckworth, C.A., Guan, Y., and Montrose, M.H. (2009). Mechanisms of Epithelial Cell Shedding in the Mammalian Intestine and Maintenance of Barrier Function. *Annals of the New York Academy of Sciences* **1165**, 135-142. https://doi.org/10.1111/j.1749-6632.2009.04027.x.

Wong, R.S.Y. (2011). Apoptosis in Cancer: From Pathogenesis to Treatment. *Journal of Experimental and Clinical Cancer Research* **30**, 87. https://doi.org/10.1186/1756-9966-30-87.

Woronicz, J.D., Calnan, B., Ngo, V., and Winoto, A. (1994). Requirement for the Orphan Steroid Receptor Nur77 in Apoptosis of T-Cell Hybridomas. *Nature* **367**, 277-281. https://doi.org/10.1038/367277a0.

Wu, D., Wallen, H.D., Inohara,N., and Nuñez, G. (1997). Interaction and Regulation of the *Caenorhabditis elegans* Death Protease CED-3 by CED-4 and CED-9. *Journal of Biological Chemistry* **272**, 21449-21454. https://doi.org/10.1074/jbc.272.34.21449.

Wu, Y.C., and Horvitz, H.R. (1998a). *C. elegans* Phagocytosis and Cell-Migration Protein CED-5 Is Similar to Human DOCK180. *Nature* **392**, 501-504. https://doi.org/10.1038/33163.

Wu, Y.C., and Horvitz, H.R. (1998b). The *C. elegans* Cell Corpse Engulfment Gene Ced-7 Encodes a Protein Similar to ABC Transporters. *Cell* **93**, 951-960. https://doi.org/10.1016/S0092-8674(00)81201-5.

Wyllie, A.H. (1980). Glucocorticoid-Induced Thymocyte Apoptosis Is Associated with Endogenous Endonuclease Activation. *Nature* **284**, 555–556. https://doi.org/10.1038/284555a0.

Xia, Z., Dickens, M., Raingeaud, J., Davis, R.J., and Greenberg, M.E. (1995). Opposing Effects of ERK and JNK-P38 MAP Kinases on Apoptosis. *Science* **270**, 1326-1331. https://doi.org/10.1126/science.270.5240.1326.

Xue, D., Shaham, S., and Horvitz, H.R. (1996). The *Caenorhabditis elegans* Cell-Death Protein CED-3 Is a Cysteine Protease with Substrate Specificities Similar to Those of the Human CPP32 Protease. *Genes and Development* **10**, 1073-1083. https://doi.org/10.1101/gad.10.9.1073.

Xue, D., and Horvitz, H.R. (1997). *Caenorhabditis elegans* CED-9 Protein Is a Bifunctional Cell-Death Inhibitor. *Nature* **390**, 305–8. https://doi.org/10.1038/36889.

Yan, N., Chai, J., Eui, S.L., Gu, L., Liu, Q., He, J., Wu, J.W., Kokel, D., Li, H., Hao, Q., Xue, D., and Shi, Y. (2005). Structure of the CED-4-CED-9 Complex Provides Insights into Programmed Cell Death in *Caenorhabditis elegans*. *Nature* **437**, 831–37.

https://doi.org/10.1038/nature04002.

Yan, N., Gu, L., Kokel, D., Chai, J., Li, W., Han, A., Chen, L., Xue, D., and Shi, Y. (2004). Structural, Biochemical, and Functional Analyses of CED-9 Recognition by the Proapoptotic Proteins EGL-1 and CED-4. *Molecular Cell* **15**, 999-1006. https://doi.org/10.1016/j.molcel.2004.08.022.

Yan, N., Xu, Y., and Shi, Y. (2006). 2:1 Stoichiometry of the CED-4-CED-9 Complex and the Tetrameric CED-4: Insights into the Regulation of CED-3 Activation. *Cell Cycle* **5**, 31-34. https://doi.org/10.4161/cc.5.1.2263.

Yang, J., Liu, X., Bhalla, K., Kim, C.N., Ibrado, A.M., Cai, J., Peng, T.I., Jones, D.P., and Wang, X. (1997). Prevention of Apoptosis by Bcl-2: Release of Cytochrome c from Mitochondria Blocked. *Science* **275**, 1129–32. https://doi.org/10.1126/science.275.5303.1129.

Youle, R.J., and Strasser, A. (2008). The BCL-2 Protein Family: Opposing Activities That Mediate Cell Death. *Nature Reviews Molecular Cell Biology* **9**, 47-59. https://doi.org/10.1038/nrm2308.

Yuan, J., and Horvitz, H.R. (1990). The *Caenorhabditis elegans* Genes *ced-3* and *ced-4* Act Cell Autonomously to Cause Programmed Cell Death. *Developmental Biology* **138**, 33-41. https://doi.org/10.1016/0012-1606(90)90174-H.

Yuan, J., Shaham, S., Ledoux, S., Ellis, H.M., and Horvitz, H.R. (1993). The *C. elegans* Cell Death Gene *ced-3* Encodes a Protein Similar to Mammalian Interleukin-1β-Converting Enzyme. *Cell* **75**, 641-652. https://doi.org/10.1016/0092-8674(93)90485-9.

Zhou, Z., Hartwieg, E., and Horvitz, H.R. (2001). CED-1 Is a Transmembrane Receptor That Mediates Cell Corpse Engulfment in *C. elegans*. *Cell* **104**, 43-56. https://doi.org/10.1016/S0092-8674(01)00190-8.

Zou, H., Henzel, W.J., Liu, X., Lutschg, A., and Wang, X. (1997). Apaf-1, a Human Protein Homologous to *C. elegans* CED-4, Participates in Cytochrome c-Dependent Activation of Caspase-3. *Cell* **90**, 405-413. https://doi.org/10.1016/S0092-8674(00)80501-2.

Chapter Two

The Pro-Apoptotic Function of the *C. elegans* BCL-2 homolog CED-9 Requires Interaction with the APAF-1 Homolog CED-4

Nolan Tucker, Peter Reddien, Bradley Hersh and H. Robert Horvitz

I collected all of the data described in this chapter including all cell counts, generation of strains via CRISPR, and biochemical assays. Peter Reddien isolated the two original strains that inspired this work *ced-9(n3377)* and *ced-4(n5611 n3392)* via EMS, and Bradley Hersh made the initial observation that *ced-9(n3377)* prevents CED-4 localization to mitochondria via an anti-CED-4 polyclonal antibody, generated by Bradley Hersh and used in this study.

Abstract

Apoptotic cell death is required for animal development and tissue homeostasis. In *Caenorhabditis elegans* apoptosis is inhibited by the BCL-2 homolog CED-9. In addition to its canonical anti-apoptotic role, CED-9 possesses an apparent pro-apoptotic function – in certain circumstances, a loss-of CED-9 function can result in decreased rather than increased cell death. This pro-apoptotic function of CED-9 is poorly understood. CED-9 has been thought to inhibit apoptosis by binding to and inhibiting the pro-apoptotic protein CED-4, the *C. elegans* homolog of APAF-1. In this work we show that mutations in either CED-9 or CED-4 located in their CED-9-CED-4 binding regions as defined by X-ray crystallography reduce apoptosis, i.e. disrupt the pro-apoptotic function of CED-9, without affecting the anti-apoptotic function of CED-9. We further show that these mutant CED-9 and CED-4 proteins are defective in CED-9-CED-4 interaction *in vivo*. These data indicate that the known CED-9-CED-4 interaction is required for the pro-apoptotic function of CED-9 but is dispensable for its anti-apoptotic function. Given the high evolutionary conservation of cell-death genes, we suggest that similar interactions between human anti-apoptotic CED-9/BCL-2 family members and APAF-1 might promote apoptotic cell death and play important roles in human diseases that involve disruptions in apoptosis, such as certain neurodegenerative disorders and cancers.

Introduction

Programmed cell death is an evolutionarily conserved process essential for proper development and tissue homeostasis in metazoans[1,2]. In humans, either excessive or insufficient cell death can result in diseases, including cancers and certain

autoimmune and neurodegenerative disorders[3,4,5]. In *Caenorhabditis elegans*, four genes – *egl-1, ced-9, ced-4, and ced-3* – are primarily responsible for the control of apoptotic cell death[6,7,8]. It has been proposed based on genetic, protein interaction, and localization studies that CED-9 (a homolog of mammalian BCL-2) protects cells from apoptosis by sequestering the pro-apoptotic protein CED-4 (APAF-1 in mammals) to mitochondria[9,10,11]. According to this model, in cells fated to die, EGL-1 (a BH3-only member of the Bcl-2 superfamily) binds CED-9, causing a conformational change in CED-9 that results in the release of CED-4[12]. After its release from CED-9, CED-4 localizes to the perinuclear membrane where it activates the caspase CED-3[10,11]. A strong *ced-9* loss-of-function mutation leads to maternal-effect lethality, presumably as a consequence of excessive cell death, and animals carrying loss-of-function mutations in both *ced-9* and a cell-death promoting gene – either *ced-4* or *ced-3* – are viable because cell death is prevented. However, and counter-intuitively, a loss-of-function mutation in *ced-9* can enhance the partial cell-death defect of animals with a weak loss-of-function mutation in the pro-apoptotic caspase gene *ced-3*[13]. This finding suggests that in addition to its anti-apoptotic role, CED-9 possesses an pro-apoptotic function.

The existence of a pro-apoptotic function of CED-9 implies that the canonical model for *C. elegans* cell death, in which CED-9 functions only as an anti-apoptotic protein, is incomplete. Furthermore, the canonical model proposes that in living cells, cell death is blocked by the CED-9-dependent sequestration of CED-4 to mitochondria. However, in *ced-9(n1653ts)* mutant animals – which carry a temperature-sensitive allele that (like *ced-9(0)* alleles) causes lethality at non-permissive temperatures but (like *ced-9(+)* and weak *ced-9(lf,* loss-of-function*)* alleles) at permissive temperatures

allows viability – at a permissive temperature some CED-4 protein is localized to the perinuclear membrane, as assayed by anti-CED-4 polyclonal antibody localization[9]. This observation suggests that CED-4 localization at the perinuclear membrane is not sufficient to drive apoptosis. In addition, despite the ability of *ced-9(lf)* alleles to enhance ectopic cell-survival caused by weak-loss-of function alleles in the cell-death promoting *ced-3* gene, loss-of *ced-9* function in the presence of a weak *ced-3* loss-of-function mutation results in CED-4 localization to the perinuclear membrane[9], again uncoupling CED-4 localization at the perinuclear membrane from the activation of apoptotic death. In short, these observations suggest that CED-4 localization at the perinuclear membrane is not sufficient to cause cell death.

Here we report that mutations in the known CED-9-CED-4 binding region cause a loss of the pro- but not the anti-apoptotic function of CED-9. In addition, these mutations prevent the CED-9-dependent sequestration of CED-4 to mitochondria. Our results suggest that – opposite to the canonical model for *C. elegans* cell death in which CED-9-CED-4 interaction and consequent CED-4 mitochondrial localization are anti-apoptotic – a CED-9-CED-4 interaction and possibly CED-4 mitochondrial localization are required for the pro-apoptotic function of CED-9. Since *C. elegans* cell-death genes show striking homology to mammalian cell-death genes[13,14,15,16], these findings have implications for our understanding of the functions of mammalian BCL-2 family members in cell death and how perturbation of their functions can affect human diseases, including certain neurogenerative disorders and cancers.

Results

CED-9 possesses a pro-apoptotic function.

The canonical model of *C. elegans* apoptosis positions CED-9 as an anti-apoptotic protein, preventing apoptosis through mitochondrial sequestration of the pro-apoptotic CED-4 protein (Fig. 1A, B). *ced-9(lf)* mutations cause maternal-effect lethality, presumably via excessive apoptosis given that mutations in downstream cell-death genes – *ced-3* and *ced-4* – suppress this lethality. However, *ced-9(lf)* mutations can enhance the cell-death defect caused by a weak loss-of-function mutation in either *ced-3* or *ced-4*[13], indicating the existence of some poorly understood pro-apoptotic role for CED-9. One example of such an enhancement of a cell-death defect by *ced-9(lf)* mutations involves cells in the ventral nervous system. In wild-type animals, six VC neurons (P3-8.aap) survive and express the GFP reporter *nIs106[P_{lin-11}::GFP]*, whereas six VC homologs (P1-2,9-12.aap) undergo apoptosis[17]. In mutants carrying a null allele of either *ced-3* or *ced-4,* the six VC homologs that normally die instead survive and differentiate to express characteristics of the VC neurons[18], including expression of the *P_{lin-11}::GFP* reporter; five of these six “undead” VC neurons can be reliably scored using this GFP reporter. Whereas *ced-3* null mutants show ectopic survival of about 5 extra cells, animals carrying a weak loss-of-function allele of *ced-3, ced-3(n2427),* show ectopic survival of roughly 1.7 extra VC-like cells on average[19] (Fig. 1C, D). By contrast, when *ced-3(n2427)* is paired with the *ced-9* null allele *ced-9(n2812),* these double-mutant animals show roughly 4.7 extra VNC-like cells (Fig. 1E). This result indicates that a lack of *ced-9* function can cause a significant increase in cell survival, indicative of the poorly understood pro-apoptotic function of *ced-9*.

An EMS screen for *ced-3(lf)* enhancers generated CED-9 and CED-4 mutations altered in their CED-9-CED-4 binding regions.

In earlier work, we described an EMS screen for enhancers of the cell-killing defect caused by *ced-3(n2427)* (Fig. 2A)[19]. In addition to those mutations previously reported, this screen generated an atypical allele of *ced-9, ced-9(n3377).* Like most *ced-9(lf)* alleles, such as the null allele *ced-9(n2812), ced-9(n3377)* enhanced the cell-killing phenotype caused by *ced-3(n2427)* and did so to an extent similar to that caused by a *ced-9* null allele (Fig.1 E and Fig. 2B). By contrast, unlike typical *ced-9(lf)* alleles, which on their own cause maternal-effect recessive lethality because of excessive cell death[7], *ced-9(n3377)* when *c*rossed into a *ced-3(+)* background was viable and caused a decrease in cell death: in *ced-3(+); ced-9(n3377)* animals, about 2.6 extra VC-like cells survived, in contrast to 0 extra VC-like cells in *ced-3(+); ced-9(+)* animals (Fig. 1C, Fig. 2C). Thus, *ced-9(n3377)* mutants lack the maternal-effect lethal (excess cell death) phenotype characteristic of most loss-of-function alleles of *ced-9*, such as *ced-9(n2812)* (Fig. 2D), and hence retains the anti-apoptotic function of *ced-9*. To preclude background mutations as the cause of the atypical phenotype observed in *ced-9(n3377)* animals, we used CRISPR to regenerate the *n3377* mutation. The new allele, *ced-9(n6676),* resulted in the same phenotype as *n3377* (Fig. 2E), confirming that *n3377* caused the atypical phenotype.

ced-9(n3377) could in principle cause either an increase in the cell-death inhibitory function of *ced-9* or a decrease in the cell-death promoting function of *ced-9*. To distinguish between these possibilities, we assessed whether the cell-death defect of *ced-9(n3377)* animals is dominant or recessive. *n3377/+* animals did not show decreased cell death relative to *ced-9(+)/ced-9(+)* animals, indicating that the cell-death

defect of *ced-9(n3377)* animals is recessive (Fig. 2F). The simplest interpretation is that *n3377* causes loss-of-function of the cell-death promoting role of *ced-9.* In other words, because *ced-9(n3377)* animals showed a defect in executing cell death but did not show maternal-effect lethality, *ced-9(n3377)* animals seem to lack the pro-apoptotic function of *ced-9* but to retain its anti-apoptotic function.

ced-9(n3377) encodes a missense mutation (E74K) in a domain of CED-9 thought to be involved in binding CED-4, based on the crystal structure of a CED-9-CED-4 complex[20] (Fig. 2G, H). The location and nature of the E74K mutation indicate that *n3377* likely disrupts CED-4 binding. Given the cell-killing defect of *ced-9(n3377)* mutants, one possibility is that the pro-apoptotic function of *ced-9* depends upon an interaction with CED-4. This hypothesis contradicts the canonical model for *C. elegans* apoptosis, according to which a loss of CED-9-CED-4 interaction should cause widespread ectopic apoptosis and maternal-effect lethality.

In addition to *ced-9(n3377),* the screen described above also generated the *ced-4* allele *n3392*. We recreated this mutation using CRISPR in a strain free from background mutations caused by EMS and named the new allele *ced-4(n6703)* (see Methods). This *ced-4* allele was of interest because it has a missense mutation, R117S, located in the presumptive CED-9-binding region of CED-4 (Fig. 3C, D) and is therefore likely to disrupt CED-9-CED-4 interaction. *ced-4(n6703)* animals were viable and caused a weak cell-killing defect: an average of 1.0 extra VC-like cells were present in these animals, as opposed to the 4.9 extra VC-like cells in *ced-4(n1162)* null mutant animals (Fig. 3A, B and Table 1). *ced-4(n6703)* did not suppress the maternal-effect lethal phenotype caused by the strong loss-of-function allele *ced-9(n1950 n2161)*; in

this way *ced-4(n6703)* is similar to a wild-type *ced-4* allele but unlike a *ced-4* null allele, e.g, *n1162* (Table 1). These two observations are consistent with the hypothesis that *n6703* causes a partial loss of *ced-4* function. However, (1) *ced-4(n6703)* mutants displayed a greater cell-killing defect (1.0 extra VC-like cells) than did two distinct weak hypomorphic reduction-of-function *ced-4* mutants, *ced-4(n2879)* and *ced-4(n2860)* (0.02 and 0.44 extra VC-like cells, respectively); and (2) *ced-4(n6703)* failed to rescue the maternal-effect lethality of *ced-9(n1950 n2161)*, whereas both of the apparently weaker alleles, *ced-4(n2879)* and *ced-4(n2860)*, did so (Table 1). These observations indicate that *ced-4(n6703)* does not cause a slight general reduction in *ced-4* function, but rather – just like *ced-9(n3377)* – specifically results in extra VC-like cells while not affecting the maternal-effect lethal phenotype caused by *ced-9* loss-of-function. Since *ced-9(n3377)* mutants are likely deficient in their ability to form a CED-9-CED-4 interaction and lack the pro-apoptotic but not the anti-apoptotic function of *ced-9,* we conclude that *ced-4(n6703)* mutants analogously lack a function of *ced-4* needed for the pro-apoptotic function of *ced-9.* In short, these observations suggest that *ced-4(n6703)* causes a cell-killing defect because of a lack of a CED-4(R117S) interaction with CED-9 and that CED-4(R117S) is otherwise functional. These results further suggest that perturbing CED-9-CED-4 interaction by altering a CED-9-CED-4 interaction domain in either CED-9 or CED-4 is sufficient to cause a cell-killing defect.

Additional mutations in the CED-4 binding region of CED-9 cause a cell-killing defect and result in viability in a *ced-3(+)* background.

Our observations concerning *ced-9(n3377)* raise the possibility that other *ced-9* mutations affecting CED-9-CED-4 interaction also specifically disrupt the cell-killing

function of *ced-9.* To test this possibility, we used CRISPR-Cas9 to generate additional mutations in the known CED-4 binding region of CED-9[20]. We performed these experiments using *ced-3(+)* animals carrying the transgene *nIs106* and screened for worms that that were both viable and showed ectopic VC-like cell survival. This approach generated five alleles of *ced-9* that, like *ced-9(n3377)*, led to viable animals and caused a recessive cell-killing defect and therefore likely maintain the anti-apoptotic but disrupt the pro-apoptotic function of *ced-9*. These alleles – *n6697, n6698, n6704, n6705,* and *n6712* – all contain indels, and in some cases additional missense mutations, in the presumptive CED-4-binding pocket and resulted in a cell-killing defect (as assayed by survival of VC-like cells) that was similar in strength to that caused by *ced-9(n3377)* (Fig. 4). Additionally, we used CRISPR to generate the allele *ced-9(n6730),* which contains two CED-9 mutations in the presumptive CED-4 binding region, R211E and N212G. CED-9(R211E, N212G) was generated previously by others, expressed in *E. coli*, and shown to be defective in CED-4 binding *in vitro*[21]. We found that *ced-9(n6730)* mutants displayed the same phenotype as *n3377*, *n6697, n6698, n6704, n6705,* and *n6712* mutants – viability and a recessive cell-killing defect (Fig. 4M, N). This observation supports the hypothesis that the phenotype caused by these mutations is a consequence of a disruption in an interaction between CED-9 and CED-4.

These *ced-9* mutations, which are apparently defective in the pro-apoptotic function of *ced-9*, have no apparent defect on the anti-apoptotic function of *ced-9*, as assayed by maternal-effect lethality (Supplemental Table 1). In short, we identified seven alleles of *ced-9* – as well as one allele of *ced-4* – that prevent the pro-apoptotic

function of *ced-9* and disrupt the presumptive CED-9-CED-4 binding region but have no apparent effect on the anti-apoptotic function of *ced-9*. The nature, location, and effects of these mutations suggest that an interaction between CED-9 and CED-4 is required for the pro-apoptotic function of *ced-9* and further suggest that this interaction is not required for the canonical anti-apoptotic function of *ced-9*.

CED-9 and CED-4 mutations in the CED-9-CED-4 binding region prevent sequestration of CED-4 to mitochondria *in vivo.*

We next tested if the mutations described above perturb CED-9-dependent sequestration of CED-4 to mitochondria *in vivo*[9]. We used a polyclonal antibody against CED-4 previously generated by our laboratory and that in our prior work revealed mitochondrial localization of CED-4 protein in wild-type embryos and perinuclear localization of CED-4 protein in embryos carrying *ced-9(lf)* alleles and a *ced-3* loss-of-function allele (which allowed viability of the strain)[9]. We confirmed the ability of this antibody to detect CED-4 protein via western blotting (Supplemental Fig. 1). Using immunofluorescence staining, we also confirmed that wild-type *C. elegans* show mitochondrial localization of CED-4 (Fig. 5A and Supplemental Fig. 2A) and that embryos carrying the *ced-9* null allele *n2812* and the *ced-3* partial loss-of-function allele *n2427* show perinuclear CED-4 localization (Fig. 5B and Supplemental Fig. 2B). Interestingly, we further observed that embryos carrying *ced-3(n2427)* and any of the eight CED-9-CED-4 binding region mutant alleles described above – *n3377, n6697, n6698, n6703, n6704, n6705, 6712,* and *n6730* – showed perinuclear localization of CED-4 (Fig. 5C-E, Supplemental Fig. 2C-J, and Supplemental Fig. 3A-E). These observations suggest that these eight mutations, which affect the presumptive CED-9-

CED-4 binding regions of CED-4 or CED-9 and cause loss of the pro-apoptotic but not anti-apoptotic function of *ced-9,* are defective in a CED-9-CED-4 interaction required to localize CED-9 to mitochondria. We conclude that mutations that likely disrupt a CED-9-CED-4 physical interaction as defined by crystal structure[20] disrupt an *in vivo* CED-9-CED-4 interaction that localizes CED-4 to mitochondria. We suggest that loss of this CED-9-CED-4 interaction and, possibly, the loss of mitochondrial localization of CED-4, is responsible for the loss-of *ced-9*'s pro-apoptotic function in these mutants and that neither this interaction nor CED-9-dependent mitochondrial sequestration of CED-4 is required for the anti-apoptotic function of *ced-9*.

Discussion

The pro-apoptotic function of the canonically anti-apoptotic *C. elegans* gene *ced-9* has long been mysterious, suggesting a poorly understood fundamental process at the core of the control of apoptotic cell death. We identified seven alleles of *ced-9* and one allele of *ced-4* that disrupt the pro-apoptotic but not the anti-apoptotic function of *ced-9*. All seven *ced-9* alleles contain mutations in the presumptive CED-4-binding region of CED-9, and the *ced-4* allele contains a mutation in the presumptive CED-9-binding region of CED-4; all eight are thus likely to disrupt an interaction between CED-9 and CED-4. Furthermore, one of these mutant CED-9 proteins, CED-9(R211E, N212G), was found by others to disrupt CED-9-CED-4 interaction *in vitro*[21]. We asked if these CED-9 and CED-4 mutations disrupt CED-9-CED-4 interaction *in vivo.* Specifically, we tested the one *ced-4* allele and the seven *ced-9* alleles and showed that they all perturb CED-9-CED-4 interaction *in vivo,* as assayed by the CED-9-dependent sequestration of CED-4 to mitochondria in embryos. None of the seven *ced-9* alleles

appeared to cause any detectable defect in the anti-apoptotic function of *ced-9*, despite being very likely to disrupt the known CED-9-CED-4 interaction. Taken together, our data support a model in which a CED-9-CED-4 interaction is required for the pro-apoptotic function of *ced-9* but is dispensable for its anti-apoptotic function – similar to apoptosis in mammals, in which the anti-apoptotic function of BCL-2 (the mammalian homolog of *ced-9*) does not depend on a direct interaction with APAF-1 (the mammalian homolog of *ced-4*). Such a model contrasts with the canonical model for caspase-mediated apoptosis in *C. elegans* in which a CED-9-CED-4 protein interaction is required for the anti-apoptotic function of *ced-9.* These findings raise important questions for future inquiry.

First, how does CED-9-CED-4 interaction promote apoptosis? Possible mechanisms could involve a local binding partner of CED-4, a conformational change or chemical modification of CED-4, or – given the mitochondrial localization of CED-9 and CED-4 in wild-type cells[9] – a mitochondrial process that is impacted by a CED-9-CED-4 complex. Second, what is the anti-apoptotic function of CED-9? The uncoupling of the anti-apoptotic role of *ced-9* from CED-4 mitochondrial localization in CED-9-CED-4 interaction mutants indicates that CED-9 inhibits some process other than CED-4 perinuclear localization. Third, what is the pro-apoptotic event triggered by EGL-1 interaction with CED-9 in cells fated to die, if this event is <u>not</u> disruption of the CED-9-CED-4 interaction? Whereas cell death is reduced when CED-9-CED-4 interaction is perturbed, such a perturbation results in an incomplete block in cell death (e.g., 2.6 extra VC-like cells in *ced-9(n3377); ced-3(+)* animals vs. 4.7 extra cells in *ced-9(n3377); ced-3(2427)* animals (Fig. 2B-C)); by contrast, an *egl-1* null allele results in a near

complete block in cell death[12]. This difference indicates that EGL-1 interaction with CED-9 promotes cell death by doing more than simply disrupting the presumptive CED-9-CED-4 interaction.

In principle, the answers to these three questions might all involve a single unknown mechanism. Two non-mutually exclusive possibilities consistent with our data are:

1. The binding of EGL-1 to the CED-9-CED-4 complex triggers a pro-apoptotic process (Fig. 6A). Loss of a CED-9-CED-4 interaction prevents this interaction and the pro-apoptotic process that it promotes.
2. The anti-apoptotic function of CED-9 is to block a pro-apoptotic process dependent on CED-4 and CED-3 but independent of CED-4 sequestration to mitochondria by CED-9 (Fig. 6B).

One possible more specific model Incorporating both of these concepts is depicted in Fig. 6D-G: EGL-1 interaction with CED-9 activates a cell-death promoting factor or process (labeled "X") that activates CED-4. CED-4 activation by “X” occurs more efficiently at mitochondria but can still occur, albeit less effectively, when CED-4 is not at mitochondria (such as in CED-9-CED-4 interaction mutants). X could reflect a pro-apoptotic factor from mitochondria that interacts with CED-4, a CED-4 conformational change, a chemical modification of CED-4, or CED-4 oligomerization. A model in which CED-9 sequesters a pro-apoptotic factor that activates CED-4 upon its release from mitochondria closely mirrors the mechanism of APAF-1 activation by mammalian BCL-2 family members via the release of cytochrome c from mitochondria[22,23,24,25,26].

It is also possible that CED-9 and CED-4 have two distinct physical interactions, one that is anti-apoptotic and one that is pro-apoptotic. In such a model, viable CED-9 mutations that result in ectopic cell survival and CED-4(R117S) disrupt the pro-apoptotic but not the anti-apoptotic interaction. The anti-apoptotic role of CED-9 is as in the canonical model and dependent on a CED-9-CED-4 interaction distinct from that defined by crystal structure studies to date[20], while the pro-apoptotic role of CED-9 depends on the CED-4 interaction defined by crystal structure[20], which is distinct from the canonical, anti-apoptotic interaction.

In short, we report that an interaction between the BCL-2 homolog CED-9 and its pro-apoptotic binding partner the APAF-1 homolog CED-4 promotes apoptosis in *C. elegans,* the animal in which caspase-driven apoptosis was discovered. Like CED-9, the mammalian protein BCL-2 and other anti-apoptotic BCL-2 family members can be pro-apoptotic, as is the case for BCL-2 in the presence of the nuclear hormone receptor NUR77[27] . Despite extensive research spanning decades, the pro-apoptotic mechanism(s) of these bifunctional proteins remains poorly understood. One difficulty in elucidating such mechanisms might be the complexity of mammalian apoptosis pathways, a consequence in part of the relatively large number of BCL-2 family members in mammals. By contrast, CED-9 is the only BCL-2 family member in *C. elegans*. Additionally, by using *C. elegans* the functions of and interactions among cell-death proteins expressed at endogenous levels can be easily analyzed in the intact organism, features more difficult to attain using mammals or mammalian cell-culture *in vitro* systems.

Given the highly conserved nature of cell-death proteins and pathways between *C. elegans* and humans, we think it plausible that a pro-apoptotic interaction analogous to the CED-9-CED-4 interaction regulates apoptosis in humans. Such an interaction could involve canonically anti-apoptotic BCL-2 family members and one or more of their pro-apoptotic interactors, such as BAX and BAK, or an unknown interactor that activates APAF-1. The elucidation of such a mechanism might add a key insight concerning the basic process of apoptosis and suggest novel targets for therapeutics aimed at treating disorders that involve dysregulated apoptosis, such as certain neurodegenerative disorders and cancers.

Acknowledgments

We thank D. Lee, J. Kong, I. Kesisova, C. Diehl and other members of the Horvitz laboratory for discussions. N.T. was supported by a Ludwig Center Graduate Student Fellowship and NIH grant T32 GM007287. This work was supported by NIH grant R01 GM024663. H.R. Horvitz is the David H. Koch Professor of Biology at MIT and an investigator of the Howard Hughes Medical Institute.

Author Contributions

Conceptualization, N.T., P.R., and H.R.H; Methodology N.T., P.R., B.H., and H.R.H.; Investigation, N.T., P.R. and B.H; Writing – Original Draft, N.T. and H.R.H; Funding Acquisition, N.T. and H.R.H; Resources, N.T., B.H., and H.R.H; Supervision, H.R.H

Declaration of Interest

The authors declare no competing interests.

Methods

C. elegans strain maintenance

All strains were cultured on Nematode Growth Media (NGM) plates seeded with the *E. coli* strain OP50 at 20°C as described[28] unless otherwise indicated.

Immunostaining

Embryos were collected by dissolving adult worms in bleach solution (0.5 M NaOH/0.8% sodium hypochlorite) for approximately 10 min[29]. Embryos were then fixed and permeabilized essentially as described[30]. Previously described rat antiserum against CED-4 was used for this study[9]. We purified the rat antiserum against CED-4 using a Melon™ Gel IgG Purification Kit from Thermo Fisher Scientific, Waltham, MA (catalog # 45206). Purified anti-CED-4 antibody was diluted to 10 μg/mL for immunofluorescence staining, and then stained with a secondary antibody, goat anti-Rat IgG (H+L) Cross-Adsorbed Secondary Antibody, Alexa Fluor™ 647 from Thermo Fisher Scientific, (catalog # A-21247, RRID AB_141778). Embryos were then mounted using SlowFade™ Diamond Antifade Mountant with DAPI from Thermo Fisher Scientific (catalog #S36964). Images of anti-CED-4 stained embryos were obtained using a 63x objective on an LSM 800 confocal microscope from Zeiss, Oberkochen, Germany (Zeiss LSM 800 with Airyscan Microscope, RRID:SCR_015963) and ZEN software. Images obtained via confocal microscopy and, due to variability in intensity of signal associated with *in vivo* immunofluorescent staining due to the freeze-cracking protocol

used, channels (DAPI, MitoFluor, and CED-4) were processed individually using FIJI software[31] (Fiji, RRID:SCR_002285). MitoFluor™ Red 589 from Thermo Fisher Scientific (catalog # M-22424) was fed to adult worms at a concentration of 10 μg/mL by covering the lawn of OP50 and incubating overnight at 20°C essentially as described[32]. Images were then cropped to reduce background. Cartoon images were created in Adobe Illustrator (Adobe Illustrator, RRID:SCR_010279) and Microsoft PowerPoint software.

VC-like cell counts

The number of ventral cord VC-like cells was assessed by counting the number of cells expressing the transgene *nIs106* in L4-stage worms (n=50 for each genotype) using a Nikon SMZ18 fluorescent dissecting microscope[19]. Counts were visualized using GraphPad Prism (*RRID*:SCR_002798).

CRISPR-induced mutations

CRISPR mutants were generated by injecting early adult-stage worms carrying the transgene *nIs106* with Cas9 protein with a gRNA targeting the gene *dpy-10* as well as a *dpy-10* repair template DNA and *ced-9* or *ced-4* repair template DNA (varying with each round of injection based on the gRNA) as described[33]. *ced-9* mutations in the CED-4 binding pocket were generated by using target gRNAs against various locations in the CED-4 binding pocket based on the CED-9-CED-4 crystal structure[20]; viable progeny showing extra VC-like cells were then picked and propagated. Structural images of the

CED-9-CED-4 complex were generated based on the CED-9-CED-4 crystal structure using PyMOL[20,34].

Western blot analysis

Protein was extracted from mixed stage *C. elegans* embryos via 10 minutes of sonication at 80°C and 2 minutes of boiling at 95°C essentially as described[35]. 100 μg of protein extracted from mixed staged embryos was then resolved by SDS-PAGE on a Bio-Rad, Hercules, CA 10% Mini-PROTEAN® TGX™ Precast Protein Gel (catalog #456-1034) and transferred to a Bio-Rad 0.45μm nitrocellulose membrane (catalog #1620115) using a Thermo Fisher Scientific Pierce™ G2 Fast Blotter (catalog #62289). CED-4 protein was detected using the previously described purified rat anti-CED-4 antibody at a concentration of 12 μg/mL and the secondary antibody, goat anti-Rat IgG (H+L) Cross-Adsorbed Secondary Antibody, Alexa Fluor™ 647 from Thermo Fisher Scientific, (catalog # A-21247, RRID AB_141778) was used at a concentration of 2 μg/mL essentially as described[35].Protein band size was determined using Bio-Rad Precision Plus Protein Dual Color Standards (catalog **#1610374).**

Figure 1. *ced-9* possess a non-canonical pro-apoptotic function. A) The canonical model for apoptosis in *C. elegans*. CED-9 acts to prevent cell death by sequestering the pro-apoptotic protein CED-4 to mitochondria. Cells fated to die express the pro-apoptotic EGL-1, which binds CED-9, causing a conformational change in CED-9 that results in the release of CED-4 from mitochondria. After its release from CED-9, CED-4 localizes to the perinuclear membrane, where it activates the caspase CED-3, thus inducing cell death. B) The canonical genetic pathway for apoptosis in *C. elegans.* C-E) Defects in cell killing, as assayed using the transgene *nIs106[P_{lin-11}::GFP],* a GFP reporter expressed in both the ventral cord VC motor neurons and "extra" VC-like undead cells. C) In wild-type animals this transgene detects no extra VC-like cells (n=50). D) *ced-3(n2427)* causes the ectopic survival of ~1.7 extra VC-like cells (n=50). E) The null allele *ced-9(n2812)* enhances the cell-killing defect caused by *ced-3(n2427)* from ~1.7 to ~4.7 extra VC-like cells (n=50).

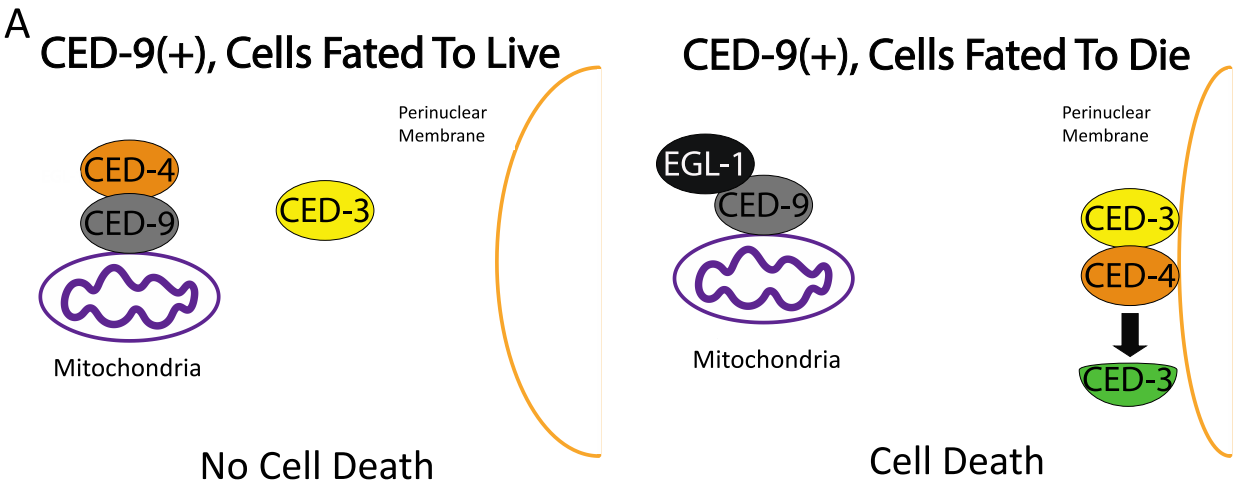
A
CED-9(+), Cells Fated To Live
CED-9(+), Cells Fated To Die
Perinuclear Membrane
CED-4
CED-9
CED-3
Mitochondria
EGL-1
CED-9
Mitochondria
Perinuclear Membrane
CED-3
CED-4
CED-3
No Cell Death
Cell Death


B
EGL-1
CED-9
CED-4
CED-3
Cell Death

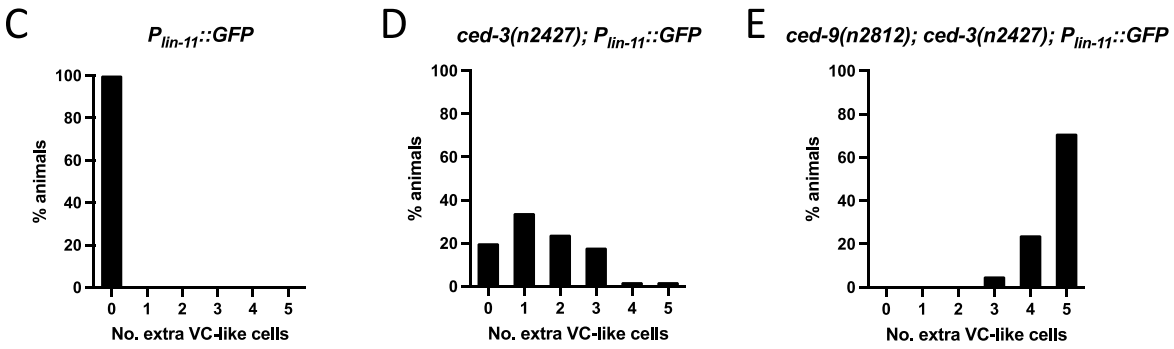
C
P_{lin-11}::GFP
D
ced-3(n2427); P_{lin-11}::GFP
E
ced-9(n2812); ced-3(n2427); P_{lin-11}::GFP
% animals
No. extra VC-like cells
0
20
40
60
80
100
0 1 2 3 4 5

Figure 2. An EMS screen for enhancers of *ced-3(n2427)* isolated a mutation that disrupts the CED-4-binding region of CED-9. A) An EMS screen for enhancers of the cell-death defect mediated by a weak loss-of-function allele of *ced-3*, *ced-3(n2427)*[19]. B-C) This screen identified *ced-9(n3377),* which is homozygous viable, enhances the cell-killing defect caused by *ced-3(n2427),* and results in the ectopic survival of ~2.6 extra VNC-like cells on its own (n=50). D) The *ced-9* null allele, *ced-9(n2812)*, does not produce viable progeny at 15°C, 20°C, and 25°C. A partial-loss-of-function allele of *ced-9*, *ced-9(n6715)*, shows some maternal-effect lethality at 15°C and 20°C and fails to produce viable progeny at 25°C; this allele causes the ectopic survival of 0.08 VC-like cells one average at 20°C. 100% of eggs laid by *ced-9(n3377)* hatch at 15°C, 20°C, and 25°C and *ced-9(n3377)* animals possess ~2.6 ectopically surviving VC-like cells on average at 20°C. E) *n3377* was recreated in a new background to rule out the possibility that background mutations caused by EMS cause the loss of cell-killing phenotype. F) The cell-killing defect caused by *n3377* is recessive. G-H) *ced-9(n3377)* carries a missense mutation (E74K) in the CED-9-CED-4 binding region as defined by crystallographic studies[20].

A

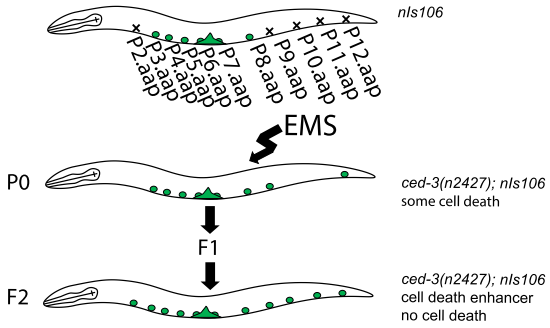

B

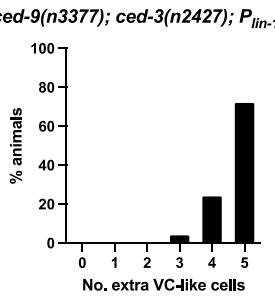

C

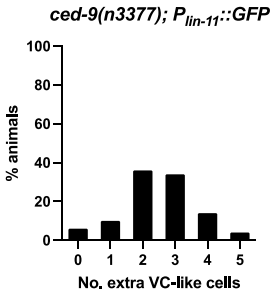

D

	Allele	Molecular Change	% Hatching (n=100) 15°C	20°C	25°C	Avg. Extra VC-like Cells at Permissive Temp.
null	*ced-9(n2812)*	Q44*	N/A	N/A	N/A	N/A
hypomorph	*ced-9(n6715)*	Q110P111Δ	96	88	N/A	0.08
	ced-9(n3377)	E74K	100	100	100	2.6

E

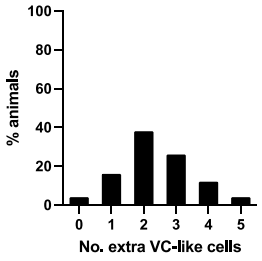

F

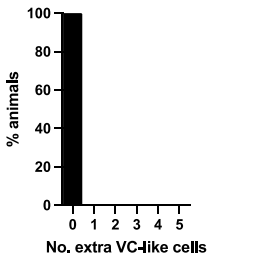

G

	71		CED-9 amino acid sequence				77
WT	N	D	W	E	E	P	R
n3377	N	D	W	K	E	P	R

H

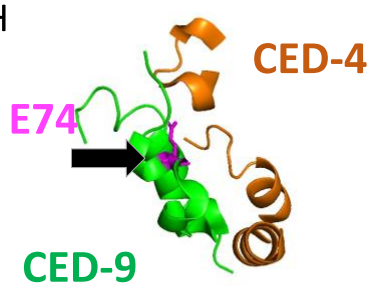

Figure 3. *ced-4(n6703)* causes ectopic VC-like cell survival and contains a mutation in the CED-9-binding region. A-B) *ced-4(n6703)* enhances the cell-killing defect caused by *ced-3(n2427)* and results in the ectopic survival of ~1.0 extra VC-like cells on its own (n=50). C-D) CED-4[R117S] is a missense mutation in the CED-9 binding region of CED-4, as defined by crystallographic studies[20].

A

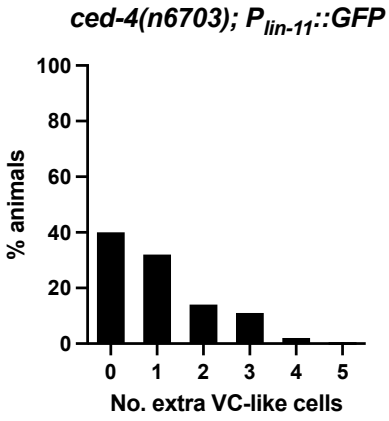

B

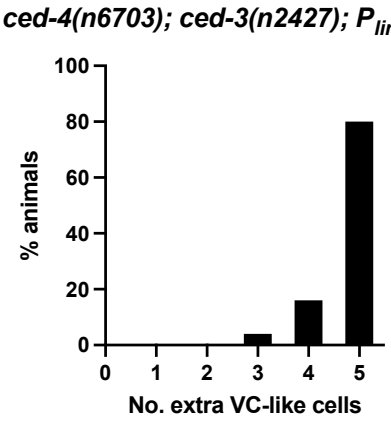

C

CED-4 amino acid sequence

	114						120
WT	M	L	D	R	K	L	L
n6703	M	L	D	S	K	L	L

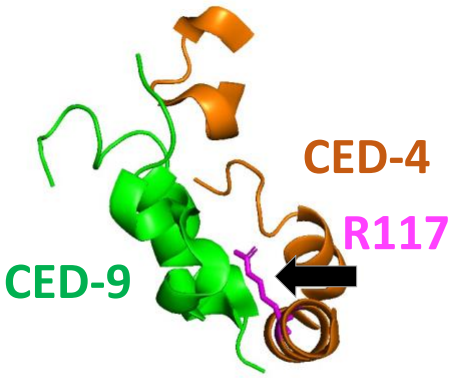

Table 1. *ced-4(n6703)* does not result in a simple reduction of *ced-4* function. *ced-4(n6703)* causes a stronger cell-killing defect than *ced-4(n2860)* and *ced-4(n2879),* as shown by VC-like cell survival. However, *ced-4(n2879)* and *ced-4(n2860)* but not *ced-4(n6703)* can rescue the maternal-effect lethality caused by the *ced-9* loss-of-function allele *ced-9(n1950 n2161)* (n=50). The mutation *unc-69(e587)* is present in the background of all listed *ced-4 ced-9(n1950 n2161)* double mutants as this marker is closely linked to *ced-9* and was used to follow *ced-9(n1950 n2161)* during crossing.

***ced-4* Allele**	**Molecular Change**	**Avg. Extra VC-Like Cells (P_{lin-11}::*GFP*)**	**Rescues *ced-9(n1950 n2161)***
WT	-	0	No
n2879	E276K	0.02	Yes
n2860	E263K	0.44	Yes
n6703	R117S	1.0	No
n3141	R53K	3.4	Yes
n1162 (null)	Q80Ochre	4.9	Yes

Figure 4. CRISPR-induced mutations in the CED-9-CED-4 binding region of CED-9 result in cell-killing defects. Six alleles of *ced-9* generated by CRISPR-Cas9 carry mutations likely to disrupt the CED-4 binding region. A-B) *ced-9(n6697)* carries an 11 amino acid insertion in the CED-4 binding pocket; *ced-9(n6698)* carries a five amino acid deletion in the CED-4 binding pocket; *ced-9(n6730)* carries two missense mutations, R211E and N212G; *ced-9(n6704)* carries a four amino acid insertion in the CED-4 binding pocket as well as two missense mutations, E75G and P76T; *ced-9(n6705)* carries a four amino acid insertion in the CED-4 binding pocket; and *ced-9(n6712)* carries a three amino acid insertion in the CED-4 binding pocket as well as two missense mutations, P76K and R77W. C-N) These mutations cause ectopic survival of VC-like cells on their own (n=50), enhance the cell-killing defect caused by *ced-3(n2427),* and are viable in a wild-type background.

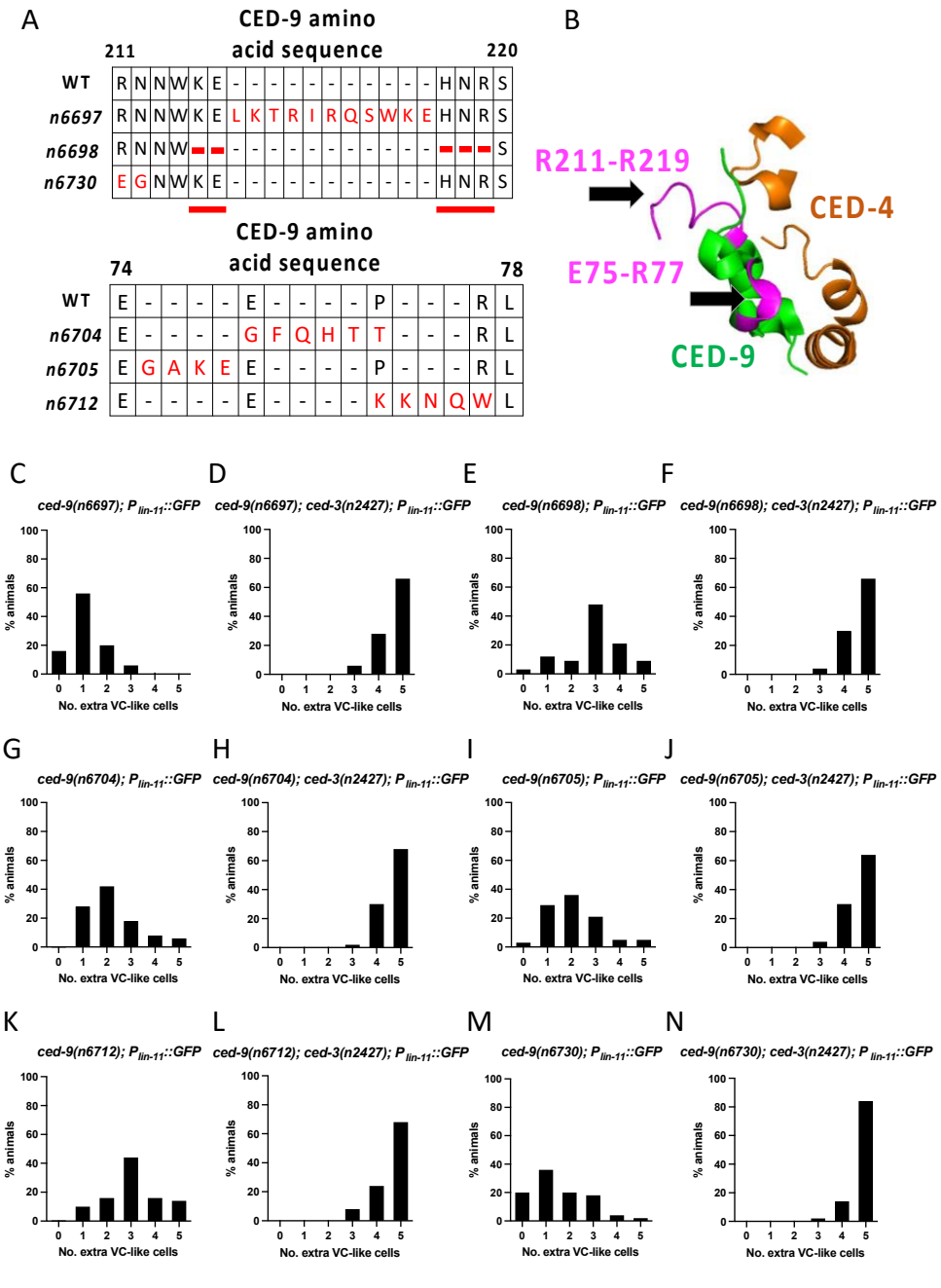
A
CED-9 amino acid sequence
211
220
WT R N N W K E - - - - - - - - - - H N R S
n6697 R N N W K E L K T R I R Q S W K E H N R S
n6698 R N N W - - - - - - - - - - - - - - - S
n6730 E G N W K E - - - - - - - - - - H N R S
CED-9 amino acid sequence
74
78
WT E - - - - E - - - - P - - - R L
n6704 E - - - - G F Q H T T - - - R L
n6705 E G A K E E - - - - P - - - R L
n6712 E - - - - E - - - - K K N Q W L
B
R211-R219
CED-4
E75-R77
CED-9
C
ced-9(n6697); P lin-11::GFP
D
ced-9(n6697); ced-3(n2427); P lin-11::GFP
E
ced-9(n6698); P lin-11::GFP
F
ced-9(n6698); ced-3(n2427); P lin-11::GFP
G
ced-9(n6704); P lin-11::GFP
H
ced-9(n6704); ced-3(n2427); P lin-11::GFP
I
ced-9(n6705); P lin-11::GFP
J
ced-9(n6705); ced-3(n2427); P lin-11::GFP
K
ced-9(n6712); P lin-11::GFP
L
ced-9(n6712); ced-3(n2427); P lin-11::GFP
M
ced-9(n6730); P lin-11::GFP
N
ced-9(n6730); ced-3(n2427); P lin-11::GFP
% animals
No. extra VC-like cells

Figure 5. Mutations that disrupt the CED-9-CED-4 binding regions of either CED-9 or CED-4 result in the mislocaliztion of CED-4 to the perinuclear membrane. A) Mitochondrial localization of CED-4 in wild-type embryos, as shown previously[9] (and Supplemental Fig. 3). B) Perinuclear localization of CED-4 in *ced-9(n2812); ced-4(n2427)* embryos; *ced-9(n2812)* is a null allele of *ced-9.* C) Perinuclear localization of CED-4 in *ced-9(n3377); ced-4(n2427)* embryos. D) Perinuclear localization of CED-4 in *ced-4(n6703); ced-4(n2427)* embryos. E) Perinuclear localization of CED-4 in *ced-9(n6704); ced-4(n2427)* embryos. Images were cropped to avoid background noise and the brightness and contrast of the DAPI and CED-4 channels were adjusted individually using Fiji software.

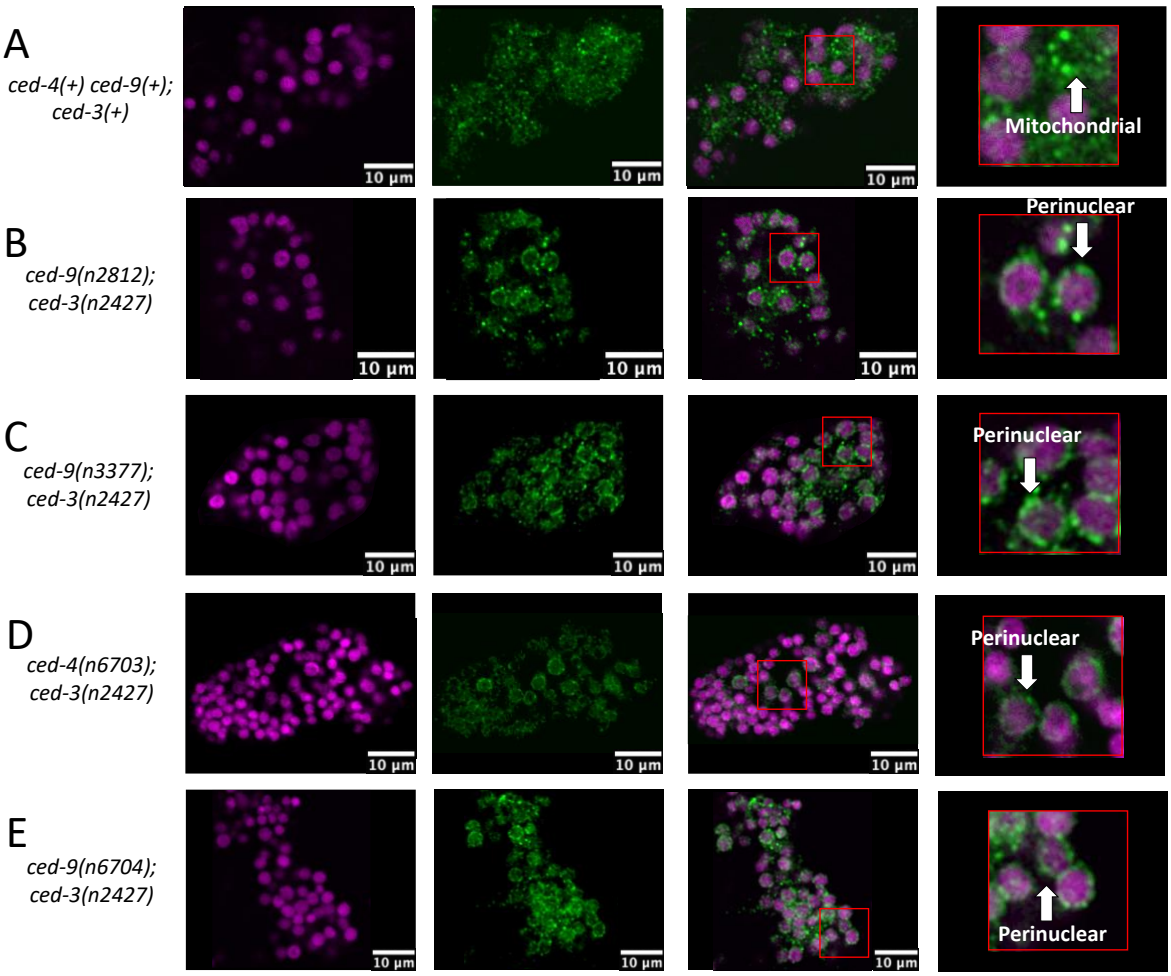
A
ced-4(+) ced-9(+);
ced-3(+)
Mitochondrial
B
ced-9(n2812);
ced-3(n2427)
Perinuclear
C
ced-9(n3377);
ced-3(n2427)
Perinuclear
D
ced-4(n6703);
ced-3(n2427)
Perinuclear
E
ced-9(n6704);
ced-3(n2427)
Perinuclear
10 µm

Figure 6. Possible alternatives to the canonical apoptosis pathway. A) EGL-1 binding to the CED-9-CED-4 complex promotes a pro-apoptotic process dependent on CED-9-CED-4 interaction. B) EGL-1 blocks the ability of CED-9 to prevent a pro-apoptotic process occurring independently of CED-4 sequestration by CED-9. C) An alternative genetic pathway in which CED-9 has both an anti-apoptotic and pro-apoptotic function that depend on CED-4 and CED-3. D-G) An unknown (essential or genetically redundant) factor X promotes apoptosis through CED-4 activation. D) In CED-9(+) cells fated to live, both factor X and CED-4 are sequestered to mitochondria by CED-9. E) In CED-9(+) cells fated to die, EGL-1 changes the conformation of CED-9, releasing factor X-activated CED-4, which then translocates to the perinuclear membrane and initiates cell death. F) CED-9-CED-4 binding mutants, such as *ced-9(n3377)* [E74K], maintain CED-9-dependent factor X sequestration, preventing killing in cells fated to live. G) In cells fated to die carrying CED-9-CED-4 binding mutations, EGL-1 releases factor X from CED-9; CED-4 and factor X do not interact at mitochondria leading to inefficient CED-4 activation by factor X and resulting in only some cell death.

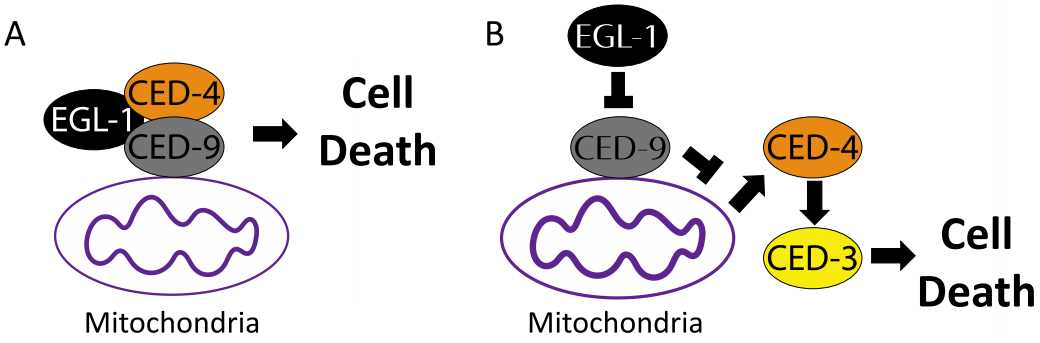
A
EGL-1
CED-4
CED-9
Cell Death
Mitochondria
B
EGL-1
CED-9
CED-4
CED-3
Cell Death
Mitochondria


C
EGL-1
CED-9
CED-4
CED-3
Cell Death

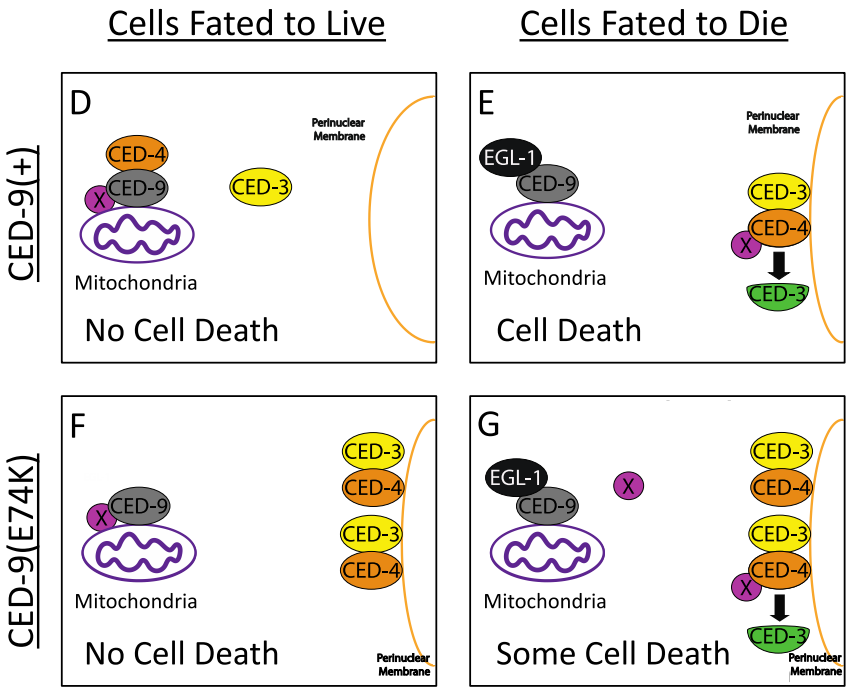
Cells Fated to Live
Cells Fated to Die
CED-9(+)
CED-9(E74K)
D
Perinuclear Membrane
CED-4
CED-9
X
CED-3
Mitochondria
No Cell Death
E
Perinuclear Membrane
EGL-1
CED-9
Mitochondria
CED-3
CED-4
X
CED-3
Cell Death
F
CED-9
X
Mitochondria
CED-3
CED-4
CED-3
CED-4
No Cell Death
Perinuclear Membrane
G
EGL-1
CED-9
X
Mitochondria
CED-3
CED-4
CED-3
CED-4
X
CED-3
Some Cell Death
Perinuclear Membrane

Supplemental Table 1. *ced-9* alleles that cause a cell-killing defect and *ced-4(n6703)* are viable as homozygotes, lacking the maternal-effect lethality typical of *ced-9* null alleles. n=100 embryos were observed at 15°C, 20°C, and 25°C and % Hatching was recorded for *ced-9* and *ced-4* alleles with no mutations in any other cell-killing gene such as *ced-3*.

	% Hatching (n=100)		
Allele	15°C	20°C	25°C
ced-9(n2812)	0	0	0
ced-9(n3377)	100	100	100
ced-9(n6697)	100	100	100
ced-9(n6698)	100	100	100
ced-9(n6704)	100	100	100
ced-9(n6705)	100	100	100
ced-9(n6712)	100	100	98
ced-9(n6730)	100	96	94
ced-4(n6703)	100	100	100
ced-4(+) ced-9(+)	100	100	100

Supplemental Figure 1. CED-4 protein is detected by anti-CED-4 antibody. A western blot showing that a polyclonal antibody made against CED-4 protein identifies a band between 50 kD and 75 kD (see Methods), roughly the size of CED-4 protein (63 kD), in a lane containing protein extracted from mixed-staged embryos carrying a wild-type *ced-4* allele. The antibody failed to detect this band in embryos carrying the null allele *ced-4(n1162).* These two lines were cropped from a larger filter.

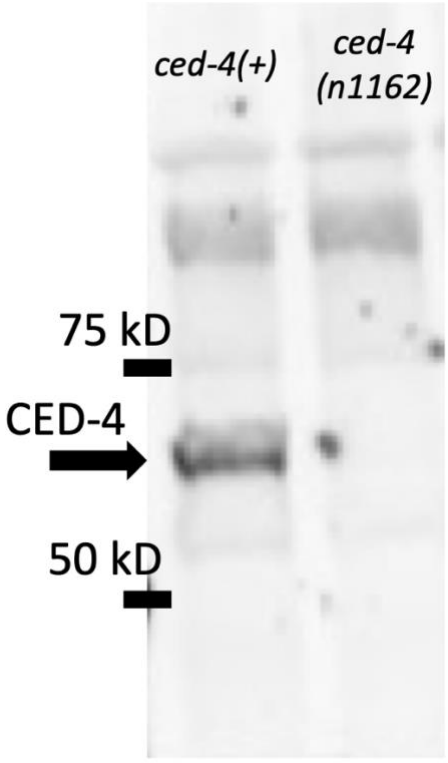
ced-4(+)
ced-4
(n1162)
75 kD
CED-4
50 kD

Supplemental Figure 2. Mutations that disrupt the CED-9-CED-4 binding regions of either CED-9 or CED-4 disrupt sequestration of CED-4 to mitochondria. A) Mitochondrial localized CED-4 in wild-type embryos, B) perinuclear localization of CED-4 in *ced-9(n2812); ced-4(n2427)* embryos, C) perinuclear localization of CED-4 in *ced-9(n3377); ced-4(n2427)* embryos, D) perinuclear localization of CED-4 in *ced-4(n6703); ced-4(n2427)* embryos, E) perinuclear localization of CED-4 in *ced-9(n6704); ced-4(n2427)* embryos, F) perinuclear localization of CED-4 in *ced-9(n6697); ced-4(n2427)* embryos, G) perinuclear localization of CED-4 in *ced-9(n6698); ced-4(n2427)* embryos, H) perinuclear localization of CED-4 in *ced-9(n6705); ced-4(n2427)* embryos, I) perinuclear localization of CED-4 in *ced-9(n6712); ced-4(n2427)* embryos, and J) perinuclear localization of CED-4 in *ced-9(n6730); ced-4(n2427)* embryos. Images were cropped to avoid background and the brightness and contrast of the MitoFluor and CED-4 channels were adjusted individually using Fiji software.

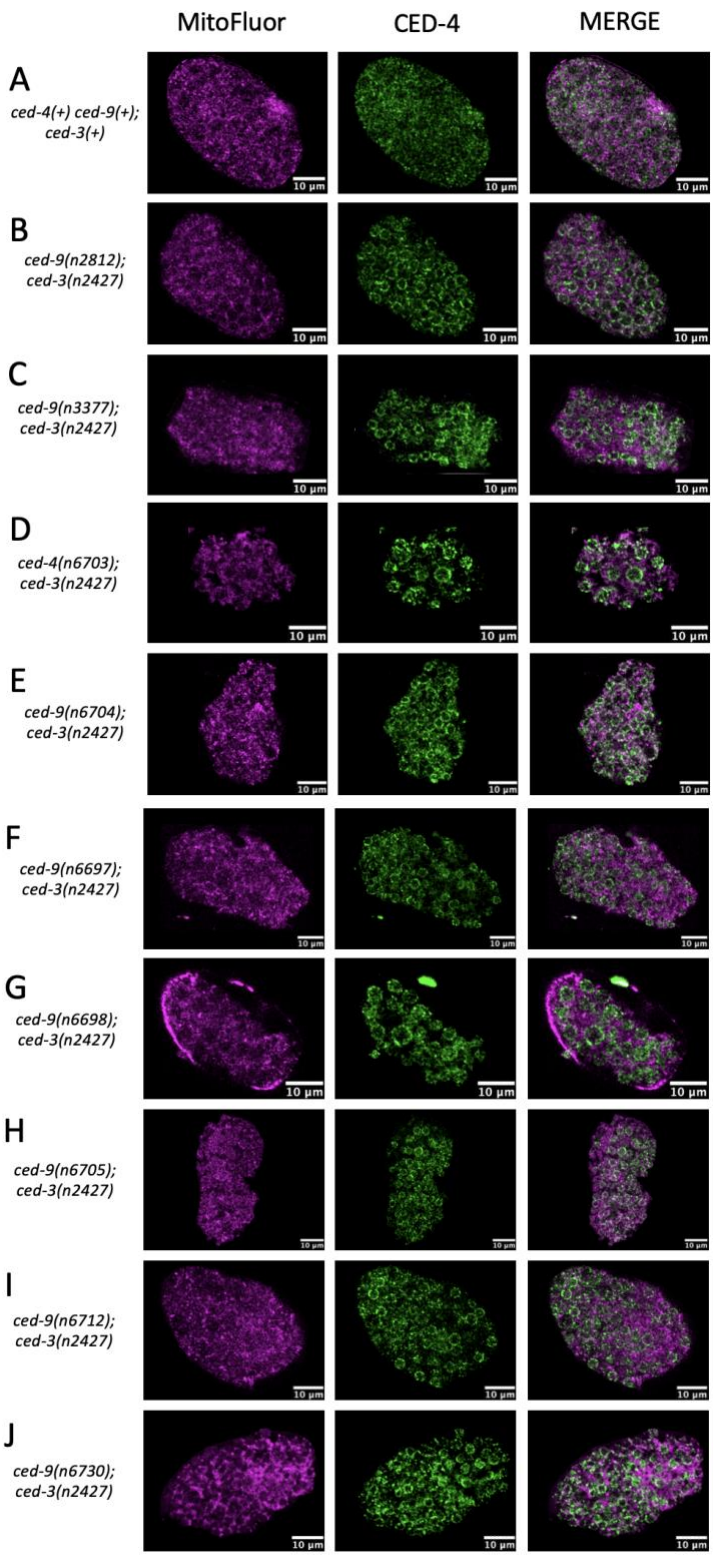
MitoFluor
CED-4
MERGE
A
ced-4(+) ced-9(+);
ced-3(+)
B
ced-9(n2812);
ced-3(n2427)
C
ced-9(n3377);
ced-3(n2427)
D
ced-4(n6703);
ced-3(n2427)
E
ced-9(n6704);
ced-3(n2427)
F
ced-9(n6697);
ced-3(n2427)
G
ced-9(n6698);
ced-3(n2427)
H
ced-9(n6705);
ced-3(n2427)
I
ced-9(n6712);
ced-3(n2427)
J
ced-9(n6730);
ced-3(n2427)
10 µm

Supplemental Figure 3. Mutations that disrupt the CED-9-CED-4 binding regions of either CED-9 or CED-4 result in the mislocalization of CED-4 to the perinuclear membrane. A) Perinuclear localization of CED-4 in *ced-9(n6697); ced-4(n2427)* embryos. B) Perinuclear localization of CED-4 in *ced-9(n6698); ced-4(n2427)* embryos. C) Perinuclear localization of CED-4 in *ced-9(n6705); ced-4(n2427)* embryos. D) Perinuclear localization of CED-4 in *ced-9(n6712); ced-4(n2427)* embryos. E) Perinuclear localization of CED-4 in *ced-9(n6730); ced-4(n2427)* embryos. Images were cropped to avoid background and the brightness and contrast of the DAPI and CED-4 channels were adjusted individually using Fiji software.

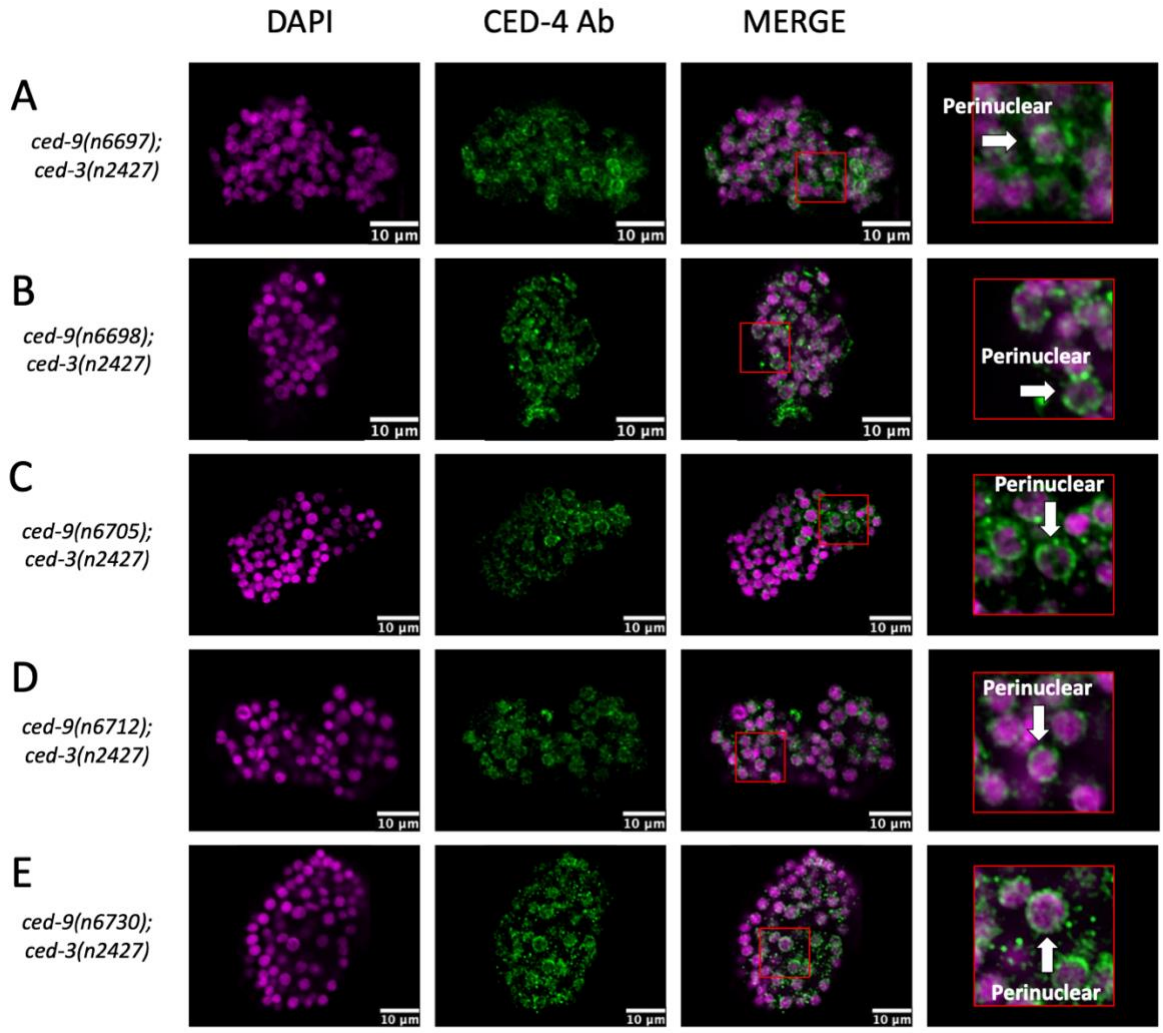
DAPI
CED-4 Ab
MERGE
A
ced-9(n6697);
ced-3(n2427)
Perinuclear
B
ced-9(n6698);
ced-3(n2427)
Perinuclear
C
ced-9(n6705);
ced-3(n2427)
Perinuclear
D
ced-9(n6712);
ced-3(n2427)
Perinuclear
E
ced-9(n6730);
ced-3(n2427)
Perinuclear
10 µm

References

1. Jacobson, M. D., Weil, M. & Raff, M. C. (1997). Programmed cell death in animal development. *Cell* **88**, 347–354. https://doi.org/10.1016/s0092-8674(00)81873-5

2. Fuchs, Y., & Steller, H. (2011). Programmed cell death in animal development and disease. *Cell* **147**, 742–758. https://doi.org/10.1016/j.cell.2011.10.033

3. Hipfner, D. R. & Cohen, S. M. (2004) Connecting proliferation and apoptosis in development and disease. *Nature Reviews Molecular Cell Biology* **5**, 805–815. https://doi.org/10.1038/nrm1491.

4. Takeuchi, O., Fisher, J., Suh, H., Harada, H., Malynn, B. A., & Korsmeyer, S. J. (2005). Essential role of BAX, BAK in B cell homeostasis and prevention of autoimmune disease. *Proc. Natl. Acad. Sci. U. S. A.* **102**, 11272-11277. https://doi.org/10.1073/pnas.0504783102.

5. Hyman, B. T. & Yuan, J. (2012) Apoptotic and non-apoptotic roles of caspases in neuronal physiology and pathophysiology. *Nature Reviews Neuroscience* **13**, 395–406. https://doi.org/10.1038/nrn3228

6. Ellis, H. M. & Horvitz, H. R. (1986). Genetic control of programmed cell death in the nematode *C. elegans*. *Cell* **44**, 817–829. https://doi.org/10.1016/0092-8674(86)90004-8

7. Hengartner, M. 0, Ellis, R. E. & Horvitz, H. R. (1992). *Caenorhabditis elegans* gene *ced-9* protects cells from programmed cell death. *Nature* **356**, 494–499. https://doi.org/10.1038/356494a0

8. Lettre, G. & Hengartner, M. O. (2006). Developmental apoptosis in *C. elegans*: A complex CEDnario. *Nature Reviews Molecular Cell Biology* **7**: 97–108. https://doi.org/10.1038/nrm1836

9. Chen, F., Hersh, B.M., Conradt, B., Zhou, Z., Riemer, D., Gruenbaum, Y., Horvitz, H.R. (2000). Translocation of *C. elegans* CED-4 to nuclear membranes during programmed cell death. *Science* **287**, 1485-1489. https://doi.org/10.1126/science.287.5457.1485

10. Chinnaiyan, A.M., O'Rourke, K., Lane, B.R., and Dixit, V.M. (1997). Interaction of CED- 4 with CED-3 and CED-9: a molecular framework for cell death. *Science* **275**, 1122– 1126. https://doi.org/10.1126/science.275.5303.1122

11. Spector, M.S., Desnoyers, S., Hoeppner, D.J., and Hengartner, M.O. (1997). Interaction between the *C. elegans* cell-death regulators CED-9 and CED-4. *Nature* **385**, 653–656. https://doi.org/10.1038/385653a0

12. Conradt, B., and Horvitz, H.R. (1998). The *C. elegans* protein EGL-1 is required for programmed cell death and interacts with the Bcl-2–like protein CED-9. *Cell* **93**, 519– 529. https://doi.org/10.1016/s0092-8674(00)81182-4

13. Hengartner, M., Horvitz, H.R. (1994). *C. elegans* cell survival gene *ced-9* encodes a functional homolog of the mammalian proto-oncogene bcl-2. *Cell* **76**, 665-676. https://doi.org/10.1016/0092-8674(94)90506-1

14. Duan, H., Chinnaiyan, A.M., Hudson, P.L., Wing, J.P., He, W.W., Dixit, V.M. (1996). ICE-LAP3, a novel mammalian homologue of the *Caenorhabditis elegans* cell death protein CED-3 is activated during Fas- and tumor necrosis factor-induced apoptosis. *J. Biol. Chem.* **271**, 1621–1625. https://doi.org/10.1074/jbc.271.3.1621

15. Cecconi, F., Alvarez-Bolado, G., Meyer, B. I., Roth, K. A. & Gruss, P. (1998). Apaf1 (CED-4 homolog) regulates programmed cell death in mammalian development**.** *Cell* **94**, 727–737. https://doi.org/10.1016/s0092-8674(00)81732-8

16. Nehme, R. & Conradt, B. (2008). egl-1: A key activator of apoptotic cell death in *C. elegans*. *Oncogene* **27**, S30–S40. https://doi.org/10.1038/onc.2009.41

17. Sulston, J. E. & Horvitz, H. R. (1977). Post-embryonic cell lineages of the nematode, *Caenorhabditis elegans*. *Dev. Biol.* **56**, 110–156. https://doi.org/10.1016/0012-1606(77)90158-0

18. White, J. G., Southgate, E., Thomson, J. N. & Brenner, S. (1986). The structure of the nervous system of the nematode *Caenorhabditis elegans*. *Philos. Trans. R. Soc. London. B, Biol. Sci.* **314**, 1–340. https://doi.org/10.1098/rstb.1986.0056

19. Reddien, P. W., Andersen, E. C., Huang, M. C., & Horvitz, H. R. (2007). DPL-1 DP, LIN-35 Rb and EFL-1 E2F act with the MCD-1 zinc-finger protein to promote programmed cell death in *Caenorhabditis elegans*. *Genetics* **175,** 1719–1733. https://doi.org/10.1534/genetics.106.068148

20. Yan, N., Chai, J., Lee, E.S., Gu, L., Liu, Q., He, J., Wu, J.W., Kokel, D., Li, H., Hao, Q., Xue, D. Shi Y. (2005). Structure of the CED-4–CED-9 complex provides insights into programmed cell death in *Caenorhabditis elegans*. *Nature* **437**, 831–837. https://doi.org/10.1038/nature04002

21. Yan N., Gu L., Kokel D., Chai J., Li W., Han A., Chen L., Xue D., Shi Y. (2004). Structural, biochemical, and functional analyses of CED-9 recognition by the proapoptotic proteins EGL-1 and CED-4. *Mol. Cell* **15**, 999-1006. https://doi.org/10.1016/j.molcel.2004.08.022

22. Liu, X., Kim, C. N., Yang, J., Jemmerson, R., Wang, X. (1996). Induction of apoptotic program in cell-free extracts: Requirement for dATP and cytochrome c. *Cell* **86**, 147-157. https://doi.org/10.1016/s0092-8674(00)80085-9

23. Kluck, R. M., Bossy-Wetzel, E., Green, D. R. & Newmeyer, D. D. (1997). The release of cytochrome c from mitochondria: A primary site for Bcl- 2 regulation of apoptosis. *Science* **275**, 1132–1136. https://doi.org/10.1126/science.275.5303.1132

24. Yang J., Liu X., Bhalla K., Kim C.N., Ibrado A.M., Cai J., Peng T.I., Jones D.P., Wang X. (1997). Prevention of apoptosis by Bcl-2: Release of cytochrome c from mitochondria blocked. *Science* **275**, 1129–1132. https://doi.org/10.1126/science.275.5303.1129

25. Zou, H., Henzel, W. J., Liu, X., Lutschg, A. & Wang, X. (1997). Apaf-1, a human protein homologous to *C. elegans* CED-4, participates in cytochrome c-dependent activation of caspase-3. *Cell* **90**, 405-413. https://doi.org/10.1016/s0092-8674(00)80501-2

26. Li, P., Nijhawan, D., Budihardjo, I., Srinivasula, S.M., Ahmad, M., Alnemri, E.S., Wang, X. (1997). Cytochrome c and dATP-dependent formation of Apaf-1/caspase-9 complex initiates an apoptotic protease cascade. *Cell* **91**, 479-489. https://doi.org/10.1016/s0092-8674(00)80434-1

27. Lin, B., Kolluri, S.K., Lin, F., Liu, W., Han, Y.H., Cao, X., Dawson, M.I., Reed, J.C., Zhang, X.K. (2004). Conversion of Bcl-2 from Protector to Killer by Interaction with Nuclear Orphan Receptor Nur77/TR3. *Cell* **116**, 527–540. https://doi.org/10.1016/s0092-8674(04)00162-x

28. Brenner, S. (1974). The genetics of *Caenorhabditis elegans***.** *Genetics* **77**, 71–94. https://doi.org/10.1093/genetics/77.1.71

29. Guenther, C. & Garriga, G. (1996). Asymmetric distribution of the *C. elegans* HAM-1 protein in neuroblasts enables daughter cells to adopt distinct fates. *Development* **122**, 3509–3518. https://doi.org/10.1242/dev.122.11.3509

30. Korčeková, D., Gombitová, A., Raška, I., Cmarko, D. & Lanctôt, C. (2012). Nucleologenesis in the *Caenorhabditis elegans* embryo**.** *PLoS One* **7**, e40290. https://doi.org/10.1371/journal.pone.0040290

31. Schindelin, J., Arganda-Carreras, I., Frise, E., Kaynig, V., Longair, M., Pietzsch, T., Preibisch, S., Rueden, C., Saalfeld, S., Schmid, B., Tinevez, J.Y., White, D.J., Hartenstein, V., Eliceiri, K., Tomancak, P., Cardona, A. (2012). Fiji: An open-source platform for biological-image analysis. *Nat. Methods* 9, 676–682. https://doi.org/10.1038/nmeth.2019

32. Dingley, S., Polyak, E., Lightfoot, R., Ostrovsky, J., Rao, M., Greco, T., Ischiropoulos, H., Falk, M.J. (2010). Mitochondrial respiratory chain dysfunction variably increases oxidant stress in *Caenorhabditis elegans*. *Mitochondrion* **10**, 125–136. https://doi.org/10.1016/j.mito.2009.11.003

33. Dickinson, D. J. & Goldstein, B. (2016). CRISPR-based methods for *Caenorhabditis elegans* genome engineering**.** *Genetics* **202**, 885–901. https://doi.org/10.1534/genetics.115.182162

34. Schrödinger, LLC. The PyMOL Molecular Graphics System, Version~1.8. (2015).

35. Jeong, D.-E., Lee, Y. & Lee, S.-J. V. (2018). Western Blot Analysis of *C. elegans* Proteins. *Methods Mol. Biol.* **1742**, 213–225. https://doi.org/10.1007/978-1-4939-7665-2_19

Chapter Three

Replication Stress Promotes Cell Elimination by Extrusion

Vivek K. Dwivedi, Carlos Pardo-Pastor*, Rita Droste, Ji Na Kong, Nolan Tucker, Daniel P. Denning, Jody Rosenblatt*, & H. Robert Horvitz

I made the discovery that reduction-of nucleotide metabolism gene function causes ectopic cell extrusion in the presence of caspase activity. Based on Vivek Dwivedi's discovery that replication stress promotes cell extrusion in *C. elegans* Carlos Pardo-Paster, a postdoc in Jody Rosenblatt's laboratory, performed cell extrusion experiments using MDCK cells treated with hydroxyurea. Ji Na Kong performed TUNEL staining experiments. Rita Droste aided in the genome-wide RNAi screen. Daniel Denning created key strains used in confocal imaging and established the project. Vivek Dwivedi wrote this paper, published in *Nature* (https://doi.org/10.1038/s41586-021-03526-y), and performed all other cell extrusion experiments in *C. elegans* including imaging and screening.

* Kings College London, London, UK SE1 1UL

Abstract

Cell extrusion is a mechanism of cell elimination that is used by organisms as diverse as sponges, nematodes, insects and mammals[1–3]. During extrusion, a cell detaches from a layer of surrounding cells while maintaining the continuity of that layer[4]. Vertebrate epithelial tissues primarily eliminate cells by extrusion, and the dysregulation of cell extrusion has been linked to epithelial diseases, including cancer[1,5]. The mechanisms that drive cell extrusion remain incompletely understood. Here, to analyse cell extrusion by *Caenorhabditis elegans* embryos[3], we conducted a genome-wide RNA interference screen, identified multiple cell-cycle genes with S-phase-specific function, and performed live-imaging experiments to establish how those genes control extrusion. Extruding cells experience replication stress during

S phase and activate a replication-stress response via homologues of ATR and CHK1. Preventing S-phase entry, inhibiting the replication-stress response, or allowing completion of the cell cycle blocked cell extrusion. Hydroxyurea-induced replication stress[6,7] triggered ATR–CHK1- and p53-dependent cell extrusion from a mammalian epithelial monolayer. We conclude that cell extrusion induced by replication stress is conserved among animals and propose that this extrusion process is a primordial mechanism of cell elimination with a tumour-suppressive function in mammals.

Introduction

Mutants of *C. elegans* that are defective in caspase-mediated apoptosis — for example, *ced-3(lf)* loss-of-function mutants — provide an excellent system for studies

of cell extrusion[3]. Cell extrusion functions as a 'backup' mechanism in *ced-3(lf)* embryos to eliminate certain cells that would normally be eliminated by caspase-mediated apoptosis[3]. To identify genes that control cell extrusion, we screened the *C. elegans* ORFeome RNA interference (RNAi) library of 11,511 bacterial clones for RNAi clones that in *ced-3(lf)* animals generated the two-excretory cell (Tex) phenotype[3] (Fig. 1a–c, Supplemental Fig. 1a), which occurs when the cell ABplpappap fails to be extruded. From this screen, we identified 30 RNAi clones corresponding to 27 genes that produced a Tex phenotype (Supplemental Data Fig. 1a). Notably, 10 of the 27 genes identified were cell-cycle genes with functions that were mostly specific to the S phase[8] (Fig. 1d, e). Additional RNAi screens identified an additional four such genes (Fig. 1d, Supplemental Table 1). Consistent with their function in cell extrusion, RNAi against 13 of the 14 identified cell-cycle genes produced a Tex phenotype only in the *ced-3(lf)* background and not in a *ced-3(+)* wild-type background (Supplemental Table 2).

Results

Cell-cycle genes promote cell extrusion

To characterize the functional role of cell-cycle genes in cell extrusion, we used time-lapse confocal microscopy to observe ABplpappap in embryos treated with RNAi against *cye-1* or *cdk-2* or with an empty vector (control embryos). We tracked the fate of ABplpappap over a 50-min period ending in ventral enclosure, which normally coincides with cell extrusion[3] (Fig. 1f, Supplemental Fig. 1b). Virtual lateral sections of the embryos at the end of ventral enclosure confirmed that ABplpappap was extruded from

control embryos (10 of 11 embryos) (Fig. 1g). By contrast, ABplpappap was not extruded from *cye-1(RNAi)* (11 of 11) (Fig. 1g) or *cdk-2(RNAi)* embryos (10 of 11) (Fig. 1g), consistent with the highly penetrant Tex phenotype observed for *cye-1(RNAi)* and *cdk-2(RNAi)* larval animals (Fig. 1d, e). We conclude that *cye-1* and *cdk-2* are required for extrusion of the cell ABplpappap.

To identify the cellular site of cell-cycle gene function in ABplpappap cell extrusion, we performed genetic mosaic analyses. We examined *cye-1(lf); ced-3(lf)* double mutants and found that these animals dis- played a Tex phenotype similar to that of *ced-3(lf); cye-1(RNAi)* animals (Fig. 1d, h), suggesting that extrusion is more sensitive to a reduction in cell-cycle gene levels than general embryonic development, for which maternal contribution of *cye-1* is sufficient[9]. We generated an extrachromosomal array carrying the cell-autonomous RFP reporter $P_{sur\text{-}5}$*::RFP* and a *cye-1(+)* transgene, which partially rescued the Tex phenotype of *cye-1(lf); ced-3(lf)* animals (Fig. 1h). Extrachromosomal arrays are mitotically unstable and are randomly lost during development, which produces mosaic animals. We examined ten mosaic animals that carried the *cye-1(+)*-rescuing array, as indicated by the presence of RFP in any set of cells or tissues, but were not rescued for the Tex phenotype (Fig. 1i). The RFP expression pattern indicated that the array was absent from ABplpappap in all ten animals, despite being present in the ABplpappap niece cell (the excretory cell) in nine of the ten animals (Fig. 1i–k, Supplemental Fig. 2a–i). We conclude that *cye-1* and probably other cell-cycle genes function cell-autonomously for the extrusion of ABplpappap.

Cells arrest in S phase before extrusion

To characterize the cell-cycle phase of cells that are extruded, we used two cell-cycle reporters: (i) tDHB–GFP[10], a truncated DNA helicase B fragment fused to GFP, and (ii) GFP–PCN-1, an N-terminal translational fusion of GFP to the *C. elegans* homologue of the DNA replication processivity factor PCNA[11]. tDHB–GFP is enriched in the nuclei of quiescent, post-mitotic and G1-phase cells and transits to the cytoplasm for all other cell-cycle phases[10] (Fig. 2a); GFP–PCN-1 exhibits a punctate sub-nuclear localization only during S phase in both mammalian and early *C. elegans* embryonic cells[11,12] (Fig. 2b). In control embryos, tDHB– GFP reporter fluorescence was mostly absent from the ABplpappap nucleus (Fig. 2c) both before ventral enclosure (five of five embryos) (Supplemental Fig. 3a) and after extrusion (five of five embryos) (Supplemental Fig. 3b). Cells extruded from other sites of control or untreated embryos also displayed low levels of nuclear tDHB–GFP (Supplemental Fig. 4a–d). Therefore, ABplpappap and other extruded cells appear to enter but never complete the cell cycle during extrusion. The GFP–PCN-1 reporter localized to bright sub-nuclear punctate foci in ABplpappap cells (Fig. 2d) both before extrusion (five of five embryos) (Supplemental Fig. 3c) and after extrusion (five of five embryos) (Supplemental Fig. 3d) from control embryos, indicating that ABplpappap entered but did not exit S phase. Time-lapse confocal microscopy of an embryo progressing towards ventral enclosure confirmed that GFP–PCN-1 localization did not change in either ABplpappap or a second, unidentified extruding cell, indicating that S phase was arrested in both cells during the period that ended in their extrusion (Fig. 2e, Supplementary Video). Nearly all cells extruded from *ced-3(lf)* embryos displayed bright sub-nuclear foci of GFP–PCN-1 (Supplemental Fig. 4e, f). We

conclude that cells extruded by *ced-3(lf)* embryos enter the cell cycle before extrusion, arrest in S phase, and are then extruded. The treatment of embryos with RNAi against *cye-1* or *cdk-2* markedly altered the localization of tDHB–GFP and GFP–PCN-1 in ABplpappap. tDHB–GFP localized to the ABplpappap nucleus (Fig. 2c) and GFP– PCN-1 was diffusely nuclear in ABplpappap (Fig. 2d) in *cye-1(RNAi)* and *cdk-2(RNAi)* embryos both before (five of five embryos each) (Supplemental Fig. 3a, c) and after ventral enclosure (five of five embryos each) (Supplemental Fig. 3b, d). These observations show that ABplpappap fails to enter the cell cycle in embryos with reduced CYE-1 and CDK-2 and indicate that progression to S phase is required for cell extrusion. Next we tested whether the previously identified cell-extrusion regulators[3] *pig-1* and *grp-1* also promote S-phase arrest. Unexpectedly, we found that ABplpappap in *pig-1(RNAi)* embryos completed the cell cycle and divided into daughter cells before ventral enclosure (Supplemental Fig. 3e, Supplementary Video 5); virtual lateral sections confirmed that the daughter cells were not extruded (five of six embryos) (Fig. 2f). ABplpappap similarly divided to generate surviving daughters in *grp-1(RNAi)* embryos (six of six embryos) (Supplemental Fig. 3f). Thus, failure either to initiate the cell cycle, as in *cye-1(RNAi)* or *cdk-2(RNAi)* embryos, or to arrest at S-phase, as in *pig-1(RNAi)* or *grp-1(RNAi)* embryos (Fig. 2f, Supplemental Fig. 3f–h), is associated with impaired cell extrusion. Given that *pig-1* and *grp-1* regulate unequal cell divisions in multiple *C. elegans* cell lineages (for example, the QR/L neuroblast lineages[13]), we tested whether they control the unequal division of ABplpappa, which produces the extruded cell ABplpappap and a sister cell almost 2.5-fold larger in diameter (Fig. 2g, Supplemental Fig. 3i). Both *pig-1(RNAi)* and *grp-1(RNAi)* generated an abnormally large

ABplpap- pap cell (Fig. 2g, Supplemental Fig. 3i–k); by contrast, RNAi against *cye-1* or *cdk-2* did not affect the highly unequal ABplpappa division (Fig. 2g, Supplemental Fig. 3i, l, m). Thus, unequal cell division precedes S-phase cell-cycle arrest in the small daughter cell that is fated for extrusion, whereas an abnormally large ABplpappap is competent to complete the cell cycle.

Extruding cells show replication stress

We speculated that ABplpappap enters S-phase arrest because it inherits from the unequal ABplpappa division a pool of resources that is insufficient to support DNA replication. We therefore examined ABplpappap for evidence of replication stress using a reporter of RPA-1, the *C. elegans* homologue of mammalian replication protein A. RPA-1 binds in distinct nuclear foci to single-stranded DNA segments generated during replication stress[14]. We observed that an RPA-1–YFP fusion protein localized to a small number of distinct foci in ABplpappap in control embryos (Fig. 3a, b), indicating that this cell undergoes replication stress; other extruded cells exhibited a similar pattern of RPA-1–YFP foci (Supplemental Fig. 4g–j). By contrast, RPA-1–YFP was more diffuse in ABplpappap in *pig-1(RNAi)* or *cdk-2(RNAi)* embryos (Fig. 3b, Supplemental Fig. 5a, b), indicating, respectively, the absence of replication stress when ABplpappap is either abnormally large (with sufficient resources for DNA synthesis) or prevented from S-phase entry. In addition, most cells extruded from *ced-3(lf)* embryos displayed punctate TUNEL staining, indicative of limited DNA damage[15] (Fig. 3c, d) and unlike the diffuse staining of cells undergoing caspase-mediated apoptosis[16], such as those visible in *ced-5(lf)* embryos (Fig. 3c, d). This observation suggests that a replication-stress

response might limit TUNEL-reactive DNA damage[17] in extruded cells. In short, cells extruded by *ced-3(lf)* embryos exhibited multiple hallmarks of replication stress.

To determine whether the replication-stress response directly promotes cell extrusion, we treated *ced-3(lf)* animals with RNAi against genes that encode critical replication-stress response proteins: TopBP1 (*mus-101*), Claspin (*clsp-1*), Timeless (*tim-1*), Tipin (*tipn-1*), Rad9 (*hpr-9*), ATR (*atl-1*) and CHK1 (*chk-1*)[18]. These RNAi treatments produced a Tex phenotype (Figs. 1d, 3e), indicating that the replication-stress response pathway is necessary for cell extrusion. Furthermore, RNAi against *atm-1* (*ATM* homologue), *brc-1* (*BRCA1* homologue), or both *atl-1* (*ATR* homologue) and *chk-1* (*CHEK1* homologue) prevented ABplpappap extrusion in three to four of the ten embryos examined after each treatment, despite the presence of RPA-1–YFP foci in the unextruded ABplpappap cell (Fig. 3a, b, Extended Data Fig. 5c, d). Thus, inhibition of the canonical replication-stress response signaling pathway prevented extrusion of cells undergoing replication stress.

We hypothesized that the source of replication stress in ABplpappap and other extruded cells is an insufficient pool of DNA replication proteins or nucleotides resulting from the unequal division of their mother cells (for example, ABplpappa). We noted that genes previously identified from a screen for suppression of *lrr-1(lf)*-induced sterility[19] also suppressed cell extrusion by *ced-3(lf)* animals (Supplemental Fig. 5e). *lrr-1* encodes an adaptor protein for the $CRL2^{LRR\text{-}1}$ E3 ubiquitin ligase and is required for the disassembly of terminated replisomes[20,21]. Loss of *lrr-1* produces abnormalities in mitotic germline cells similar to those we observed in cells extruded from *ced-3(lf)* embryos: activation of the ATL-1–CHK-1-dependent replication-stress response, S-

phase arrest, and DNA damage[22]. In addition, we found that *lrr-1(RNAi)* caused ectopic extrusion of unidentified cells in a wild-type background (Fig. 3f, g). These findings indicate that LRR-1 insufficiency in the small ABplpappap cell can drive its extrusion from *ced-3(lf)* embryos, presumably by preventing the efficient removal of terminated replisomes. We also found that RNAi against a gene required for pyrimidine nucleotide synthesis (*pyr-1*) or a gene required for the maintenance of purine nucleotide balance (*gmpr-1*) similarly caused ectopic extrusion of unidentified cells in wild-type animals (Fig. 3g, Supplemental Fig. 5f). (The *C. elegans* gene *F32D1.5* is referred to here as *gmpr-1*. A request to change the name of *F32D1.5* to *gmpr-1* has been approved by WormBase and this change will be reflected in a future WormBase release.) *pyr-1* and *gmpr-1* encode the *C. elegans* homologues of mammalian CAD and GMP reductase enzymes, respectively. Thus, perturbation of nucleotide levels is sufficient to drive cell extrusion. We propose that low levels of LRR-1 combined with insufficient nucleotide pools can result in replication stress and S-phase arrest in, and ultimately cell extrusion of, the small daughter cells of unequal cell divisions.

An evolutionarily conserved cell-extrusion mechanism

To test whether replication stress-mediated cell extrusion is an evolutionarily conserved process, we examined monolayers of Madin-Darby canine kidney (MDCK-II) cells treated with 2 mM hydroxyurea (HU) to induce replication stress[6,7] (Fig. 4a, Extended Data Fig. 6a) and measured the rate of apically directed cell extrusions via time-lapse microscopy. HU treatment increased the rate of cell extrusion from the MDCK-II monolayer by more than threefold over vehicle control (Fig. 4b, c,

Supplementary Videos 6, 7). Using MDCK-Fucci cells, which produce a cell-cycle phase-specific fluorescence (G0/G1, red; S/G2/M, green), we found that cells extruded stochastically from the monolayers (as observed with vehicle treatment) mostly exhibited red fluorescence indicative of the G0 or G1 phase (Fig. 4d). By contrast, most cells extruded from HU-treated monolayers displayed green fluorescence, consistent with S-phase arrest (Fig. 4d).

Several observations indicate that cell death (for example, apoptosis) did not cause the HU-mediated cell extrusions: (i) similar percentages of HU-induced and stochastically extruded cells showed trypan blue staining (Fig. 4e); (ii) cells extruded following HU treatment were viable and proliferated within 24 h of being cultured in fresh medium (Fig. 4f); and (iii) the caspase inhibitor zVAD-FMK did not prevent HU-induced cell extrusion (Fig. 4g, Supplemental Fig. 6b). These findings demonstrate that HU induces the extrusion of living cells.

Last, we tested the requirement for ATR and CHK1 in replication stress-mediated extrusions from MDCK-II cell layers. HU treatment significantly increased the level of phosphorylated ATR (pATR) in MDCK-II cells (Fig. 4h, Supplemental Fig. 6c). Also, the small molecule CHK1 inhibitors SB 218078 and PF477736 suppressed HU-induced cell extrusion (Fig. 4g, Supplemental Fig. 6b), indicating that HU-induced mammalian cell extrusion requires the ATR–CHK1 pathway. In mammals, the ATR–CHK1-mediated replication-stress response activates p53[23]. HU treatment increased p53 levels, as did treatment with Nutlin-3, a chemical activator of p53 (Extended Data Fig. 6d, e). Furthermore, the p53 inhibitor pifithrin-α (PFT) completely suppressed HU-induced cell extrusion (Fig. 4g, Supplemental Fig. 6b). Although Nutlin-3 increased extrusion rates of

MDCK-II cells (Fig. 4g), it did not result in replication stress (Fig. 4a, Supplemental Fig. 6a), indicating that p53 activation is sufficient to induce cell extrusion in the absence of replication stress.

Discussion

Our findings are summarized in Fig. 4i and suggest the following four-step mechanistic model for replication-stress induced cell extrusion (Fig. 4j): (i) a cell in S phase experiences replication stress following a genotoxic insult (for example, HU) or the inheritance of insufficient replicative resources from an unequal cell division; (ii) ATR and CHK1 (and p53 in mammals) mediate a replication-stress response; (iii) cell adhesion molecules are downregulated[3], possibly through inhibition of CDK1, a regulator of cell adhesion during S phase[24]; and (iv) the cell is extruded as a consequence of this reduced adhesion[25] and mechanical forces generated by neighboring cells (for example, constrictive forces preceding ventral enclosure in developing *C. elegans* embryos[26]) or physiological crowding[27].

Our finding that replication stress drives cell elimination by extrusion for both *C. elegans* and mammalian cells demonstrates that cell extrusion in *ced-3(lf)* embryos is not simply a result of the genetic perturbation of the caspase-mediated apoptosis pathway and indicates that this mechanism is evolutionarily conserved. The cell cycle is similarly conserved and is ancient. As cell elimination caused by an inducible cell-cycle state does not require specialized molecular or cellular machinery (unlike caspase-mediated apoptosis and phagocytosis), we propose that replication-stress-driven cell extrusion is a primordial process of cell elimination. The observation that cells targeted

for caspase-dependent cell death extrude when caspases are inactivated suggests that extrusion as a primitive form of cell elimination has in some instances been supplanted by caspase-mediated apoptosis. We further suggest that a developmentally controlled replication-stress response might be used by metazoans for cell elimination via extrusion in a variety of biological contexts.

Replication stress and cell extrusion are key features of cancer biology[1,28], but their relationship has not been explored. We pro- pose that the extrusion of cells undergoing replication stress can be tumour-suppressive. Non-cancerous cells that fail to respond to replication stressors can accrue DNA damage, genomic rearrangements and ploidy defects associated with oncogenesis[28]. Pre-cancerous and cancerous cells experience persistent replication stress[28] resulting from the overexpression, amplification or mutational activation of genes that drive uncontrolled proliferation. In such contexts, cell extrusion activated by replication stress could function as an early checkpoint to eliminate pre-cancerous and malignant cells.

In other contexts, cell extrusion induced by replication stress might be subverted to promote metastatic tumorigenesis. Indeed, the mouse p53 R172H mutation (equivalent to the R175H mutation common to human tumours) causes a high frequency of metastatic tumours[29,30]. Mouse p53(R172H) induces a replication-stress response by increasing both CHK1 expression and basal CHK1 phosphorylation[31,32]. We suggest that this ectopic replication-stress response triggers the extrusion of cells harbouring this mutation and that an oncogenic mutation in APC or K-RAS[5], or perhaps p53(R172H) itself, reverses the direction of extrusion from apical (causing elimination) to basal (causing dis- semination) to promote metastasis. In addition, reports that

chemo- therapeutic inhibitors of DNA replication, such as doxorubicin and cyclophosphamide, promote the metastatic spread of tumour cells[33] also support this notion.

In short, we have identified a conserved mechanism that links replication stress to the process of cell extrusion. We suggest that cell extrusion driven by replication stress is a primordial mechanism of cell elimination common to all metazoa and that cell extrusion arising from replication stress regulates the survival and spread of tumour cells.

Acknowledgements

We thank S. van den Heuvel and the CGC, which is funded by NIH Office of Research Infrastructure Programs (P40 OD010440), for providing strains; L. Hufnagel and X. Trepat for providing MDCK-Fucci cells; G. van Meer and the ECACC for providing MDCK-II cells (ECACC 62107); N. An for strain management; S. Luo, S. R. Sando, E. L. Q. Lee, A. Doi, A. Corrionero and other members of the Horvitz laboratory for helpful discussions; and D. Ghosh, C. L. Pender, M. G. Vander Heiden, P. W. Reddien, and R. O. Hynes for suggestions regarding the manuscript. This work was supported by the Howard Hughes Medical Institute and by NIH grant R01GM024663. V.K.D. was a Howard Hughes Medical Institute International Student Research fellow. C.P.-P. was the recipient of Human Frontiers Science Program postdoctoral fellowship LT000654/2019-L. J.N.K. was supported by NIH grant R01GM024663. N.T. was supported by NIH Pre-Doctoral Training Grant T32GM007287. D.P.D. was supported by postdoctoral fellowships from the Damon Runyon Cancer Research Foundation and

from the Charles A. King Trust. J.R. and C.P.-P. were funded by King's College London startup funds. H.R.H. is the David H. Koch Professor of Biology at MIT and an Investigator at the Howard Hughes Medical Institute.

Author contributions

H.R.H. supervised the project. V.K.D. and H.R.H. conceptualized the project. V.K.D. and H.R.H. designed the experiments that used *C. elegans*. V.K.D., R.D., J.N.K. and N.T. performed the experiments that used *C. elegans*. V.K.D., R.D. and D.P.D. generated reagents. C.P.-P. and J.R. designed the experiments that used mammalian cells. C.P.-P. performed the experiments that used mammalian cells. V.K.D., D.P.D. and H.R.H. wrote the original and revised manuscript drafts. All authors contributed to data analysis, interpretation, and reviewing and editing of the manuscript.

Competing interests

The authors declare no competing interests.

Methods

Strains

C. elegans hermaphrodite strains were maintained on nematode growth medium (NGM) plates containing 3 g/l NaCl, 2.5 g/l peptone and 17 g/l agar supplemented with 1 mM $CaCl_2$, 1 mM $MgSO_4$, 1 mM KPO_4 and 5 mg/l cholesterol with *E. coli* OP50 as a source of food[34]. All strains were derived from Bristol N2. *ced-3(lf)* refers to the *n3692* deletion allele of *ced-3*[3]. *cye-1(lf)* refers to the *eh10* allele of *cye-1*[35]. *ced-5(lf)* refers to

the *n1812* allele of *ced-5*[36]. *C. elegans* strains carrying the transgenes *nIs861* and *isIs17* were maintained at 25 °C. All other strains were maintained at 22 °C. The transgenes and mutations used are listed below:

LGI: *nIs433[P$_{pgp-12}$::4xNLS::GFP::unc-54 3'UTR; p76-16B(unc-76(+))]*, *cye-1(eh10)*

LGII: *heSi192[P$_{eft-3}$::tDHB::eGFP::tbb-2 3'UTR + Cbr-unc119(+)]*

LGIII: *unc-119(ed3)*

LGIV: *ced-3(n3692), ced-5(n1812)*

LGV: *ltIs44[P$_{pie-1}$::mCherry::PH(PLC1delta1) + unc-119(+)]*

LGX: *nIs434[P$_{pgp-12}$::4xNLS::GFP::unc-54 3'UTR; p76-16B(unc-76(+))]* Unknown linkage: *stIs10026[P$_{his-72}$::HIS-72::GFP]*, *isIs17[pGZ295(P$_{pie-1}$::GFP ::pcn-1(W03D2.4)), pDP#MM051 (unc-119(+))]*, *nIs861[pDD111(P$_{egl-1}$::mCherry::PH::unc-54 3'UTR)]*, *nIs632[pDD111(P$_{egl-1}$::mCherry::PH::unc-54 3'UTR), pML902 (dlg-1::GFP),p76-16B(unc-76(+))]*, *opIs263[P$_{rpa-1}$::rpa-1::YFP + unc-119(+)]*

Extrachromosomal array: *nEx3043[cye-1(+); P$_{sur-5}$::RFP]*

nIs632 and *nIs861* express membrane-localized mCherry from the *egl-1* promoter, which facilitated the identification of ABplpappap (an *egl-1*-expressing cell). *nIs632* does not express *dlg-1::GFP*, presumably as a result of partial transgene silencing[37–39]. *stIs10026*[40] ubiquitously expresses a GFP-tagged histone HIS-72 from its endogenous promoter, which produces fluorescence in the nuclei of all cells and helps to high- light extruded cells with respect to surrounding unextruded cells.

The following strains were used: N2 (Wild-type strain), MT4434 *ced-5(n1812) IV*, MT12054 *ced-3(n3692) IV*, MT20083 *nIs433 I*, MT20084 *nIs434 X*, MT20117 *nIs433 I;*

ced-3(n3692) IV, MT20131 *ced-3(n3692) IV; nIs434 X*, MT26340 *cye-1(eh10)/hT2[qIs48] I; hT2[qIs48]/+ III; nIs434 X*, MT26342 *cye-1(eh10)/hT2[qIs48] I; hT2[qIs48]/+ III; ced-3(n3692) IV; nIs434 X*, MT26360 *cye-1(eh10)/hT2[qIs48] I; hT2[qIs48]/+ III; ced-3(n3692) IV; nIs434 X; nEx3043*, MT22450 *ced-3(n3692) IV; stIs10026; nIs632*, MT25639 *ced-3(n3692) IV; stIs10026; nIs861*, MT25640 *heSi192 II; ced-3(n3692) IV; nIs861*, MT25692 *ced-3(n3692) IV; ltIs44 V; stIs10026*, MT25807 *ced-3(n3692) IV; nIs861; isIs17*, MT26335 *ced-3(n3692) IV; ltIs44 V; opIs263*.
Strains MT25640, MT25692, MT25807 and MT26335 might carry the *unc-119(ed3)* mutation in the background, which is rescued by the transgenes *heSi192*, *ltIs44*, *isIs17* and *ltIs44* in these strains, respectively.

Plasmids and fosmids

pDD111 ($P_{egl\text{-}1}$*::mCherry::PH::unc-54 3′UTR*) was generated with the following steps: i) 6.8 kb of the *egl-1* promoter was amplified from genomic DNA with Phusion DNA polymerase using the primers 5′-CGCCTGCAGTTGAAATTTGGGGATATTTTGG-3′ and 5′- CGC GAGCTCCTGGAAATTAGTAAGGTTTTGAAGGGGG-3′; ii) the amplicon was digested with PstI and SacI (New England Biolabs) and ligated into pPD122.56, which encodes 4×NLS–GFP to generate $P_{egl\text{-}1}$*::4xNLS::GFP::unc-54 3′UTR*; iii) mCherry–PH (pleckstrin homology) sequence was amplified from pAA173 using primers 5′-CGCACCGGTCCAGATGGCTCAAACAAAGC-3′ and 5′- CGCGAATTC GGCACAAGTTCATTCACAGG-3′ and digested with EcoRI and AgeI (New England Biolabs) and ligated into pDD122.56 ($P_{egl\text{-}1}$*::4xNLS::GFP ::unc-54 3′UTR*), which generated the plasmid pDD122.56 ($P_{egl\text{-}1}$*::4xNL S::mCherry::PH::unc-54 3′UTR*); iv)

the 4×NLS sequence was removed with the primers 5′-ggagctcAGAAAAAATGGTCTCAAAGGGTG-3′ and 5′-CACCCTTTGAGACCATTTTTTCTGAGCTCC-3′ using QuikChange Site-Directed Mutagenesis (Agilent) to generate pDD111 (*P_{egl-1}::mCherry::PH::unc-54 3′UTR*).

Sequences of all RNAi constructs that affected cell extrusion are provided in the Supplementary Information. RNAi clones were con- structed for *atl-1*, *mat-2* and *lin-15B*. Genomic regions of about 1 kb length were amplified from wild-type genomic lysates using Q5 Hot Start high-fidelity polymerase (New England Biolabs) with the following primers:

atl-1: 5′-TCGAATTCCTGCAGCTCCTCGAACCCATCATCCCT-3′; 5′-TGACGCGTGGATCCCATGAAGCTGCGTGGTTGTTG-3′. *mat-2*: 5′-TCGAATTCCTGCAGCCTGGAACTCATCCCATACGC-3′; 5′-TGACGCGT GGATCCCCATTGGAACCTCCAGATGCT-3′. *lin-15B*: 5′-TCGAAT TCCTGCAGCGCTGACACAATTGCGAACAT-3′; 5′-TGACGCGTGGATCCC CGTGTGCATAAAGACCAAGG-3′. *atl-1* + *chk-1*: *atl-1* fragment 5′-TCGAATTCCTGCAGCTCCTCGAACCCATCATCCCT-3′; 5′- ACACGACA GCGTCCGCAGAAATGAAGCTGCGTGGTTGTTG-3′; *chk-1* fragment 5′-TTCTGCGGACGCTGTCGTGTCAAGCGGATCCGTGGTATCA-3′; 5′- TGA CGCGTGGATCCCCCGAGTGCTCCACATTGACT-3′.

These inserts were cloned into the pL4440 vector linearized with XmaI (New England Biolabs) using the In-Fusion HD cloning kit (TaKaRa) according to the manufacturer’s instructions. The cloned vector was then transformed into competent HT115 bacterial cells. Correct RNAi clones were identified by Sanger sequencing.

Geneious 10.2.6 (Bio- matters, Inc.) was used to guide all plasmid design and construction.

The fosmid WRM0637bF05 (Source Bioscience), which contains the genomic *cye-1* sequence, was used for genomic rescue of the Tex phenotype in *cye-1(eh10); ced-3(n3692); nIs434* animals. A plasmid containing the sequence for $P_{sur\text{-}5}$*::RFP*, which expresses RFP cell-autonomously, was used as a fluorescent marker of cells carrying a mitotically unstable extrachromosomal array for genetic mosaic analysis.

Germline transformation

Germline transformation experiments were performed as described[41]. To generate the *cye-1*-rescuing transgene *nEx3043*, the fosmid WRM0637bF05, a plasmid containing the sequence for $P_{sur\text{-}5}$*::RFP* and 1 kb plus DNA ladder (Invitrogen), was injected into *hT2[qIs48]/ cye-1(eh10); ced-3(n3692); nIs434* animals at 3 ng/µl, 20 ng/µl and 80 ng/µl.

RNAi treatments

Previously described feeding RNAi constructs and reagents were used to perform RNAi feeding experiments[42,43]. In brief, HT115 *E. coli* bacteria carrying RNAi clones in the pL4440 vector were grown for at least 12 h in Luria broth (LB) liquid medium with 75 mg/l ampicillin at 37 °C. These cultures were seeded onto 6-cm Petri plates with NGM containing 1 mM isopropyl-β-d-thiogalactopyranoside (IPTG) (Amresco) and 75 mg/l ampicillin and incubated for 24 h at 22 °C. For imaging experiments using confocal microscopy, ten L4 animals were added to each RNAi plate

and imaging of progeny embryos was performed on the next day as described in 'Microscopy' (below). For excretory cell counts, five L4 animals were added to each RNAi plate and L3–L4 progeny were scored for the number of excretory cells, as described in 'Excretory cell counts' (below). If a bacterial clone targeting a certain gene was not available in previously constructed libraries[42,44], we generated our own RNAi clone as described in 'Plasmids and fosmids' (above). Each RNAi experiment included an empty pL4440 vector negative control. Larvae and embryos were randomly selected for experiments after RNAi treatment. Experiments requiring imaging of *C. elegans* embryos after candidate RNAi treatments could not be effectively blinded, as the RNAi treatments produced developmental phenotypes that made the identity of the target gene obvious.

Genome-wide RNAi screen

The ORFeome RNAi library was used to conduct a genome-wide RNAi screen[42]. For each day of the RNAi screen, all bacterial colonies from two 96-well plates were cultured for at least 12 h at 37 °C in LB with 75 mg/l ampicillin. These cultures were then pre-incubated with 1 mM IPTG (Amresco) for 1 h to maximize induction of dsRNA production. We prepared 24-well plates with each well containing 2 ml NGM with 1 mM IPTG (Amresco) and 75 mg/l ampicillin in advance and stored them at 4 °C until needed; they were brought to room temperature a few hours before seeding. Each bacterial colony culture was then seeded onto an individual well of a 24-well plate and incubated for 24 h at 20 °C. Three L4 animals were picked into a 10-µl drop of M9 medium, which facilitated their transfer into a well using a pipette. The progeny of these

three animals were screened 3 days later. Each set of RNAi clones screened also included a *pig-1* RNAi positive control and an empty pL4440 vector negative control. The scorer was blinded to the identity of the RNAi clones. Excretory cell counts were performed as described in 'Excretory cell counts' (below). Sanger sequencing was used to confirm the identities of RNAi clones that reproducibly generated a Tex phenotype for more than 10% of the animals scored.

Microscopy

All RNAi screens scoring excretory cells were performed using a Nikon SMZ18 fluorescent dissecting microscope.

DIC and epifluorescence images of L3-L4 larval stage animals carrying the transgene *nIs433[$P_{pgp\text{-}12}$::4xNLS-GFP]* or *nIs434[$P_{pgp\text{-}12}$::4xNLS-GFP]*, which mark the excretory cell and ectopic excretory-like cells, were obtained using a 63× objective lens (Zeiss) on an AxioImager Z2 (Zeiss) compound microscope and Zen Blue software (Zeiss).

For confocal microscopy of cell extrusion (or its absence) from *ced-3(lf)* embryos, embryos staged at the 200–300-cell stage were picked and mounted onto a glass slide (Corning) with a freshly prepared 2% agarose pad. Embryos with ventral surfaces facing the objective were selected for imaging. Confocal images of embryos were obtained using a 63× objective lens (Zeiss) on a Zeiss LSM800 confocal microscope.

For observing extrusion (or absence of extrusion) from *ced-3(lf)* embryos, we focused particularly on the cell ABplpappap, the identification of which is facilitated by its

central position on the ventral surface[45]. The fluorescent transgene *nIs861[P$_{egl-1}$::mCherry::PH]* or *nIs632[P$_{egl-1}$::mCherry::PH; dlg-1::GFP]*, which express the Pleckstrin homology domain of PLC-δ fused to mCherry from the promoter of *egl-1*, was used to label the membrane of the ABplpappap cell, an *egl-1*-expressing cell[3], to further facilitate cell identification. Another fluorescent transgene (*stIs10026[his-72::GFP]*, which expresses GFP-tagged HIS-72 histone protein) was used to label the nuclei of all cells to help to define ABplpappap's location within the embryo. Time-lapse confocal microscopy was used to monitor the location of ABplpappap in embryos, keeping the cell in view by refocusing on it every 30 s. Confocal imaging during a period of about 50 min ending in ventral enclosure (the point at which hypodermal cells meet on the ventral surface of the embryo) was sufficient to determine whether ABplpappap did or did not undergo extrusion. To determine whether specific RNAi treatments caused cell extrusion from wild-type embryos, RNAi-treated embryos were examined using a 63× objective lens (Zeiss) on a Zeiss LSM800 confocal compound microscope for the presence of one or more cell(s) outside the embryonic body and some such embryos with extruded cells were imaged.

To determine whether ABplpappap and other cells that are extruded entered the cell cycle, embryos carrying the transgene *heSi192[P$_{eft-3}$::tD HB::eGFP::tbb-2 3'UTR]* expressing a codon-optimized (for *C. elegans*) C-terminal fragment of human DNA helicase B, which translocates from the nucleus to the cytoplasm in response to the activity of the cell cycle CDKs 1 and 2[10], were examined using confocal microscopy after various RNAi treatments. *nIs861* labelled the membrane of ABplpappap with mCherry and facilitated cell identification in these embryos.

To determine the cell cycle phase of ABplpappap and other cells that are extruded, embryos carrying the transgene *isIs17[P$_{pie-1}$::GFP::PCN-1]* expressing GFP-tagged PCN-1 protein, which produces a phase-specific fluorescence intensity and localization pattern[11], were examined using confocal microscopy after various RNAi treatments. *nIs861* labelled the membrane of ABplpappap with mCherry and facilitated cell identification in these embryos.

For examining ABplpappap and other extruded cells for replica- tion stress, embryos carrying the transgene *opIs263[P$_{rpa-1}$::rpa-1::YFP]* expressing YFP-tagged RPA-1, which localizes to foci under conditions of replication stress[14], were examined using confocal microscopy after various RNAi treatments. *ltIs44[P$_{pie-1}$::mCherry::PH]* labelled the mem- brane of all cells with mCherry and facilitated the identification of cell boundaries in these embryos. Microscopy for the genetic mosaic analysis experiments are described in the 'Mosaic analysis' section below.

Images were processed with ImageJ software (NIH), Photoshop CC 2019 (Adobe) and Illustrator CC 2019 (Adobe) software. The Time Stamper function in the Stowers ImageJ plugin was used to mark elapsed time on time-lapse videos.

Excretory cell counts

Excretory cell counts were performed using a dissecting microscope equipped with fluorescence at a total magnification of 270×. For the genome-scale RNAi screen, roughly 50 animals were examined in each well of a 24-well plate, and any well with more than five animals with two excretory cells was marked for confirmatory testing. Excretory cell counts in confirmatory RNAi experiments, candidate RNAi experiments

and experiments with genetic mutants were conducted using 6-cm Petri plates with appropriate medium. Animals were first immobilized by keeping the Petri plates on ice for 30 min. At least 100 animals at the L3–L4 larval stage were scored for each genotype or RNAi experiment unless there was extensive lethality or a growth defect, in which case a lower number or earlier-stage animals, respectively, were scored. A cell was scored as an excretory or an excretory-like cell if it were located in the anterior half of the animal and its nucleus had strong GFP expression.

Mosaic analysis

To perform mosaic analysis, transgenic animals of the genotype *hT2[qIs48]/cye-1(eh10); ced-3(n3692); nIs434; nEx3043[cye-1(+); P$_{sur-5}$::RFP]* were generated. Progeny of animals that lost the *hT2* balancer and were of the genotype *cye-1(eh10); ced-3(n3692); nIs434; nEx3043* were examined for the Tex phenotype. Ten such animals that displayed the Tex phenotype despite carrying the *cye-1*-rescuing array were examined using confocal microscopy with 63× (Zeiss) or 100× (Zeiss) objective lenses for the presence of the RFP-expressing extrachromosomal array in multiple cells, including the excretory cell (identified by the presence of distinctive canals extending from the cell body) and ABplpappap. Because the majority of these animals showed the presence of the rescuing array in the excretory cell, but not in ABplpappap, only the sublineage containing these cells was further analyzed.

Calculation of cell size

Confocal micrographs were obtained for multiple focal planes starting at the ventral surface and ending at the dorsal surface of the embryo, with each plane separated by a distance of 0.37 μm. The greatest area occupied by a cell in any plane was designated the ‘maximum area’ of a cell.

To determine the ratio of diameters of ABplpappaa and ABplpappap, the square root of the mean of the area ratios was calculated and the two cells were assumed to be perfect spheres.

Generation of virtual lateral sections

Confocal micrographs were obtained for multiple focal planes starting at the ventral surface and ending at the dorsal surface of embryos that had completed epidermal ventral enclosure, with each plane separated by a distance of 0.37 μm. A virtual lateral section for each *Z*-stack was generated at the plane perpendicular to the left–right axis that bisected ABplpappap using the Orthogonal Views function of Fiji[46].

Fluorescence signal quantification tDHB–GFP

The ABplpappap nuclear boundary, cell membrane boundary and tDHB–GFP fluorescence signal were identified using the DIC, mCherry and GFP channels, respectively, of confocal images of RNAi-treated *ced-3(lf)* embryos expressing the transgenes *heSi192* and *nIs861*. Mean tDHB–GFP fluorescence intensities inside the nuclear region, entire cell and background were quantified using Fiji software[46]. Mean cytoplasmic tDHB–GFP fluorescence intensity was calculated us- ing the formula $I_{\text{cytoplasm}} = ((I_{\text{cell}} \times \text{cell area}) - (I_{\text{nucleus}} \times \text{nucleus area}))/(\text{cell area} - \text{nucleus area})$,

where $I_{cytoplasm}$, I_{cell} and $I_{nucleus}$ denote the mean tDHB fluorescence intensity in the cytoplasm, cell and nucleus, respectively. The ratio of nuclear-to-cytoplasmic tDHB fluorescence intensity in Fig. 2c was adjusted for background fluorescence (measured from a random area outside the embryo boundaries); that is, the background fluorescence intensity was subtracted from both nuclear and cytoplasmic fluorescence intensity values before the ratios were calculated.

GFP–PCN-1 and RPA-1–YFP

The ABplpappap nucleus was identified from the DIC channel of confocal images of RNAi-treated *ced-3(lf)* embryos expressing the corresponding transgenes. The coefficient of variation (ratio of s.d. to mean) of fluorescence intensity inside the nuclear region was used as a measure to differentiate between diffuse and punctate fluorescence signals and was quantified using Fiji software[46]. In brief, highly localized fluorescence signals were expected to have pixel fluorescence intensity values that were either much higher or much lower than the mean fluorescence intensity of an area of interest, whereas a diffuse fluorescence signal was expected to have pixel intensity values that were closer to the mean fluorescence intensity of an area of interest. A high variation from the mean would produce a high variance and hence a higher standard deviation and vice versa. As standard deviation is also influenced by fluorescence intensity, we used coefficient of variation as a measure of signal localization to remove any artefactual differences in fluorescence intensity among embryos.

TUNEL staining

TUNEL staining was performed as described[16] with the following modifications. After being frozen with liquid nitrogen, the embryos were fixed with 4% PFA/PBS, pH 7.4 for 15 min at room temperature and then permeabilized by incubation with 0.1% Triton X-100 in PBS for 10 min at room temperature. After washing, TUNEL staining was performed according to the manufacturer's (Roche, Switzerland) instructions. Stained embryos were mounted using Fluoroshield with DAPI mounting solution (Sigma-Aldrich) to visualize the nuclei.

Cell culture

The MDCK-II[47] cells were obtained from European Collection of Authen- ticated Cell Cultures (ECACC, 00062107, 19G037). MDCK-Fucci[48] cells (originally generated in L. Hufnagel's laboratory) were a gift from X. Trepat. The MDCK-II cell line was authenticated before shipping by ECACC. The MDCK-Fucci cell line was not authenticated. Both cell lines were tested for mycoplasma contamination before shipping. Both cell lines were cultured in Dulbecco's modified Eagle's medium (DMEM) supplemented with 10% fetal bovine serum and 1% penicillin/streptomycin in a humidified incubator at 37 °C with 5% CO_2.

Chemicals

We prepared 2 mM HU (Millipore Sigma, H8627) in culture medium before each experiment. Nutlin-3 (Tocris, 3984), Pifithrin-α (Focus Biomolecules, 10-2480), SB 218078 (Tocris, 2560), PF477736 (Tocris, 4277) and zVAD-FMK (Promega, G7231) stocks were prepared in DMSO and kept at −20 °C until needed, when dilutions were

prepared in culture medium for cell treatment for final concentrations of 10 μM, 10 μM, 30 nM, 5 nM and 50 μM, respectively.

Mammalian cell imaging

These assays were performed using 6-well plastic plates. Twenty thou- sand MDCK-II cells were seeded in each well and grown to confluence for 72 h. On the day of the experiment, cells were washed twice with PBS and treated with fresh medium or various chemicals in medium. After equilibration, plates were imaged at 15-min intervals for up to 24 h, using an Evos M7000 imaging system equipped with a humidified onstage incubator (37 °C, 5% CO_2). Several positions per well were imaged in the phase contrast and green and red fluorescence channels (when applicable) available in this system.

Mammalian cell extrusion quantification

In time-lapse phase contrast images, extruding cells are easily identifiable as bright, white, rounded spots emerging from the epithelial plane. We counted the number of cells with these features for each condition using the Cell Counter plugin of Fiji[46]. The number of cell extrusions per XY position was quantified without knowing the corresponding treatment. Extrusions are reported as the number of extruding cells per hour for comparison between experiments of different duration.

Mammalian cell-cycle phase determination

The Fucci system differentially labels the nuclei of cells in G1 (red) and S/G2/M (green) phases[49]. Images of MDCK-Fucci cells with HU or control treatment were obtained in the phase contrast, red and green fluorescence channels as described in 'Mammalian cell imaging' (above). For each position, a multi-channel stack was built using Fiji[46]. After we iden- tified an extruded cell in the phase contrast channel, we determined the cell cycle phase using the fluorescence channels.

Mammalian re-seeding experiments

At the end of an imaging experiment, supernatants were collected and centrifuged (1,200 rpm, 5 min, room temperature). Pellets were re-suspended in 50 µl PBS, and 10 µl of the suspension was used for cell counting with Trypan blue in a Neubauer chamber, allowing us to simultaneously calculate the number of cells being re-seeded and the fraction of cells that was dead. The remaining cells were seeded with 1 ml fresh medium in a 24-well plate and grown in the cell culture incubator. Images were obtained at 2 h and 24 h for cell counting.

Mammalian cell immunostaining

Cells were fixed in 4% PFA-PBS for 20 min at 37 °C, permeabilized with 0.5% Triton X-100-PBS for 5 min at room temperature and stained with primary antibodies (all 1:250 in 1% BSA-PBS: p53, abcam ab26; phospho-ATR (Ser248), ThermoFisher 720107; phospho-histone H2A.X (Ser139), Cell Signaling 9718) overnight at 4 °C, and secondary antibodies (with 1:500 AF647 phalloidin and 30 µg/ml Hoechst) for 1 h at room temperature. We used 1× PBS for washing between steps and preparation of all

solutions. Samples were mounted with Fluoromount-G Mounting Medium (Invitrogen 00-4958-02).

Fixed mammalian cell imaging

Samples were imaged using 20× air and 60× oil objectives of a Nikon Eclipse Ti2-E microscope equipped with a Yokogawa CSU-W1 spinning disk system, an Andor DU-888 camera, and a Toptica multi-laser bed. All settings were kept constant between conditions.

Quantification of mammalian cell staining

All images were quantified with ad hoc Cell Profiler[50] pipelines. In brief, the IdentifyPrimaryObjects, MeasureObjectIntensity, and ExportTo- Spreadsheet modules were used sequentially for nuclear segmentation (Hoechst channel), nuclear intensity measurements (p53, pATR, or γH2AX channels) and data export, respectively. Cell staining analysis was automated, reducing the risk of human-originated bias.

Statistics and reproducibility

All experiments were repeated independently at least three times to ensure reproducibility. All representative micrographs are one example of five to ten biologically independent replicates of the same experiment, of which the remaining micrographs or quantification as a graph are provided in an associated figure panel, or have been described in the main text.

For calculation of statistical significance for fluorescence intensity and area ratios, the ratios were first transformed to logarithm values, with the assumption that logarithm of ratios produced a normal distribution of values. Normal distributions with unequal variances were assumed for coefficients of variance of GFP–PCN-1 and RPA-1–YFP signal fluorescence intensity. Normal distributions with unequal variances were assumed for rates of extrusion after different chemical treatments. No assumptions were made about the distributions of the rates of cell death under HU and vehicle treatments. Normal distributions with unequal variances were assumed for the fraction of extruded cells in different phases of the cell cycle after HU and vehicle treatments. Normal distribution was assumed for numbers of cells reseeded in fresh medium after pre-treatment in different conditions. As each mammalian-cell staining image contained from hundreds to thou- sands of cells, per-cell statistical analysis would result in extremely low *P* values. To avoid this sub-estimation, we first calculated descriptive statistics (median, average, s.d., *n*) for each image and made no assumptions about the distributions of these values for subsequent statistical analysis. All statistical analysis was performed using Prism (GraphPad Software). No statistical methods were used to predetermine sample size.

Figure 1. Cell-cycle genes control cell extrusion cell autonomously. a, Sublineage diagram showing the fate of ABplpappap (asterisk) in wild-type and *ced-3(lf)* animals and in *ced-3(lf)* animals that also had a defect in extrusion. **b**, **c**, Merged epifluorescence and Nomarski micrographs of the pharyngeal region of *nIs433[Ppgp-12::4×NLS-GFP]; ced-3(lf)* (**b**) and extrusion-defective *nIs433; ced-3(lf); pig-1(RNAi)* (**c**) animals[3]. **d**, The percentages of animals with the Tex phenotype in *ced-3(lf)* animals after the indicated RNAi treatment. **Identified from candidate RNAi screens; others identified from screen shown in Extended Data Fig. 1a. **e**, Merged epifluorescence and Nomarski micrographs of the pharyngeal region of *nIs433; ced-3(lf)* animals after the indicated RNAi treatment. **f**, **g**, Ventral and virtual lateral views of *ced-3(lf); stIs10026[his-72::GFP]; nIs632[Pegl-1::mCherry::PH]* embryos after the indicated RNAi treatment at the indicated time point. *t*ve, time point of ventral enclosure. **h**, Percentages of animals of the indicated genotypes with the Tex phenotype. **i**, Cell-lineage diagram showing the number of animals with the Tex phenotype carrying the *cye-1(+)*-rescuing array *nEx3043* in the indicated lineage or cell in ten *cye-1(lf); ced-3(lf); nIs434[Ppgp-12::4xNLS-GFP]* animals. **j**, **k**, Two confocal fluorescence micrographs of one of ten *cye-1(lf); ced-3(lf); nIs434; nEx3043* genetic mosaic worms represented in **i**. Arrowheads, excretory or ectopic excretory-like cells in **b**, **c**, **e**; ABplpappap in **f**, **g**. A, anterior; D, dorsal; R, right; V, ventral. Scale bars, 10 μm.

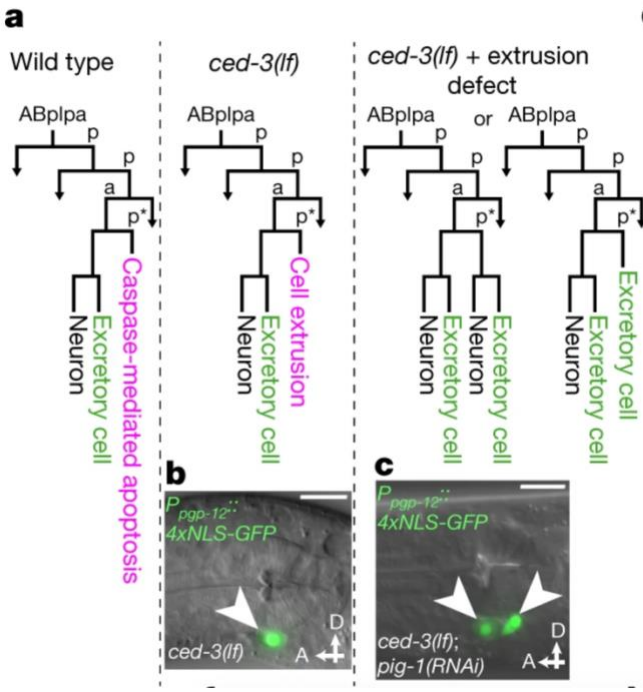

d

RNAi target gene	Percentage Tex (*n*)	Mammalian protein
Control	1 (107)	–
cdc-25.2	21 (159)	CDC25
cya-1	12 (363)	Cyclin A
cye-1	87 (165)	Cyclin E
cdk-1	15 (61)	CDK1
*cdk-2***	65 (181)	CDK2
psf-1 *psf-2* *psf-3*	36 (116) 39 (156) 50 (105)	GINS complex
csn-1 *csn-4* *csn-5*	43 (132) 47 (141) 39 (145)	COP9 signalosome
*atl-1***	9 (444)	ATR
*chk-1***	9 (220)	CHK1

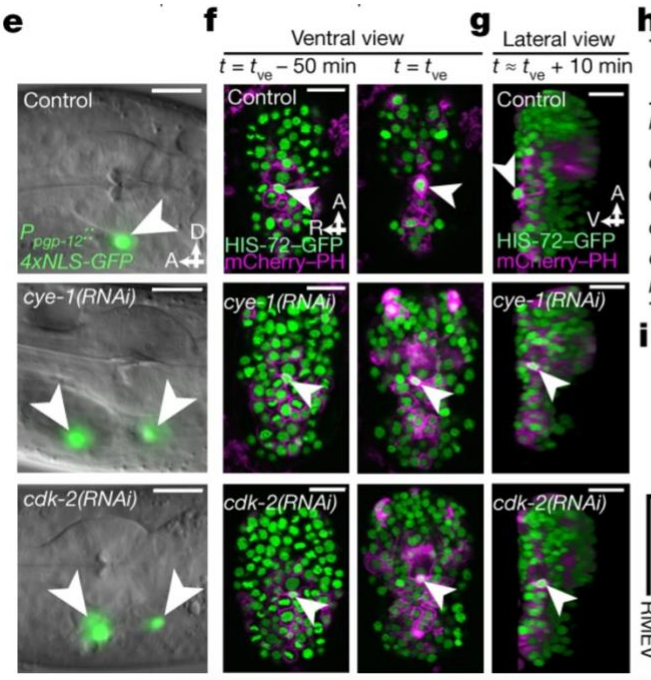

h

Genotype	Percentage Tex (*n*)
nIs434[Ppgp-12::4xNLS-GFP]	0 (100)
ced-3(n3692); nIs434	2 (100)
cye-1(eh10); nIs434	0 (100)
cye-1; ced-3; nIs434	69 (100)
cye-1; ced-3; nIs434; nEx3043[cye-1(+); Psur-5::RFP]	31 (100)

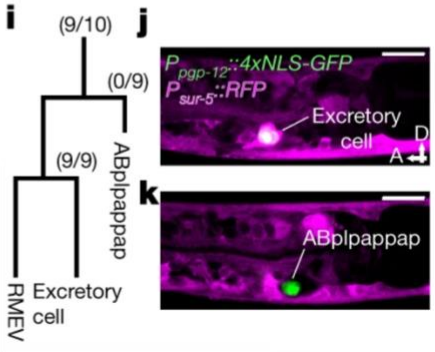

Figure 2. Cells undergoing extrusion arrest in S phase. a, Relative nuclear and cytoplasmic localization of a tDHB–GFP fusion protein in the indicated cell-cycle phases[10]. **b**, Localization pattern of GFP–PCN-1 in a typical *C. elegans* embryonic cell in the indicated cell-cycle phase. **c**, Nuclear:cytoplasmic ratio of tDHB–GFP fluorescence intensity in ABplpappap in *heSi192[P$_{eft-3}$::tDHB-GFP]; ced-3(lf); nIs861[P$_{egl-1}$::mCherry::PH]* embryos after the indicated RNAi treatment. **d**, Quantification of the coefficient of variation of GFP–PCN-1 fluorescence intensity in *ced-3(lf); isIs17[P$_{pie-1}$::GFP::pcn-1]; nIs861* embryos after indicated RNAi treatment. **e**, Time-lapse confocal fluorescence micrographs of GFP–PCN-1 fluorescence in ABplpappap (arrowhead and right insets) in *ced-3(lf); isIs17; nIs861* embryos at the indicated times after treatment with control RNAi. Arrow, unidentified extruding cell (left insets). **f**, Micrographs of virtual lateral section of *ced-3(lf); nIs861; stIs10026[his-72::GFP]* embryos showing either ABplpappap (left, arrowhead) or its daughter cells (right, arrowheads) after indicated RNAi treatment. **g**, Quantification of the ratio of the maximum area occupied by ABplpappap to that occupied by its sister cell, ABplpappaa, in *ced-3(lf); ltIs44[P$_{pie-1}$ ::mCherry::PH]; stIs10026* embryos after the indicated RNAi treatment. Insets, magnified view of ABplpappap or its daughter cells. Scale bars, 2 μm (**b**); 10 μm (all other micrographs). **c**, **d**, **g**, *n* = 10 embryos (biological replicates) for each RNAi treatment; mean ± s.d.; ordinary one-way ANOVA with Dunnett's correction for multiple comparisons. *P* values are indicated; NS, not significant.

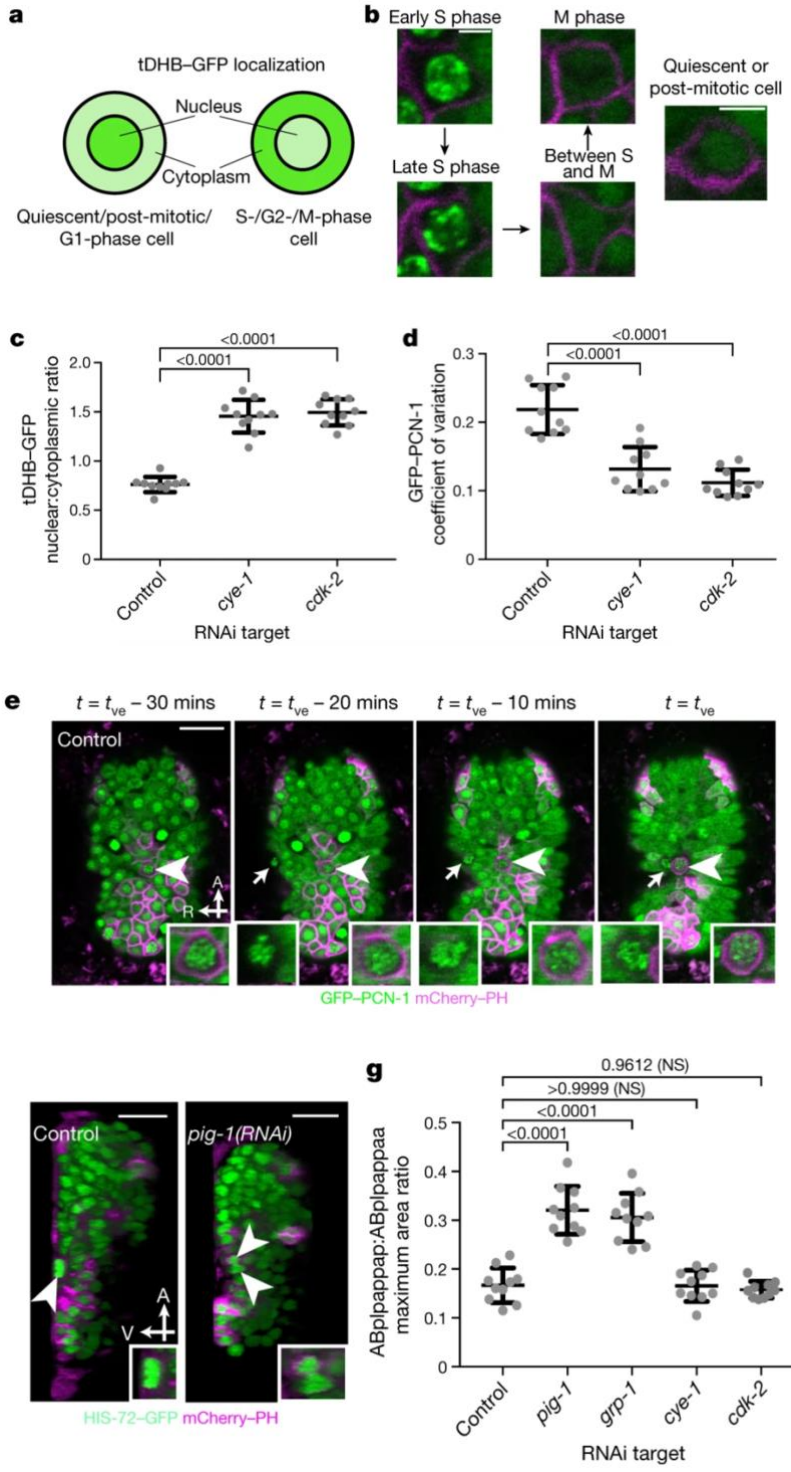
a
tDHB–GFP localization
Nucleus
Cytoplasm
Quiescent/post-mitotic/ G1-phase cell
S-/G2-/M-phase cell
b
Early S phase
M phase
Quiescent or post-mitotic cell
Late S phase
Between S and M
c
tDHB–GFP nuclear:cytoplasmic ratio
<0.0001
<0.0001
Control
cye-1
cdk-2
RNAi target
d
GFP–PCN-1 coefficient of variation
<0.0001
<0.0001
Control
cye-1
cdk-2
RNAi target
e
t = t_ve – 30 mins
t = t_ve – 20 mins
t = t_ve – 10 mins
t = t_ve
Control
A
R
GFP–PCN-1 mCherry–PH
f
Control
pig-1(RNAi)
A
V
HIS-72–GFP mCherry–PH
g
0.9612 (NS)
>0.9999 (NS)
<0.0001
<0.0001
ABplpappap:ABplpappaa maximum area ratio
Control
pig-1
grp-1
cye-1
cdk-2
RNAi target

Figure 3. Replication stress is coincident with and promotes cell extrusion.

a, Confocal fluorescence micrographs showing the localization of RPA-1–YFP in ABplpappap (arrowhead) in *ced-3(lf); ltIs44; opIs263[P$_{rpa-1}$::rpa-1::YFP]* embryos after the indicated RNAi treatment. Inset, magnified view of ABplpappap. Scale bars, 10 μm. **b**, Coefficient of variation of RPA-1–YFP fluorescence intensity in ABplpappap in *ced-3(lf); ltIs44; opIs263* embryos after the indicated RNAi treatments. *n* = 10 embryos (biological replicates) for each RNAi treatment; mean ± s.d.; *P* values shown for ordinary one-way ANOVA with Dunnett's correction for multiple comparison; NS, not significant. **c**, Merged Nomarski and fluorescence micrographs showing DAPI and TUNEL staining in extruded cells in embryos of indicated genotype. Scale bars, 2 μm. **d**, Percentage of observed extruded cells in embryos of the indicated genotypes with the indicated TUNEL staining pattern. **e**, Percentages of *ced-3(lf)* animals with the Tex phenotype after the indicated RNAi treatment along with mammalian homologues of the RNAi targets. **f**, Nomarski micrograph showing cells extruded (arrowheads) from wild-type embryos after *lrr-1(RNAi)*. Scale bar,
10 μm. **g**, Percentages of wild-type embryos exhibiting cell extrusion after the indicated RNAi treatments along with mammalian homologues of RNAi targets.

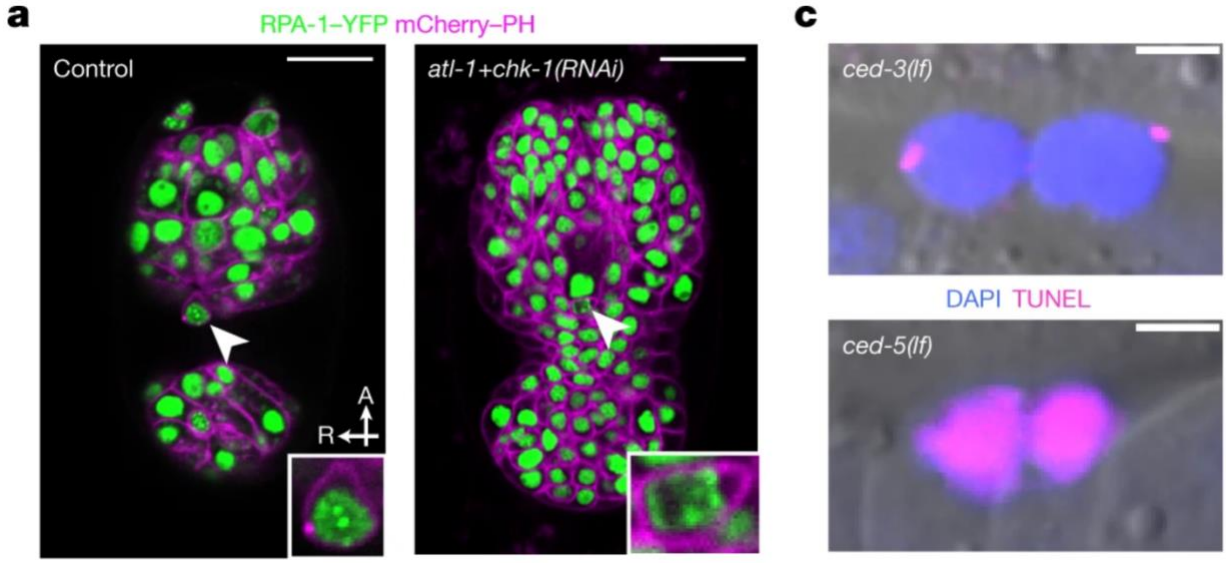

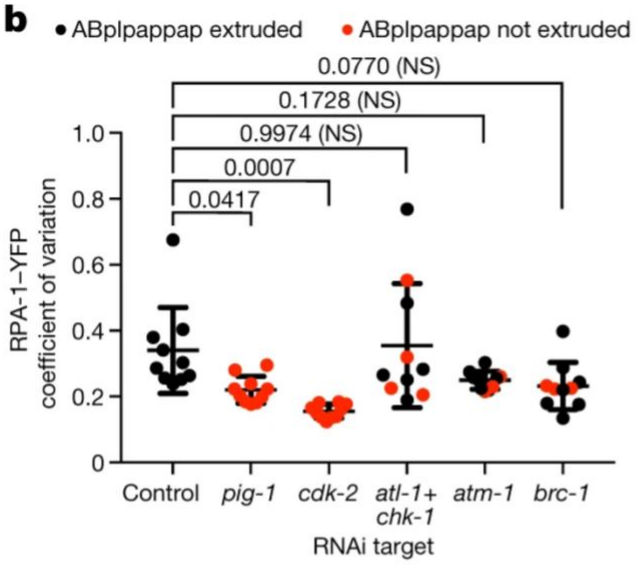

d

Genotype	TUNEL staining pattern			*n*
	Punctate	Diffuse	None	
ced-3(lf)	55%	15%	30%	40
ced-5(lf)	0%	88%	12%	40

e

RNAi target	Mammalian homologue	Percentage Tex	*n*
Control	–	4	235
hpr-9	*RAD9*	12	422
tim-1	*TIMELESS*	21	385
tipn-1	*TIPIN*	10	367
mus-101	*TOPBP1*	18	162
clsp-1	*CLSPN*	18	141

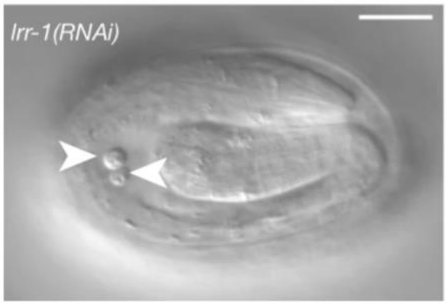

g

RNAi target	Mammalian homologue	Embryos with cell extrusion	*n*
Control	–	0%	100
lrr-1	*LRR1*	43%	100
gmpr-1	*GMPR1/2*	7%	100
pyr-1	*CAD*	18%	100

Figure 4. Replication stress promotes cell extrusion from a simple mammalian epithelial layer. a, Quantification of anti-γH2AX immunofluorescence signal in MDCK-II cells treated with vehicle, HU, or Nutlin-3. **b**, Representative micrographs of cells extruded (white rounded spots) from an MDCK-II monolayer after about 21 h of treatment with vehicle control (left) or HU (right). Scale bars, 100 μm. **c**, **g**, Quantification of extrusions per hour after the indicated treatments. **d**, The cell-cycle phases of cells extruded after treatment with vehicle control or HU. **e**, Percentage of extruded cells that stained with trypan blue after indicated treatments. **f**, The number of HU-treated or vehicle-treated extruded cells that adhered at 2 h and 24 h after reseeding in fresh medium. **h**, Quantification of anti-pATR immunofluorescence signal in vehicle- or HU-treated MDCK-II cells. **i**, **j**, Summary and model of replication-stress induced cell extrusion. Each data point, separate experiment in **c–g**; mean fluorescence intensity signal from one image of hundreds of cells in **a**, **h**. *n* = 7, 7 and 5 for vehicle, HU and Nutlin3, respectively (**a**); 5 each (**c**); 6 for vehicle, 5 for HU (**d**); 8 for vehicle, 6 for HU (**e**); 8 for vehicle, 6 for HU at 2 h and 7 each at 24 h (**f**); 13, 12, 6, 6, 5, 12 and 9 for vehicle, HU, HU + PFT, HU + zVAD-FMK, HU + PF477736, HU + SB218078 and Nutlin-3, respectively (**g**); 18 each (**h**), all biologically independent. All data in **a**, **c**–**h** are represented as mean ± s.d. Statistical analysis: Kruskal–Wallis one-way ANOVA followed by Dunn's correction (**a**); two-tailed Welch's *t*-test (**c**); ordinary one-way ANOVA with Sidak's correction (**d**, **f**, **g**); Mann–Whitney two-tailed test (**e**, **h**). *P* values are indicated; NS, not significant.

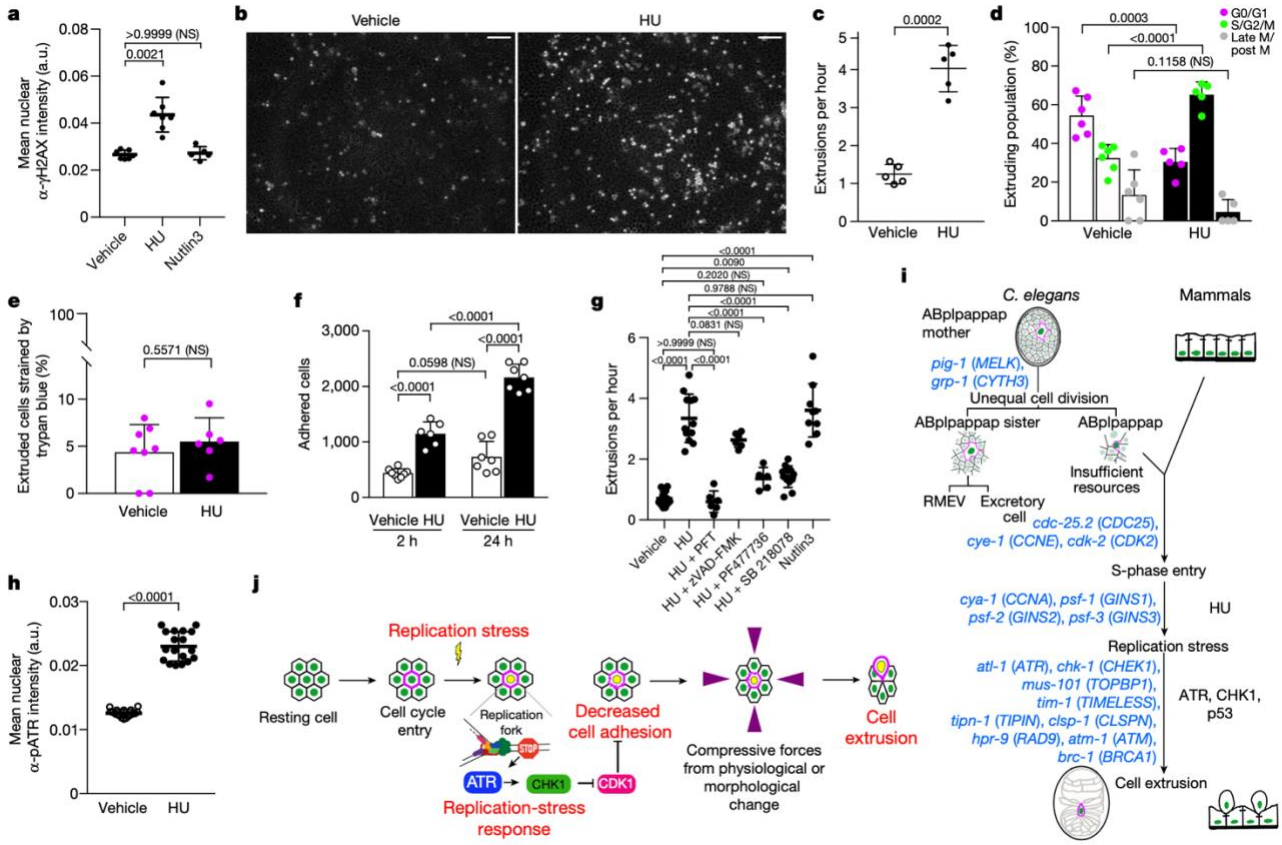
a
Mean nuclear α-γH2AX intensity (a.u.)
>0.9999 (NS)
0.0021
Vehicle
HU
Nutlin3
b
Vehicle
HU
c
Extrusions per hour
0.0002
Vehicle
HU
d
Extruding population (%)
0.0003
<0.0001
0.1158 (NS)
G0/G1
S/G2/M
Late M/ post M
Vehicle
HU
e
Extruded cells strained by trypan blue (%)
0.5571 (NS)
Vehicle
HU
f
Adhered cells
<0.0001
<0.0001
0.0598 (NS)
<0.0001
Vehicle HU
2 h
Vehicle HU
24 h
g
Extrusions per hour
<0.0001
0.0090
0.2020 (NS)
0.9788 (NS)
<0.0001
<0.0001
0.0831 (NS)
>0.9999 (NS)
<0.0001
<0.0001
Vehicle
HU
HU + PFT
HU + zVAD-FMK
HU + PF477736
HU + SB 218078
Nutlin3
h
Mean nuclear α-pATR intensity (a.u.)
<0.0001
Vehicle
HU
i
C. elegans
Mammals
ABplpappap mother
pig-1 (MELK), grp-1 (CYTH3)
Unequal cell division
ABplpappap sister
ABplpappap
Insufficient resources
RMEV
Excretory cell
cdc-25.2 (CDC25), cye-1 (CCNE), cdk-2 (CDK2)
S-phase entry
cya-1 (CCNA), psf-1 (GINS1), psf-2 (GINS2), psf-3 (GINS3)
HU
Replication stress
atl-1 (ATR), chk-1 (CHEK1), mus-101 (TOPBP1), tim-1 (TIMELESS), tipn-1 (TIPIN), clsp-1 (CLSPN), hpr-9 (RAD9), atm-1 (ATM), brc-1 (BRCA1)
ATR, CHK1, p53
Cell extrusion
Cell extrusion
j
Replication stress
Resting cell
Cell cycle entry
Replication fork
STOP
ATR
CHK1
CDK1
Replication-stress response
Decreased cell adhesion
Compressive forces from physiological or morphological change
Cell extrusion

Supplemental Figure 1. A genome-wide RNAi screen for the Tex phenotype revealed control of cell extrusion by *cye-1* and *cdk-2*. a, Schematic representation of the genome-wide RNAi screen for the Tex phenotype. RNAi using pL4440 empty vector was used as negative control and *pig-1(RNAi)* was used as positive control[3]. **b**, Time-lapse confocal fluorescence micrographs of *ced-3(lf); stIs10026[his-72::GFP]; nIs632[P$_{egl-1}$::mCherry::PH]* embryos after indicated RNAi treatment at the indicated times. *t*ve, time point of ventral enclosure. Arrowheads, ABplpappap. Scale bars, 10 μm.

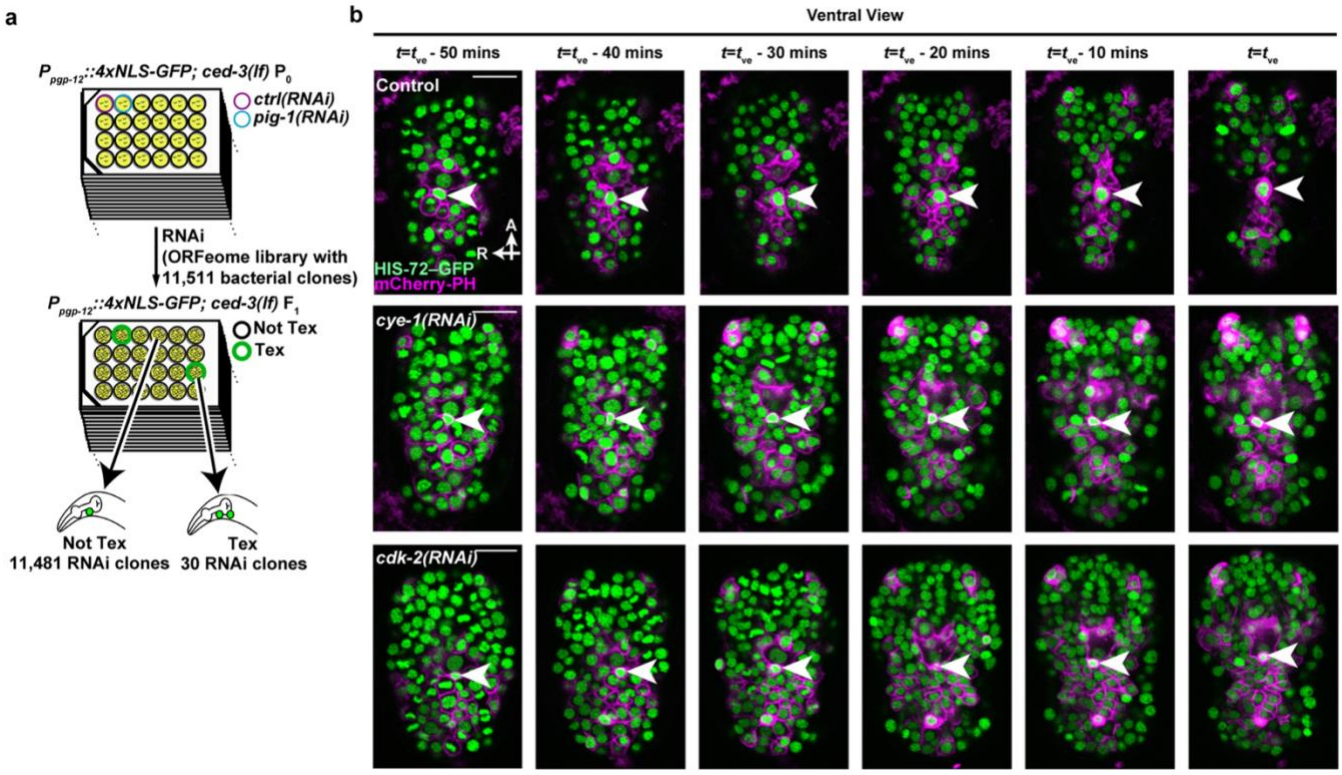
a
P_{pgp-12}::4xNLS-GFP; ced-3(lf) P_0
ctrl(RNAi)
pig-1(RNAi)
RNAi
(ORFeome library with
11,511 bacterial clones)
P_{pgp-12}::4xNLS-GFP; ced-3(lf) F_1
Not Tex
Tex
Not Tex
11,481 RNAi clones
Tex
30 RNAi clones
b
Ventral View
t=t_{ve} - 50 mins
t=t_{ve} - 40 mins
t=t_{ve} - 30 mins
t=t_{ve} - 20 mins
t=t_{ve} - 10 mins
t=t_{ve}
Control
A
R
HIS-72–GFP
mCherry-PH
cye-1(RNAi)
cdk-2(RNAi)

Supplemental Figure 2. Genetically mosaic *cye-1(lf); ced-3(lf)* animals with the Tex phenotype lack a *cye-1*-rescuing transgene in ABplpappap. a–**i**, Confocal micrographs showing the presence of the *cye-1(+)*-rescuing transgene in the excretory cell but not in ABplpappap (**a**–**h**) or in neither the excretory cell nor ABplpappap (**i**) of *cye-1(eh10); ced-3(n3692); nIs434[Ppgp-12 ::4xNLS-GFP]; nEx3043[cye-1(+); Psur-5::RFP]* animals with the Tex phenotype. Scale bars, 10 μm.

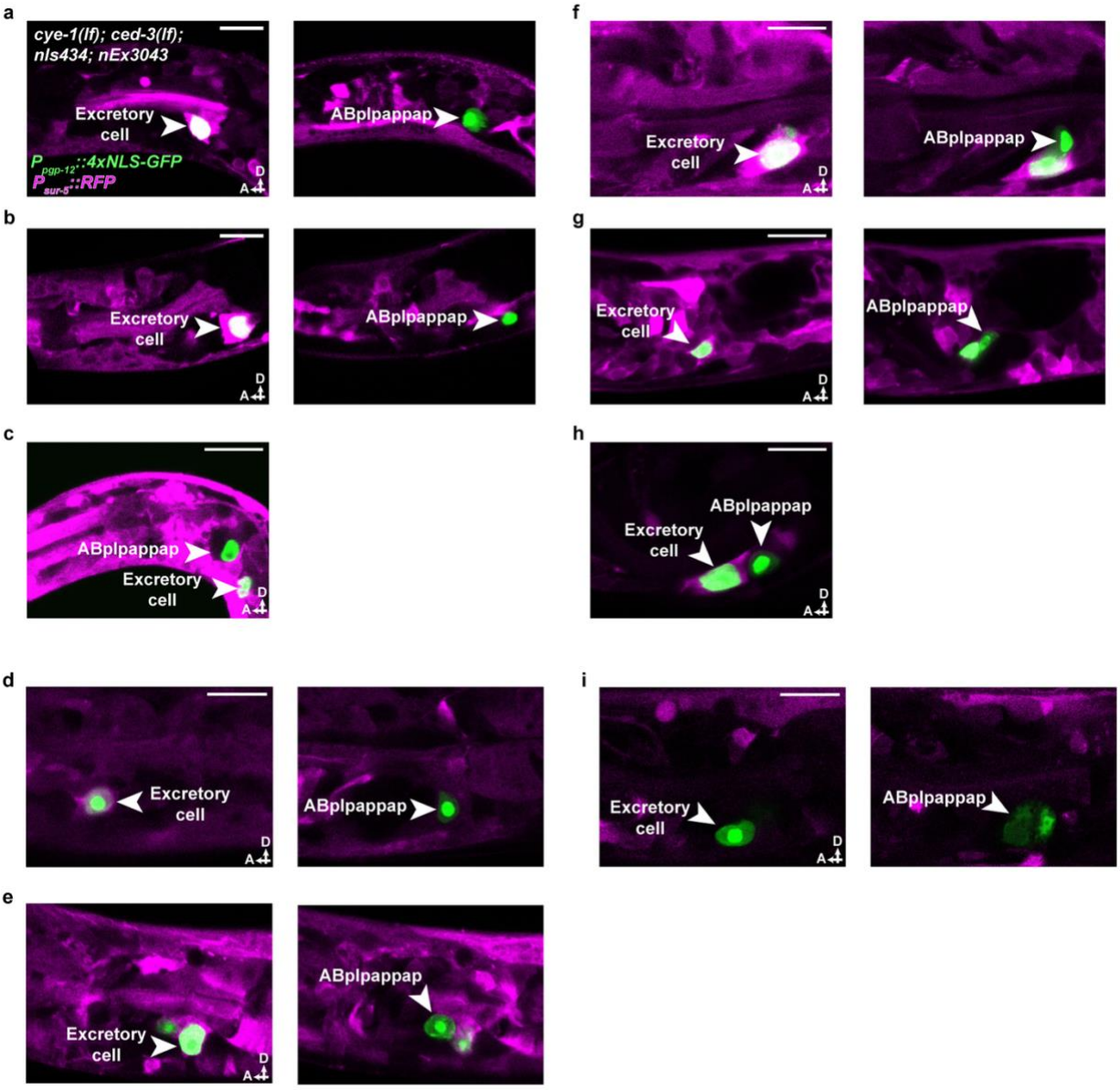
a
cye-1(lf); ced-3(lf);
nls434; nEx3043
Excretory cell
ABplpappap
b
Excretory cell
ABplpappap
c
ABplpappap
Excretory cell
d
Excretory cell
ABplpappap
e
Excretory cell
ABplpappap
f
Excretory cell
ABplpappap
g
Excretory cell
ABplpappap
h
ABplpappap
Excretory cell
i
Excretory cell
ABplpappap
D
A

Supplemental Figure 3. ABplpappap, which is generated by an unequal cell division, arrests in S phase and is extruded. a, **b**, Confocal fluorescence micrographs of tDHB–GFP fluorescence in ABplpappap (arrowheads) before (**a**) and after (**b**) ventral enclosure in *heSi192[Peft-3::tDHB-GFP]; ced-3(lf); nIs861[Pegl-1::mCherry::PH]* embryos after the indicated RNAi treatment. Dotted outline, ABplpappap nucleus, as identified by Nomarski optics. **c**, **d**, Confocal fluorescence micrographs of GFP–PCN-1 fluorescence in ABplpappap (arrowheads) before (**c**) and after (**d**) ventral enclosure in *ced-3(lf); isIs17[P*$_{pie-1}$ *::GFP::pcn-1]; nIs861* embryos after the indicated RNAi treatment. **e**, Time-lapse confocal fluorescence micrographs of GFP–PCN-1 fluorescence in ABplpappap (arrowheads) in a *ced-3(lf); isIs17; nIs861; pig-1(RNAi)* embryo at the indicated times. t_{ve}, time point of ventral enclosure. **f**–**h**, Micrographs of virtual lateral section of *ced-3(lf); nIs861; stIs10026* embryos showing either ABplpappap (arrowhead) or its daughter cells (arrowheads) after indicated RNAi treatment. **i**–**m**, Confocal fluorescence micrographs of *ced-3(lf); ltIs44[Ppie-1::mCherry::PH]; stIs10026* embryos showing the relative sizes of ABplpappap and its sister cell, ABplpappaa, in embryos after the indicated RNAi treatment. Insets, ABplpappap (**a**–**d**); ABplpappap or its daughters (**e–h**); magnified view of the region indicated, which includes ABplpappap (†) and ABplpappaa (*) (**i**–**m**). Scale bars, 10 μm.

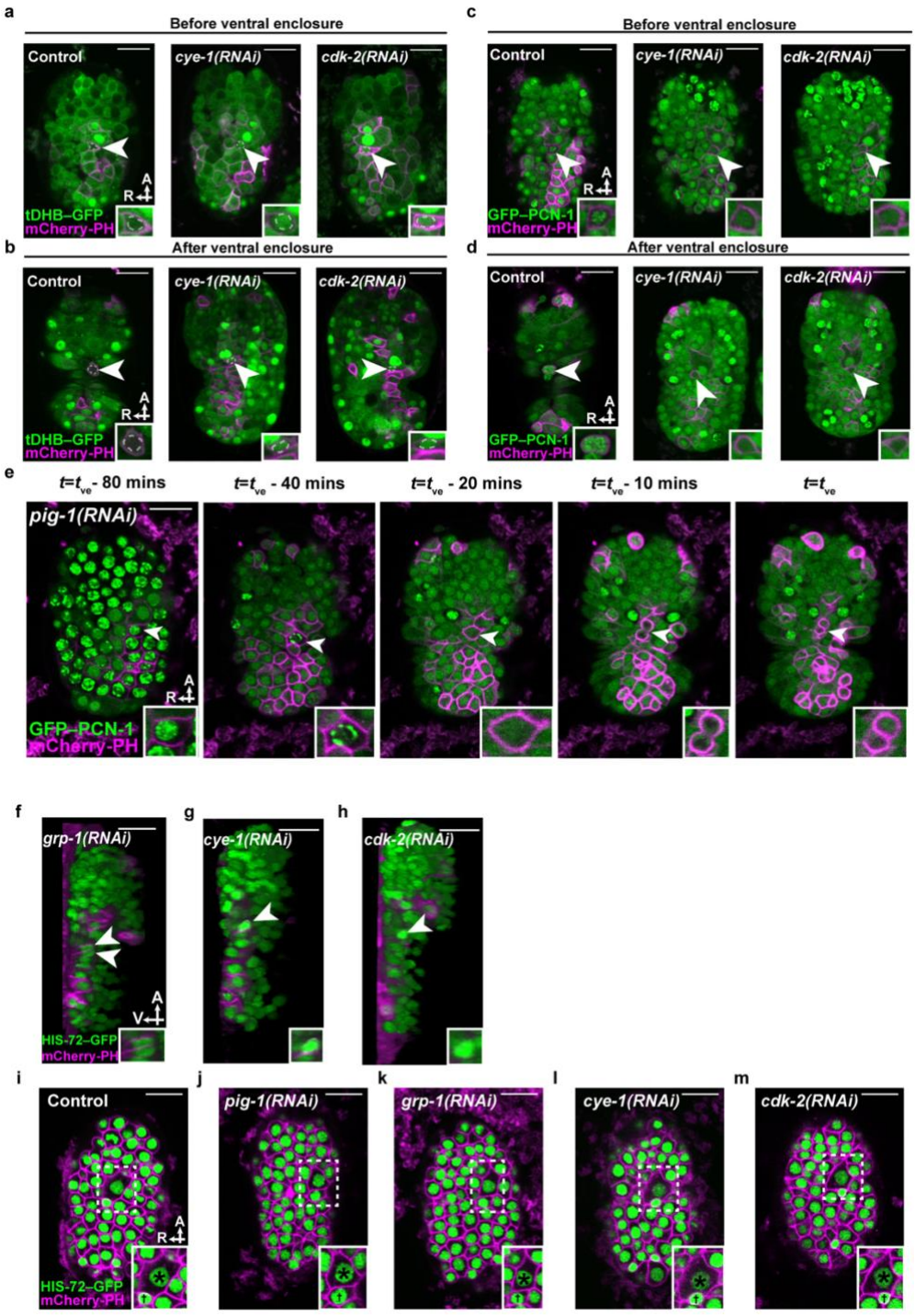
a
Before ventral enclosure
Control
cye-1(RNAi)
cdk-2(RNAi)
tDHB–GFP
mCherry-PH
b
After ventral enclosure
c
Before ventral enclosure
GFP–PCN-1
d
After ventral enclosure
e
t=tve - 80 mins
t=tve - 40 mins
t=tve - 20 mins
t=tve - 10 mins
t=tve
pig-1(RNAi)
f
grp-1(RNAi)
HIS-72–GFP
g
h
i
j
k
l
m

Supplemental Figure 4. All extruded cells display features of cell cycle entry, S-phase arrest, and replication stress. a–**d**, tDHB–GFP fluorescence in unidentified extruded cells from the anterior sensory depression (**b**), the ventral pocket (**c**), and the posterior tip (**d**) of a comma stage embryo of the genotype *heSi192; ced-3(lf); nIs861* after RNAi against empty vector control. Nuclei of extruded cells, as identified by Nomarski optics, are marked by dotted outlines. **e**, **f**, Micrographs of GFP–PCN-1 fluorescence in unidentified extruded cells (arrowhead) at the ventral pocket (**e**) or the anterior sensory depression (**f**) from *ced-3(lf); isIs17; nIs861* embryos after RNAi against empty vector control (**e**) or no RNAi (**f**). Insets, extruded cells marked by arrowheads in micrographs. **g**–**j**, RPA-1–YFP fluorescence in unidentified extruded cells from the anterior sensory depression (**h**, **i**) and ventral pocket (**j**) in a *ced-3(lf); ltIs44; opIs263[Prpa-1::rpa-1::YFP]* embryo after RNAi against empty vector control. Scale bars, 10 μm.

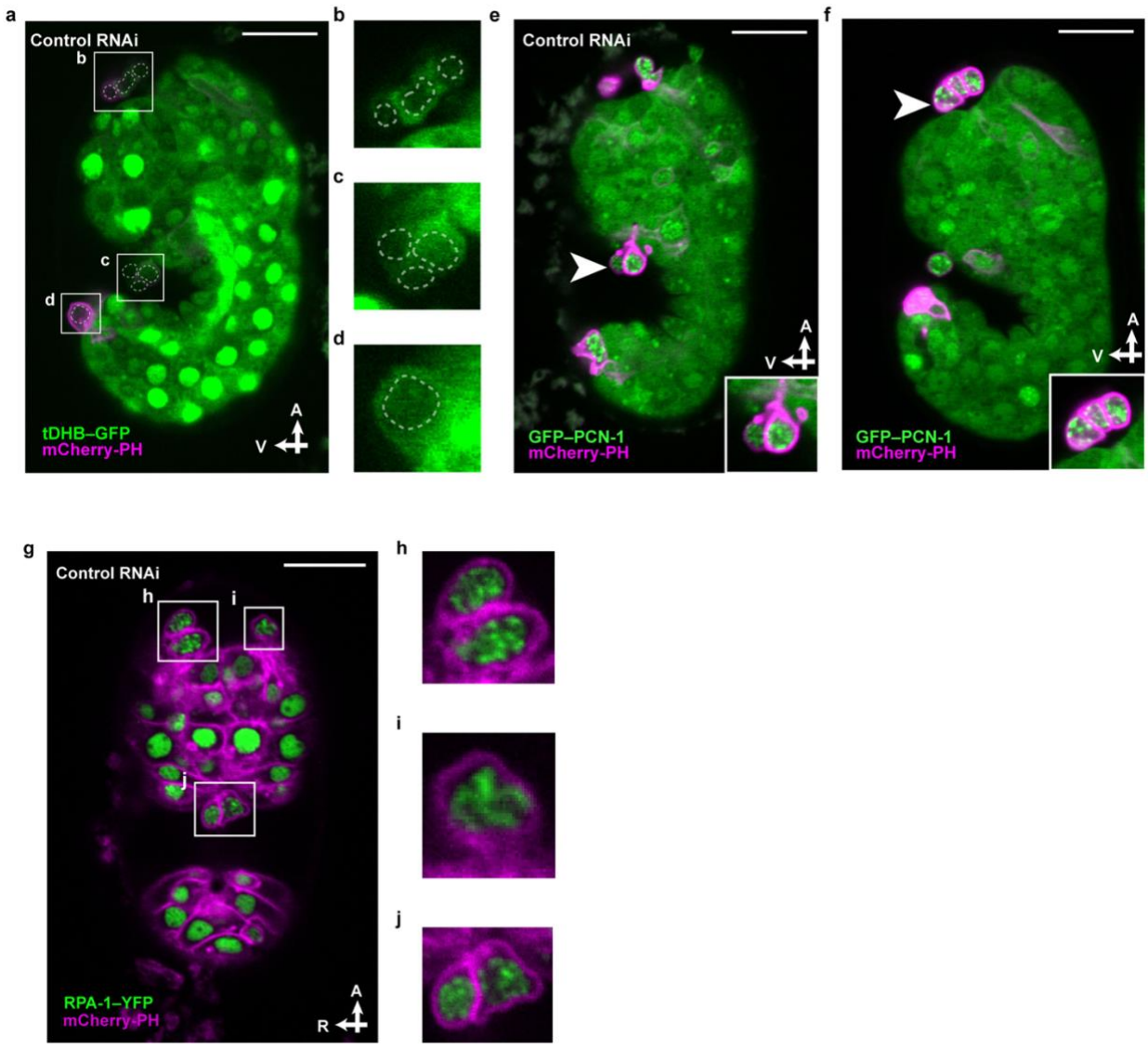
a
Control RNAi
b
c
d
tDHB–GFP
mCherry-PH
A
V
b
c
d
e
Control RNAi
GFP–PCN-1
mCherry-PH
A
V
f
GFP–PCN-1
mCherry-PH
A
V
g
Control RNAi
h
i
j
RPA-1–YFP
mCherry-PH
A
R
h
i
j

Supplemental Figure 5. The replication-stress response, probably caused by *lrr-1* and nucleotide insufficiency, promotes cell extrusion. a–**d**, Confocal fluorescence micrographs showing the localization of RPA-1–YFP in ABplpappap (arrowheads) in *ced-3(lf); ltIs44; opIs263* embryos after the indicated RNAi treatment. Insets, magnified views of ABplpappap. **e**, Genes identified as suppressors of the sterility of *lrr-1(lf)* mutants[19] were tested for suppression of cell extrusion. **f**, Nomarski micrograph showing a cell extruded (arrow) from a wild-type embryo after *gmpr-1(RNAi)* treatment. Scale bars, 10 μm.

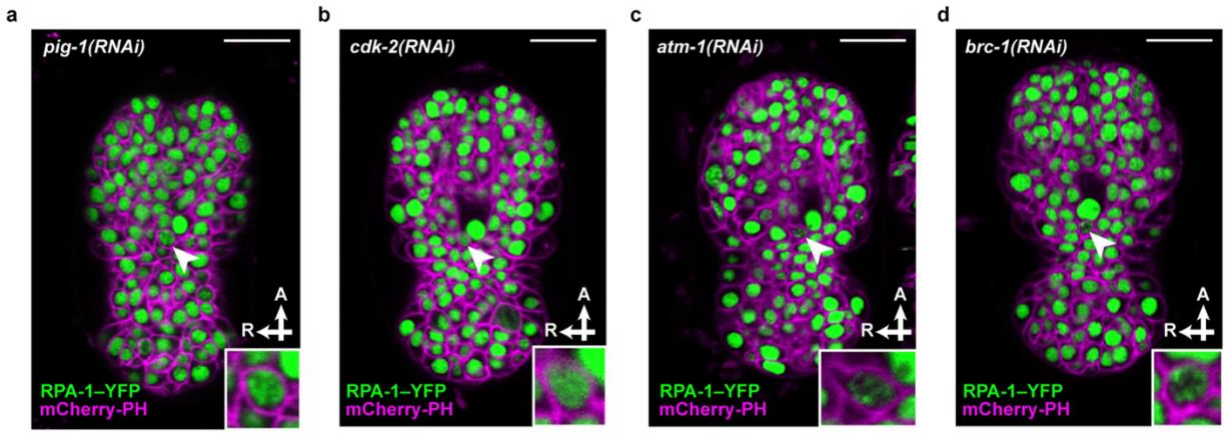

e

Suppressor of *lrr-1(lf)* sterility	Suppressor of *ced-3(lf)* extrusion?
atl-1	Yes
chk-1	Yes
mus-101	Yes
clsp-1	Yes
psf-2	Yes
psf-3	Yes

f

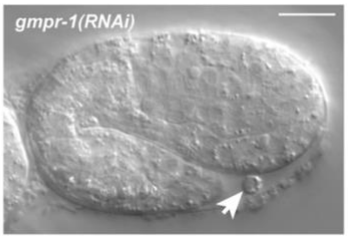

Supplemental Figure 6. Inhibitors of HU-induced replication-stress response and pan-caspase inhibitors do not alter stochastic cell extrusion. a, **c**, **d**, Representative micrographs of anti-γH2AX (**a**), anti-pATR (**c**) and anti-p53 immunofluorescence signal (**d**) in vehicle- or HU-treated MDCK-II cells (**c**), and in vehicle-, HU- or Nutlin3-treated MDCK-II cells (**a**, **d**). DNA is stained with Hoechst. Scale bars, 20 μm. **b**, Quantification of extrusions per hour after the indicated treatments. *n* = 13, 6, 5, 5 and 5 (biological replicates) each for control, PFT, zVAD-FMK, SB 218078 and PF477736 treatments, respectively. Each data point represents a separate experiment. These data were collected and analysed for statistical significance with the data in Fig. 4g. *P* values are indicated; n.s., not significant. **e**, Quantification of anti-p53 immunofluorescence signal in MDCK-II cells treated with vehicle, HU, or Nutlin-3. *n* = 9, 7 and 5 (biological replicates) for vehicle, HU and Nutlin3, respectively. Each data point represents mean fluorescence intensity signal from one image of hundreds of cells. Kruskal–Wallis one-way ANOVA followed by Dunn's correction was performed. *P* values are indicated. Data in **b**, **e** are represented as mean ± s.d.

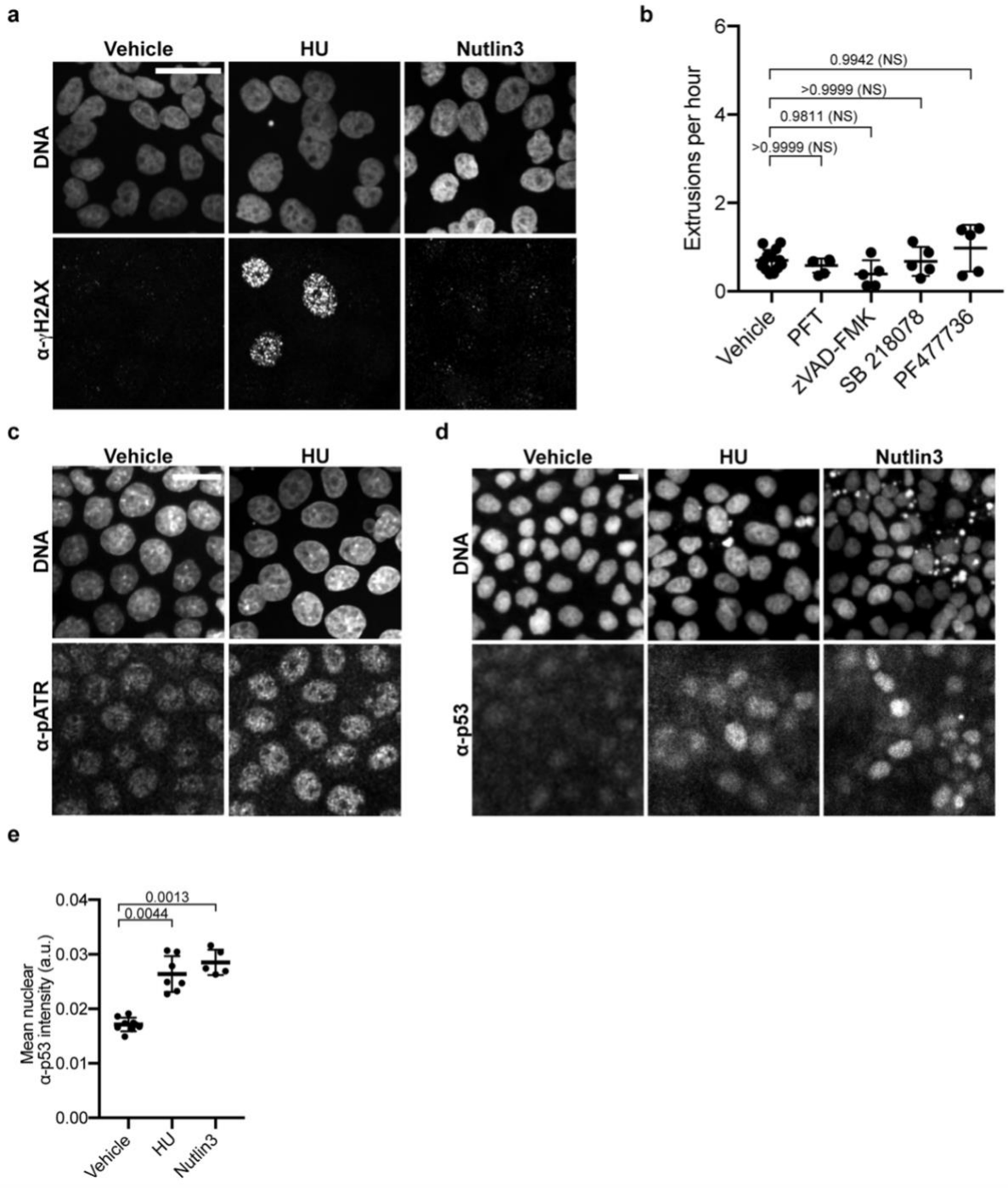
a
Vehicle
HU
Nutlin3
DNA
α-γH2AX
b
Extrusions per hour
0.9942 (NS)
>0.9999 (NS)
0.9811 (NS)
>0.9999 (NS)
Vehicle
PFT
zVAD-FMK
SB 218078
PF477736
c
Vehicle
HU
DNA
α-pATR
d
Vehicle
HU
Nutlin3
DNA
α-p53
e
Mean nuclear α-p53 intensity (a.u.)
0.0013
0.0044
Vehicle
HU
Nutlin3

Supplemental Table 1. Penetrances of the Tex phenotype produced by RNAi against cell cycle genes (and non-cell-cycle cyclins and CDKs) in *ced-3(lf)* animals.

RNAi target	Mammalian Homologue	Percent Tex	n	extensive lethality?
empty vector	-	1	159	N
atl-1	*ATR*	10	509	N
cdc-14	*CDC14A/B/C*	1	168	N
cdc-25.1	*CDC25A/B/C*	0	111	Y
cdc-25.2	*CDC25A/B/C*	12	159	N
cdc-25.3	*CDC25A/B/C*	2	168	N
cdc-25.4	*CDC25A/B/C*	0	183	N
cdk-1	*CDK1*	15	61	Y
cdk-11.1	*CDK11A/B*	0	175	N
cdk-11.2	*CDK11A/B*	1	132	N
cdk-12	*CDK12*	0	167	N
cdk-2	*CDK2*	65	181	N
cdk-4	*CDK4/6*	1	193	N
cdk-5	*CDK5*	0	155	N
cdk-7	*CDK7*	0	130	Y
cdk-8	*CDK8/19*	1	186	N
cdk-9	*CDK9*	1	155	Y
cdt-1	*CDT1*	1	147	Y
chk-1	*CHEK1*	10	164	Y
cit-1.1	*CCNT1/2*	0	105	N
cit-1.2	*CCNT1/2*	1	244	N
cki-1	*CDKN1B*	0	125	N
cki-2	*CDKN1A/B/C*	1	216	N
clk-2	*TELO2*	1	156	N
cul-1	*CUL1*	5	81	Y
cul-2	*CUL2*	0	21	Y
cul-3	*CUL3*	5	151	Y
cul-4	*CUL4*	0	141	N
cya-1	*CCNA1/2*	20	309	N
cyb-1	*CCNB1*	4	136	N
cyb-2.1	*CCNB1/2*	1	102	N
cyb-2.2	*CCNB1*	0	144	N
cyb-3	*CCNB3*	14	7	Y
cic-1	*CCNC*	1	158	N
cyd-1	*CCND1/2/3*	0	111	N
cye-1	*CCNE1/2*	89	133	Y
cyh-1	*CCNH*	0	119	Y
cyl-1	*CCNL1/2*	1	106	Y
cyy-1	*CCNY*	1	108	N
dpl-1	*TFDP1/2/3*	0	167	N
efl-1	*E2F4/5*	0	141	N
emb-27	*CDC16*	0	107	Y
emb-30	*ANAPC4*	0	130	Y
fzr-1	*FZR1*	1	146	N
fzy-1	*CDC20*	0	130	Y
hpr-17	*RAD17*	5	214	N
hus-1	*HUS1/1B*	0	132	N
lin-15	-	1	104	N
lin-23	*BTRC*	23	147	N
lin-35	*RB1/RBL1/2*	0	134	N
lin-36	-	0	111	N
lin-9	*LIN9*	1	125	N
mat-1	*CDC27*	0	80	Y
mat-2	*ANAPC1*	1	163	Y
mat-3	*CDC23*	0	108	Y
mdf-1	*MAD1L1*	3	112	N
mdf-2	*MAD2L1*	1	111	N
mrt-2	*RAD1*	0	114	N
rnr-1	*RRM1*	5	103	Y
san-1	*BUB1/1B*	1	145	N
wee-1.1	*PKMYT1*	1	159	N
wee-1.3	*PKMYT1*	0	60	Y

Tex penetrance produced by indicated RNAi treatment, mammalian homologue of the RNAi target and whether the RNAi clone produced extensive lethality are shown. Genes corresponding to RNAi clones that produced more than 9% penetrance of the Tex phenotype are in bold. *cyb-3* did not fit this criterion, as extensive lethality prevented the counting of a sufficient number of animals to assign significance. Some cyclins and CDKs that function outside the cell cycle were included and served as negative controls.

Supplemental Table 2. Penetrances of the Tex phenotype produced in wild-type animals by RNAi against cell-cycle genes with potential roles in cell extrusion.

RNAi target	Mammalian Homologue	Percent Tex	n
empty vector	-	0	127
atl-1	*ATR*	0	198
cdc-25.2	*CDC25A/B/C*	0	36
cdk-1	*CDK1*	0	51
cdk-2	*CDK2*	0	237
chk-1	*CHEK1*	0	115
csn-1	*GPS1*	0	156
csn-4	*COPS4*	0	141
csn-5	*COPS5*	0	114
cya-1	*CCNA1/2*	0	167
cye-1	*CCNE1/2*	0	143
lin-23	*BTRC*	12	96
psf-1	*GINS1*	0	150
psf-2	*GINS2*	0	190
psf-3	*GINS3*	0	72

The Tex penetrance produced in wild-type animals by RNAi clones against cell cycle genes that might be involved in cell extrusion (based on the corresponding Tex penetrance in *ced-3(lf)* animals) is provided. Bona fide candidates for cell extrusion regulation should not produce a Tex phenotype in wild-type animals, as cell extrusion does not occur in wild-type embryos. A Tex phenotype in wild-type animals could occur from other effects of RNAi against cell cycle genes, such as excessive proliferation leading to multiple excretory cells. Such proliferation is likely to be the case for *lin-23*, as RNAi against *lin-23* has been previously described to cause excessive proliferation[51]. The 13 other genes are good candidates to be regulators of cell extrusion by the criterion of dependence of the Tex phenotype on the loss of function of *ced-3*.

References

1. Ohsawa, S., Vaughen, J. & Igaki, T. Cell extrusion: a stress-responsive force for good or evil in epithelial homeostasis. *Dev. Cell* **44**, 284–296 (2018).

2. De Goeij, J. M. et al. Cell kinetics of the marine sponge *Halisarca caerulea* reveal rapid cell turnover and shedding. *J. Exp. Biol*. **212**, 3892–3900 (2009).

3. Denning, D. P., Hatch, V. & Horvitz, H. R. Programmed elimination of cells by caspase-independent cell extrusion in *C. elegans*. *Nature* **488**, 226–230 (2012).

4. Rosenblatt, J., Raff, M. C. & Cramer, L. P. An epithelial cell destined for apoptosis signals its neighbors to extrude it by an actin- and myosin-dependent mechanism. *Curr. Biol*. **11**, 1847–1857 (2001).

5. Gudipaty, S. A. & Rosenblatt, J. Epithelial cell extrusion: pathways and pathologies. *Semin. Cell Dev. Biol*. **67**, 132–140 (2017).

6. Timson, J. Hydroxyurea. *Mutat. Res*. **32**, 115–132 (1975).

7. Koç, A., Wheeler, L. J., Mathews, C. K. & Merrill, G. F. Hydroxyurea arrests DNA replication by a mechanism that preserves basal dNTP pools. *J. Biol. Chem*. **279**, 223–230 (2004).

8. Takeda, D. Y. & Dutta, A. DNA replication and progression through S phase. *Oncogene* **24**, 2827–2843 (2005).

9. Fay, D. S. & Han, M. Mutations in *cye-1*, a *Caenorhabditis elegans* cyclin E homolog, reveal coordination between cell-cycle control and vulval development. *Development* **127**, 4049–4060 (2000).

10. van Rijnberk, L. M., van der Horst, S. E. M., van den Heuvel, S. & Ruijtenberg, S. A dual transcriptional reporter and CDK-activity sensor marks cell cycle entry and progression in *C. elegans*. *PLoS One* **12**, e0171600 (2017).

11. Brauchle, M., Baumer, K. & Gönczy, P. Differential activation of the DNA replication checkpoint contributes to asynchrony of cell division in *C. elegans* embryos. *Curr. Biol*. **13**, 819–827 (2003).

12. Zerjatke, T. et al. Quantitative cell cycle analysis based on an endogenous all-in-one reporter for cell tracking and classification. *Cell Rep*. **19**, 1953–1966 (2017).

13. Teuliere, J. & Garriga, G. Size matters: how *C. elegans* asymmetric divisions regulate apoptosis. *Results Probl. Cell Differ*. **61**, 141–163 (2017).

14. Stergiou, L., Eberhard, R., Doukoumetzidis, K. & Hengartner, M. O. NER and HR pathways act sequentially to promote UV-C-induced germ cell apoptosis in *Caenorhabditis elegans*. *Cell Death Differ*. **18**, 897–906 (2011).

15. Dinant, C. et al. Activation of multiple DNA repair pathways by sub-nuclear damage induction methods. *J. Cell Sci*. **120**, 2731–2740 (2007).

16. Wu, Y. C., Stanfield, G. M. & Horvitz, H. R. NUC-1, a *Caenorhabditis elegans* DNase II homolog, functions in an intermediate step of DNA degradation during apoptosis. *Genes Dev*. **14**, 536–548 (2000).

17. Toledo, L. I. et al. ATR prohibits replication catastrophe by preventing global exhaustion of RPA. *Cell* **155**, 1088–1103 (2013).

18. Stevens, H., Williams, A. B. & Michael, W. M. Cell-type specific responses to DNA replication stress in early *C. elegans* embryos. *PLoS One* **11**, e0164601 (2016).

19. Ossareh-Nazari, B., Katsiarimpa, A., Merlet, J. & Pintard, L. RNAi-based suppressor screens reveal genetic interactions between the CRL2LRR-1 E3-ligase and the DNA replication machinery in *Caenorhabditis elegans*. *G3 (Bethesda)* **6**, 3431–3442 (2016).

20. Sonneville, R. et al. CUL-2^{LRR-1} and UBXN-3 drive replisome disassembly during DNA replication termination and mitosis. *Nat. Cell Biol*. **19**, 468–479 (2017).

21. Dewar, J. M., Low, E., Mann, M., Räschle, M. & Walter, J. C. CRL2^{Lrr1} promotes unloading of the vertebrate replisome from chromatin during replication termination. *Genes Dev*. **31**, 275–290 (2017).

22. Merlet, J. et al. The CRL2LRR-1 ubiquitin ligase regulates cell cycle progression during *C. elegans* development. *Development* **137**, 3857–3866 (2010).

23. Meek, D. W. Tumour suppression by p53: a role for the DNA damage response? *Nat. Rev. Cancer* **9**, 714–723 (2009).

24. Jones, M. C., Askari, J. A., Humphries, J. D. & Humphries, M. J. Cell adhesion is regulated by CDK1 during the cell cycle. *J. Cell Biol*. **217**, 3203–3218 (2018).

25. Grieve, A. G. & Rabouille, C. Extracellular cleavage of E-cadherin promotes epithelial cell extrusion. *J. Cell Sci*. **127**, 3331–3346 (2014).

26. Wernike, D., Chen, Y., Mastronardi, K., Makil, N. & Piekny, A. Mechanical forces drive neuroblast morphogenesis and are required for epidermal closure. *Dev. Biol*. **412**, 261–277 (2016).

27. Eisenhoffer, G. T. et al. Crowding induces live cell extrusion to maintain homeostatic cell numbers in epithelia. *Nature* **484**, 546–549 (2012).

28. Gaillard, H., García-Muse, T. & Aguilera, A. Replication stress and cancer. *Nat. Rev. Cancer* **15**, 276–289 (2015).

29. Olive, K. P. et al. Mutant p53 gain of function in two mouse models of Li-Fraumeni syndrome. *Cell* **119**, 847–860 (2004).

30. Lang, G. A. et al. Gain of function of a p53 hot spot mutation in a mouse model of Li-Fraumeni syndrome. *Cell* **119**, 861–872 (2004).

31. Singh, S. et al. Mutant p53 establishes targetable tumor dependency by promoting unscheduled replication. *J. Clin. Invest*. **127**, 1839–1855 (2017).

32. Yeo, C. Q. X. et al. p53 maintains genomic stability by preventing interference between transcription and replication. *Cell Rep*. **15**, 132–146 (2016).

33. Karagiannis, G. S. et al. Neoadjuvant chemotherapy induces breast cancer metastasis through a TMEM-mediated mechanism. *Sci. Transl. Med*. **9**, eaan0026 (2017).

34. Brenner, S. The genetics of *Caenorhabditis elegans*. *Genetics* **77**, 71–94 (1974).

35. Brodigan, T. M., Liu, Ji., Park, M., Kipreos, E. T. & Krause, M. Cyclin E expression during development in *Caenorhabditis elegans*. *Dev. Biol*. **254**, 102–115 (2003).

36. Wu, Y. C. & Horvitz, H. R. *C. elegans* phagocytosis and cell-migration protein CED-5 is similar to human DOCK180. *Nature* **392**, 501–504 (1998).

37. Hsieh, J. et al. The RING finger/B-box factor TAM-1 and a retinoblastoma-like protein LIN-35 modulate context-dependent gene silencing in *Caenorhabditis elegans*. *Genes Dev*. **13**, 2958–2970 (1999).

38. Grishok, A., Sinskey, J. L. & Sharp, P. A. Transcriptional silencing of a transgene by RNAi in the soma of *C. elegans*. *Genes Dev*. **19**, 683–696 (2005).

39. Fischer, S. E. J. et al. Multiple small RNA pathways regulate the silencing of repeated and foreign genes in *C. elegans*. *Genes Dev*. **27**, 2678–2695 (2013).

40. Boeck, M. E. et al. Specific roles for the GATA transcription factors *end-1* and *end-3* during *C. elegans* E-lineage development. *Dev. Biol*. **358**, 345–355 (2011).

41. Mello, C. C., Kramer, J. M., Stinchcomb, D. & Ambros, V. Efficient gene transfer in *C.elegans*: extrachromosomal maintenance and integration of transforming sequences. *EMBO J*. **10**, 3959–3970 (1991).

42. Rual, J.-F. et al. Toward improving *Caenorhabditis elegans* phenome mapping with an ORFeome-based RNAi library. *Genome Res*. **14** (10B), 2162–2168 (2004).

43. Fraser, A. G. et al. Functional genomic analysis of *C. elegans* chromosome I by systematic RNA interference. *Nature* **408**, 325–330 (2000).

44. Kamath, R. S. et al. Systematic functional analysis of the *Caenorhabditis elegans* genome using RNAi. *Nature* **421**, 231–237 (2003).

45. Sulston, J. E., Schierenberg, E., White, J. G. & Thomson, J. N. The embryonic cell lineage of the nematode *Caenorhabditis elegans*. *Dev. Biol*. **100**, 64–119 (1983).

46. Schindelin, J. et al. Fiji: an open-source platform for biological-image analysis. *Nat. Methods* **9**, 676–682 (2012).

47. Hansson, G. C., Simons, K. & van Meer, G. Two strains of the Madin-Darby canine kidney (MDCK) cell line have distinct glycosphingolipid compositions. *EMBO J*. **5**, 483–489 (1986).

48. Streichan, S. J., Hoerner, C. R., Schneidt, T., Holzer, D. & Hufnagel, L. Spatial constraints control cell proliferation in tissues. *Proc. Natl Acad. Sci. USA* **111**, 5586–5591 (2014).

49. Sakaue-Sawano, A. et al. Visualizing spatiotemporal dynamics of multicellular cell-cycle progression. *Cell* **132**, 487–498 (2008).

50. McQuin, C. et al. CellProfiler 3.0: next-generation image processing for biology. *PLoS Biol*. **16**, e2005970 (2018).

51. Kipreos, E. T., Gohel, S. P. & Hedgecock, E. M. The *C. elegans* F-box/WD-repeat protein LIN-23 functions to limit cell division during development. *Development* **127**, 5071–5082 (2000).

Chapter Four

Future Directions

Identifying the mechanism by which CED-9-CED-4 interaction mediates the pro-apoptotic function of CED-9

Given the highly conserved nature of cell-death proteins and pathways between *C. elegans* and humans, it is plausible that a pro-apoptotic interaction analogous to the CED-9-CED-4 interaction regulates apoptosis in humans. Such an interaction could involve canonically anti-apoptotic BCL-2 family members and one or more of their pro-apoptotic interactors, such as BAX and BAK, or an unknown interactor that activates APAF-1. The elucidation of such a mechanism might add a key insight concerning the basic process of apoptosis and suggest novel targets for therapeutics aimed at treating disorders that involve dysregulated apoptosis, such as certain neurodegenerative disorders and cancers.

In this thesis (Chapter Two), I hypothesize that an unknown factor "X" is a pro-apoptotic factor sequestered by CED-9 that activates CED-4 upon its release from mitochondria. This model closely mirrors the mechanism of APAF-1 activation by mammalian BCL-2 family members via the release of cytochrome c from mitochondria (Liu *et al.*, 1996; Kluck *et al.*, 1997; Li *et al.*, 1997; Yang *et al.*, 1997; Zou *et al.*, 1997). Despite extensive research in the field of apoptosis using both *C. elegans, Drosophila,* and mammalian systems, this factor might be a protein that has remained undetected because of lethality caused by loss-of-function mutations of the gene or genetic redundancy.

To search for such a factor in *C elegans, a* genome-wide RNAi screen for pro-apoptotic genes could be performed. In this screen L4 *nIs106* worms would be fed bacteria from the ORFeome RNAi library in a genome-wide screen and their offspring assessed for extra VC-like cells using the transgene *nIs106[*$P_{lin\text{-}11}$*::GFP].*

The ORFeome library contains 11,511 clones against 10,953 genes (out of approximately 20,000 in the *C. elegans* genome*).* This screen could identify such a factor “X” or, potentially, another essential, pro-apoptotic gene that remains unidentified.

Determining the anti-apoptotic function of CED-9

This work shows that CED-9-CED-4 interaction, previously thought to mediate the anti-apoptotic function of CED-9, is rather required for the pro-apoptotic function of CED-9. Significantly, my findings also show that CED-9-CED-4 interaction is not required for the anti-apoptotic function of CED-9. Therefore, the mechanism of the anti-apoptotic function of CED-9 remains unknown.

Though a CED-9-sequestered factor “X” would explain this function, as in this case the anti-apoptotic function of CED-9 would be to sequester both “X” and CED-4, other possibilities exist. To address this issue, alleles of *ced-9* lacking the anti-apoptotic but not the pro-apoptotic function of CED-9 (i.e. opposite to the alleles of CED-9 described in Chapter Two that lack the pro- but not the anti-apoptotic function of CED-9) could be produced and studied (described below) to determine what can cause a specific loss of the anti-apoptotic function of CED-9.

An EMS mutagenesis screen could be used to produce *ced-9* alleles of this nature. In this screen wild-type males carrying the transgenes *nIs348* and *nIs106* will be mutagenized then crossed to *ced-9(0)/qC1 III; nIs106* hermaphrodites. *nIs348* expresses mCherry in the M4 cell and will be used to mark cross-progeny, provide another marker to score a second cell death (the M4 sister), and to follow *ced-3(+)*

during the crosses described below as *nIs348* and *ced-3* are linked, and *qC1 III* (a balancer of Chromosome III) will be used to prevent crossover events from occurring. Balancer- and *nIs348*-positive F1s will be picked onto individual plates, F1s that produce maternal-effect lethal, balancer-negative progeny will be sequenced for *ced-9* mutations. Mutant *ced-9* alleles of interest (those causing maternal-effect lethality) will then be crossed to *ced-3(n2427); nIs106* to make *ced-9(mut); ced-3(n2427); nIs106* animals. *ced-9* alleles that cause maternal-effect lethality but do not enhance the cell-killing defect caused by *ced-3(n2427)* are defective specifically in the anti-apoptotic function of CED-9. The nature of such a mutation could provide important insights for understanding the anti-apoptotic function of CED-9, similar to how *ced-9(n3377),* mutant specifically in the pro-apoptotic of CED-9, provided insights into the pro-apoptotic of CED-9. As previously described in the Introduction of this thesis, such alleles might be mutant in certain amino acids within the region CED-9(1-67). This is because it appears possible that, based on my findings described in Chapter Two and that a deletion of CED-9(1-67) appears to, at least partially, disrupt the protective function of CED-9 but not CED-9-CED-4 interaction *in vitro* (Xue and Horvitz, 1997), CED-9 could have an anti-apoptotic function independent of CED-9-CED-4 interaction dependent on it N-terminus.

This screen would have the added benefit of generating new reduction-of-function and null alleles of *ced-9* that might be informative about the broader function of CED-9 by isolating *ced-9(0)* alleles that do not contain obvious null mutations such as frameshifts, large deletions, or nonsense mutations. Rather missense

mutations that result in complete loss-of CED-9 function could be informative as they would suggest the necessity of a single amino acid for CED-9 function.

RNAi screen of essential genes

An RNAi screen of essential genes can be conducted as an approach to identify a CED-9-sequestered factor “X” (Chapter Two). This factor could be a protein encoded by an essential gene in the *C. elegans* genome and thus null or strong-loss-of function mutations in this gene might not have been isolated from previous mutagenesis screens. This proposed RNAi screen would entail growing *ced-3(n2427); nIs106* L4 animals on bacteria that express RNAi against essential genes predicted to be localized to mitochondria or play a role in mitochondrial function and examining the progeny of these animals for extra VC-like cells; this screen could identify a gene encoding factor “X” as well as other cell-death genes that might have been missed by traditional mutagenesis screens due to lethality associated with loss-of-function mutations within these genes. If RNAi against essential, mitochondrial genes fails to identify any novel cell-death gene then this screen should be expanded to include all essential genes.

Identifying additional CED-9-CED-4 interaction mutations in CED-4

I describe in Chapter Two seven alleles of *ced-9* that lack the pro-apoptotic function of CED-9 and cause an apparent defect in CED-9-CED-4 interaction. Only one such allele of *ced-4* exists, *ced-4(n6703).* To further understand the pro-apoptotic nature of CED-9-CED-4 interaction alleles of *ced-4* similar to *ced-*

4(n6703), i.e. unable to rescue *ced-9(n1950 n2161)* and causing a cell-death defect, should be generated.

To generate these alleles, CRISPR should be used to make *ced-4* mutations that are predicted to disrupt CED-9-CED-4 interaction based on the known crystal structure of a CED-9-CED-4 complex (Yan *et al.*, 2005). These experiments should mutate residues in CED-4 that make hydrogen bonds with CED-9 residues to alanine; these residues of CED-4 are: I18, R24, T49, L51, E52, R53, D206, L209, E214, R215, L217, and F220 (Yan *et al.*, 2005). Mutant *ced-4* alleles that cause a defect in cell-killing (assayed using *nIs106* to identify alleles that cause ectopic VC-like cell survival) should then be tested for their ability to rescue the strong loss-of-function allele *ced-9(n1950 n2161),* as in Chapter Two for *ced-9(n6703). ced-4* alleles that, like general *ced-4(lf)* alleles, cause a defect in cell-killing but, like *ced-4(+)* alleles, do not rescue maternal-effect lethality caused by *ced-9(n1950 n2161),* are likely mutant specifically in CED-9-CED-4 interaction but otherwise functional. Antibody staining could then be used to determine the intracellular localization of CED-4 protein *in vivo* in embryos carrying these mutant alleles. Mutations that fit the above criteria and are localized to the perinuclear membrane in *ced-9(+)* embryos are alleles of CED-4 that, like *ced-4(n6703),* disrupt CED-9-CED-4 interaction, specifically.

This approach should generate more *ced-4* alleles similar to *ced-4(n6703),* which might add to our understanding of the pro-apoptotic nature of CED-9-CED-4 interaction and show that CED-4 can be robustly mutated to prevent the pro-apoptotic function of CED-9 by blocking CED-9-CED-4 interaction.

CED-4L protein might not be present in *C. elegans* embryos

To determine the roles of the individual isoforms of CED-4 (CED-4S and CED-4L) I used CRISPR/Cas9 to generate CED-4S- and CED-4L-specific alleles of CED-4. As expected, an allele presumably lacking CED-4S and retaining CED-4L (*ced-4(n6692)*) produced an ectopic cell-survival phenotype similar to a *ced-4(0)* allele (Figure 1A); in contrast, two alleles presumably lacking CED-4L and retaining CED-4S (*ced-4(n6687) and ced-4(n6696)*) created neither extra cells or ectopic cell deaths in VC-like cells (Figure 1B, C).

Additionally, *C. elegans* embryos carrying *ced-4(n6692)* produced no CED-4 protein detectable by wester blotting with an anti-CED-4 polyclonal antibody, while embryos carrying *ced-4(n6687)* and *ced-4(n6696)* both showed a seemingly normal amount of CED-4 protein (Figure 2). These data suggest that CED-4L protein is produced in *C. elegans* embryos at very low levels, undetectable by western blotting with the antibody, or not at all.

Saturation of the *ced-3(n2427)* enhancement screen

Previously, a screen for enhancers of the cell-killing defect caused by the weak loss-of function allele *ced-3(n2427)* identified mutations in *mcd-1* and *dpl-1* and the CED-9-CED-4 interaction mutations *ced-9(n3377)* and *ced-4(n5611 n3392)* (Reddien *et al.,* 2007). This sensitized screen produced mutations in cell-death genes that would have been missed in other screens because of the relatively weak effect of the mutations. This screen isolated 37 mutations by screening ~13,000

mutagenized haploid genomes. This screen is not saturated since only one mutant allele of *mcd-1* and one mutant allele of *dpl-1* were isolated, saturating this screen might produce additional mutations in novel cell-death genes that were missed by the initial screen.

Determining the endogenous function of CED-4L, an anti-apoptotic product of the canonically pro-apoptotic *ced-4* gene

Understanding the long mysterious function of the long isoform of CED-4 (CED-4L) could add to our understanding of the pro- and anti-apoptotic functions of CED-9 and CED-4 and their interactions with each other. While the short isoform of CED-4 (CED-4S) is the predominant pro-apoptotic isoform of CED-4, CED-4L has been shown to be anti-apoptotic when overexpressed (Shaham and Horvitz, 1996). However, the endogenous function of CED-4L is not understood.

CED-4L appears to conserved across different *Caenorhabditis* species, based on genomic sequences (Shaham and Horvitz, 1996) suggesting that this isoform is functional. However, I have been unable to detect CED-4L protein in *C. elegans* embryos using western blotting with an anti-CED-4 polyclonal antibody generated many years ago by Bradley Hersh (Figure 2). The anti-CED-4 polyclonal antibody cannot be used to detect CED-4 in adult worms, as this antibody detects too much background in protein extracts of mixed-staged worms. However, GFP-tagged CED-4 could be used to resolve this issue of background reactivity, as anti-GFP antibody would not have this limitation. If a GFP-tagged allele of *ced-4* lacking CED-4S expression specifically is detected by western blotting in adult worms but not

embryos, then CED-4L might provide protection post-embryonically, a function that would make sense since most cell deaths occur in the embryo rather than post embryonically and expression of anti-apoptotic CED-4 isoform might provide cells with additional protection.

CED-4L should also be tested for its ability to bind CED-9 *in vivo* using antibody staining in embryos carrying a CED-4L-specific allele or GFP-tagged CED-4L to assess whether CED-4L is localized to mitochondria or the perinuclear membrane. Since the pro-apoptotic function of CED-9 depends on CED-9-CED-4 interaction, evaluation of CED-4L localization *in vivo* could be helpful in resolving the function of CED-4L, which contains a 24 amino acid insertion relative to CED-4S that sits in the presumptive CED-9 bind region of CED-4, for example, if CED-4L shows the same localization of CED-4 where CED-4L is expressed then it might prevent apoptosis by preventing CED-4S octamerization, preventing the formation of an active apoptosome (Shaham and Horvitz, 1996; Yan *et al.*, 2005). Since the CED-4L-specific amino acid sequence contains amino acids that are conserved across *Caenorhabditis* species at the third codon position it is also possible that CED-4L functions at the RNA, not the protein level (Shaham and Horvitz, 1996).

An imbalance between purine and pyrimidine nucleotides causes ABplpappap survival in a *ced-3(+)* background

To further understand the mechanism of cell extrusion, I performed an EMS mutagenesis screen using a caspase-deficient *ced-3(n3396)* background for embryos defective in cell extrusion and screening for the survival of the normally

extruded cell ABplpappap. The embryonic survival of ABplpappap was assayed using the GFP reporter *nIs433[P$_{pgp-12}$::GFP],* which is expressed in both the normal single excretory cell in the *C. elegans* head and in the ectopic excretory-cell like ABplpappap cell when it survives in *ced-3(lf)* mutants. From this screen I isolated a mutant with multiple cells expressing the reporter, i.e. presumably exhibiting the fate of the excretory cell. Using SNP mapping, I mapped the causal mutation, *n6457,* to the left arm of chromosome V and using RNAi and rescue I identified the mutation as an allele of the GMP reductase gene *gmpr-1,* which encodes a homolog of the two human GMP reductase proteins GMPR1 and GMPR2. GMP reductase proteins convert GMP nucleotides to IMP, which can then be converted to AMP. This *n6457* allele of *gmpr-1* is a nonsense mutation in a tryptophan codon 273 amino acids from the C-terminus of the protein (W85Opal). Interestingly, the *gmpr-1(n6457)* allele also allows ABplpappap to escape caspase-mediated apoptosis in a *ced-3(+)* background, i.e. in the presence of wild-type caspase activity (Figure 3). This result suggests that the levels of purines controlled by GMP reductase can affect caspase-mediated apoptosis as well as cell extrusion, a novel finding suggesting.

To identify suppressors or enhancers of *gmpr-1* as well as other nucleotide metabolism genes that contribute to apoptosis, I performed a screen for ABplpappap survival by the presence of at least two excretory cells by using RNAi against purine and pyrimidine metabolism genes in the *gmpr-1(n6457)* mutant background as well as a wild-type background, reasoning that other nucleotide metabolism genes, in addition to *gmpr-1,* could be involved in the process by which *gmpr-1* apparently promotes apoptosis (Table 1). This screen identified two suppressors of *gmpr-1*, *pyr-*

1, a *de novo* pyrimidine synthesis gene homologous to the human CAD enzyme, and the phosphoribosyl pyrophosphate synthase gene *R151.2*. This screen also showed that when activity of either the adenlyosuccinate synthase gene *adss-1* or *pyr-1* is knocked down in a wild-type background, ABplpappap survives, similar to RNAi knockdown of *gmpr-1*. In short, I found that RNAi against some genes that effect pyrimidine metabolism (*pyr-1*) or purine metabolism *(gmpr-1* and *adss-1*) allow ABplpappap to survive in a wild-type background, but RNAi against *R151.2,* which effects both purine and pyrimidine metabolism, does not (Table 1 and Figure 4). Interestingly, the Tex phenotype caused by *gmpr-1(n6457)* is suppressed by RNAi against *R151.2* or *pyr-1* but not by RNAi against the purine metabolism gene *adss-1* (Table 1).

Based on these results, I hypothesize that when either purine or pyrimidine metabolism is perturbed using RNAi against *gmpr-1, adss-1,* or *pyr-1* in wild-type worms the cell ABplpappap escapes caspase-mediated apoptosis. However, if both purine and pyrimidine metabolism are perturbed by using RNAi against *R151.2* in wild-type worms or RNAi against either *R151.2* or *pyr-1* in *gmpr-1(n6457)* mutants ABplpappap can undergo apoptosis in an apparently normal manner. These observations suggest that it is an imbalance between purine and pyrimidine levels and not a scarcity of either that prevents cell death.

Determining how an apparent imbalance between purine and pyrimidine nucleotides disrupts cell elimination

Based on my results it appears that when either purine or pyrimidine metabolism is perturbed using RNAi against *gmpr-1, adss-1,* or *pyr-1* in wild-type worms the cell ABplpappap escapes caspase-mediated apoptosis. However, if both purine and pyrimidine metabolism are perturbed by using RNAi against *R151.2* in wild-type worms or RNAi against either *R151.2* or *pyr-1* in *gmrp-1(null)* mutants, ABplpappap can undergo apoptosis in an apparently normal manner. These observations suggest that it is an imbalance between purine and pyrimidine levels and not a scarcity of either that prevents both apoptosis and cell extrusion.

To determine how an apparent imbalance between purine and pyrimidine nucleotides might disrupt cell elimination, I propose seeking more genes involved in this process be identified. Since mutations in certain cell cycle genes prevent cell extrusion (Dwivedi *et al.*, 2021), it is plausible that the mechanism by which purine/pyrimidine balance regulates cell extrusion and apoptosis depends, at least in apart, on the cell cycle. Additionally, since mutations in cell cycle genes and nucleotide metabolism genes often result in lethality, EMS is not an attractive screening method, instead a genome-wide RNAi screen using the ORFeome library for genes that when decreased in expression block ABplpappap death in a *ced-3(+)* background should be conducted. In this screen L4 worms carrying, *nIs433[*$P_{pgp\text{-}12}$*::GFP]* (a transgene marking ABplpappap and the excretory cell) will be grown on clones from the ORFeome library, the progeny of these worms will then be examined for the Tex (Two-excretory cell) phenotype. Additionally, *gmpr-1(n6457)*;

nIs433 should also be screened similarly by RNAi to identify suppressers/enhancers of the Tex phenotype caused by loss-of *gmpr-1* function. This screen could identify genes involved in a novel cell-elimination mechanism dependent on purine/pyrimidine nucleotide balance that controls both apoptosis and cell extrusion.

A link between genes that regulate the cell cycle and cell death has been observed previously (Reddien *et al.*, 2007). This work found that the *C. elegans* genes *efl-1* (E2F), *dpl-1* (DP), and the zinc-finger protein *mcd-1* work together with the (class B Synthetic Multivulva) SynMuvB genes *lin-35* (Rb), *lin-37* (Mip40), and *lin-52* (dLin52) (human homologs in parentheses), to regulate programmed cell death. These genes encode components of the DREAM (Dp, Rb-like, E2F, and MuvB) complex, known to regulate the cell cycle through transcriptional regulation of cell cycle genes (Boxem and van den Heuvel, 2001, 2002; Korenjak *et al.,* 2004; Lewis *et al.,* 2004; Harrison *et al.,* 2006; Litovchick *et al.,* 2007; Schmit *et al.,* 2007). These genes act downstream of *egl-1* and *ced-9* to regulate cell death in *C. elegans,* suggesting that these genes might be involved in transcriptional regulation of CED-4 or CED-3 (Reddien *et al.,* 2007).

A study using GFP-tagged CED-4 expressed by a transgene showed that in the *C. elegans* germline CED-4 is localized to the perinuclear membrane, rather than mitochondria as it is in somatic cells (Pourkarimi, Greiss, and Gartner, 2012). In this work cells containing perinuclear localized CED-4 were found in germ cells in the mitotic zone, transition zone, and early and late stage pachytene zones in the *C. elegans* gonad. Apoptosis in the *C. elegans* germline occurs only in the “gonadal loop region” where germ cells are exiting the pachytene stage (the third stage of

meiotic prophase I) (Gumienny *et al.,* 1999). *egl-1* loss-of function mutations and *ced-9* gain-of-function mutations have little to no effect in these germline deaths (Gumienny *et al.,* 1999), which suggests that these deaths occur independently of EGL-1 transcription. The RAS/MAPK pathway is required for germ cells to exit the pachytene stage (Church *et al.,* 1995), and loss-of-function mutations in RAS-pathway genes prevent germline apoptosis (Gumienny *et al.,* 1999). Thus, CED-3 might be expressed following the exit of the pachytene stage of meiosis I, activating apoptosis in the presence of activated CED-4 protein. It is also possible that germ cells that have progressed into the “gonadal loop region”, where apoptosis occurs, begin to express CED-3 in response to some extracellular signal encountered in this region of the gonad. In this model, cells that have successfully exited the pachytene stage will have restored CED-9-CED-4 interaction, while those that remain in the pachytene stage undergo apoptosis in the presence of CED-3. Interestingly, E2F genes have been shown to have a role in the modulation of MAPK (Hershko *et al.,* 2006) and the transcription of caspases (Muller *et al.,* 2001); suggesting that in *C. elegans efl-1,* previously identified to have a role in regulating apoptosis and the cell cycle (Boxem and van den Heuvel, 2001, 2002; Korenjak *et al.,* 2004; Lewis *et al.,* 2004; Harrison *et al.,* 2006; Litovchick *et al.,* 2007; Reddien *et al*., 2007; Schmit *et al.,* 2007) might function to regulate apoptosis in the germline by controlling pachytene exit and CED-3 transcription.

Since in *C. elegans* embryos CED-4 is localized to mitochondria (Chen *et al.,* 2000), it is possible that CED-9-CED-4 interaction is restored following meiosis or exit of the pachytene stage of meiosis I. Exactly how CED-9-CED-4 interaction might

be blocked in the *C. elegans* germline is unknown. To address this issue an RNAi screen of genes known to be involved in meiosis could be performed using worms carrying endogenously-tagged CED-4::GFP. The pre-pachytene zone of the germline of adult worms treated with RNAi against these genes then could be examined for CED-4 mitochondrial localization to identify genes required for blocking CED-9-CED-4 interaction in the germline.

It is also possible that CED-3 is transcriptionally regulated to control apoptosis in the germline dependent on E2F and possibly other members of the DREAM complex through the regulation of the cell cycle. Since mutations in the DREAM complex also prevent apoptosis in somatic cells downstream of CED-9, these genes might act to promote apoptosis by activating CED-3 transcription in somatic cells as well. The balance of purines and pyrimidines appears to have a role in regulating apoptosis, at least in certain cells (Figure. 3 and Table. 1), as well as an apparent role in the cell cycle, due to its regulation of cell extrusion which does not occur when S-phase entry is blocked (Dwivedi *et al.,* 2021). Hence, since members of the DREAM complex and genes regulating purine and pyrimidine balance regulate the cell cycle and apoptosis, it is possible that these genes affect apoptosis indirectly through their influence on the cell cycle in *C. elegans* and, since E2F can regulate caspase expression and members of the DREAM complex control apoptosis downstream of *egl-1* and *ced-9,* the cell cycle might influence apoptosis through controlling CED-3 transcription. This role appears to be independent of p53, as its worm homolog *cep-1* was not observed to cause any defect in cells deaths regulated by members of the DREAM complex (Reddien *et al.,* 2007). To test whether

purine/pyrimidine balance modulates CED-3 expression, RNAi could be used against nucleotide metabolism genes – e.g., *gmpr-1, adss-1,* and *pyr-1* – in adult worms carrying CED-3::wrmScarlet to test for CED-3 expression in the germline, if purine/pyrimidine balance promotes apoptosis through transcriptional-regulation of CED-3, then RNAi against these genes should suppress CED-3 expression. Further, when treated with RNAi against *pyr-1* or *R151.2, gmpr-1(n6457)* worms carrying CED-3::wrmScarlet should show relatively normal levels of CED-3 expression, compared to *gmpr-1(n6457)* worms, which should decrease CED-3 expression, since RNAi against *pyr-1* or *R151.2* suppresses the cell-death defect caused by *gmpr-1(n6457)*. RNAi against members of the DREAM complex could be used in a similar way to test whether knock-down of these genes results in suppression of CED-3 expression. Control of CED-3 expression by the DREAM complex and nucleotide metabolism genes would represent a novel discovery of a mechanism of apoptosis in germ cells – and possibly somatic cells as well – that is apparently cell-cycle-dependent and p53-independent that, if evolutionarily conserved, could have implications for human germ cell death.

Acknowledgements

I thank Dongyeop Lee and Mona Liu for comments about this chapter.

Figure 1. Loss-of CED-4L causes no ectopic survival of VC-like cells. A) an allele presumably lacking CED-4S and retaining CED-4L (*ced-4(n6692)*) caused ectopic survival of VC-like cells as assayed by the reporter *nIs106[P_{lin-11}::GFP]*. B) Two alleles presumably lacking CED-4L and retaining CED-4S (*ced-4(n6687) and ced-4(n6696)*) produced no detectable ectopic survival of VC-like cells.

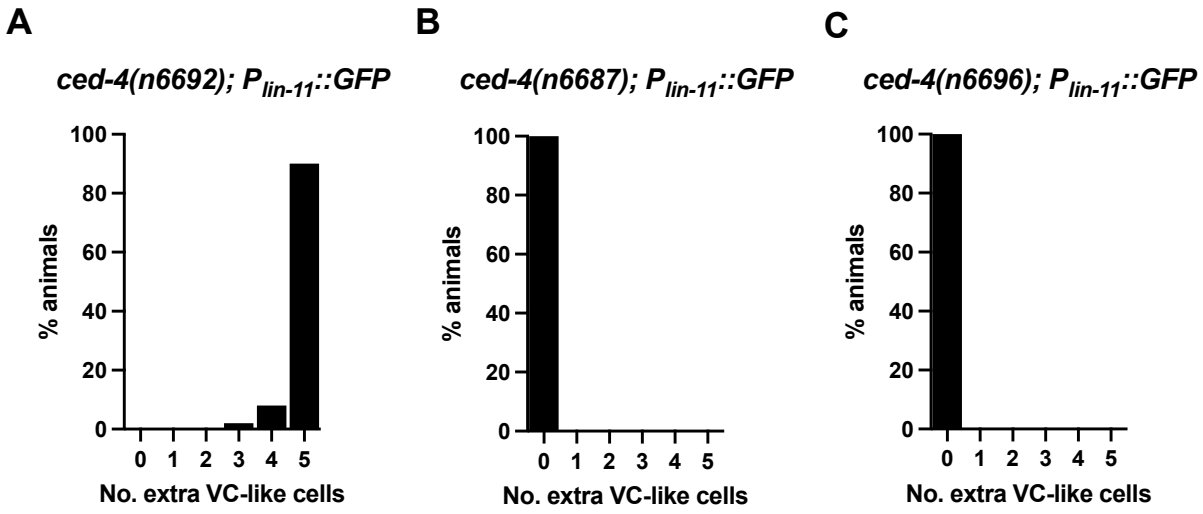
A
ced-4(n6692); P lin-11 ::GFP
100
80
60
40
20
0
% animals
0 1 2 3 4 5
No. extra VC-like cells
B
ced-4(n6687); P lin-11 ::GFP
100
80
60
40
20
0
% animals
0 1 2 3 4 5
No. extra VC-like cells
C
ced-4(n6696); P lin-11 ::GFP
100
80
60
40
20
0
% animals
0 1 2 3 4 5
No. extra VC-like cells

Figure 2. CED-4L protein is not detectable by an anti-CED-4 polyclonal antibody in *C. elegans* embryos. A western blot shows that a polyclonal antibody made against CED-4 protein identifies a band between 50 kD and 75 kD, roughly the size of CED-4 protein (63 kD), in a lane containing protein extracted from mixed-staged embryos carrying a wild-type *ced-4* allele. The antibody failed to detect this band in embryos carrying the null allele *ced-4(n1162).* The antibody does not detect this band (presumed to be CED-4) in embryos carrying *ced-4(n6692)* (CED-4S^{-}) but does in embryos carrying *ced-4(n6687)* or *ced-4(n6696)* (CED-4L^{-}).

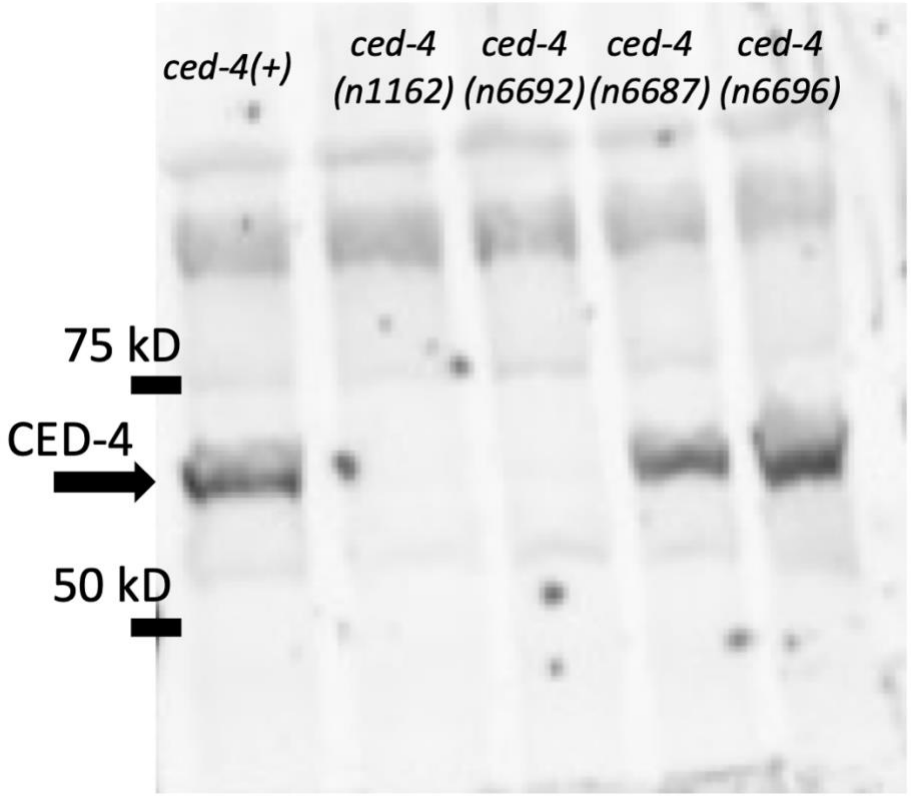
ced-4(+)
ced-4 (n1162)
ced-4 (n6692)
ced-4 (n6687)
ced-4 (n6696)
75 kD
CED-4
50 kD

Figure 3. Loss-of *gmpr-1* function causes the ectopic survival of ABplpappap in *ced-3(+)* embryos. A) *nIs433[P_{pgp-12}::GFP]* marks only the excretory cell in the head of a wild-type L4 animal. B) The nonsense allele *gmpr-1(n6457)* results in 36% apparent survival of ABplpappap (two excretory-like cells) in an otherwise wild-type background. C) and C') Embryo containing transgenes labeling histones (*stIs10026[P_{his-72}::GFP::his-72]*) and the cell membrane (*ltIs44 [P_{pie-1}::mcherry::PH(PLC1delta1)])* grown on RNAi against control vector *L4440* shows ABplpappap undergoing caspase-mediated apoptosis. D) and D') Embryo grown on RNAi against *gmpr-1* shows survival of ABplpappap.

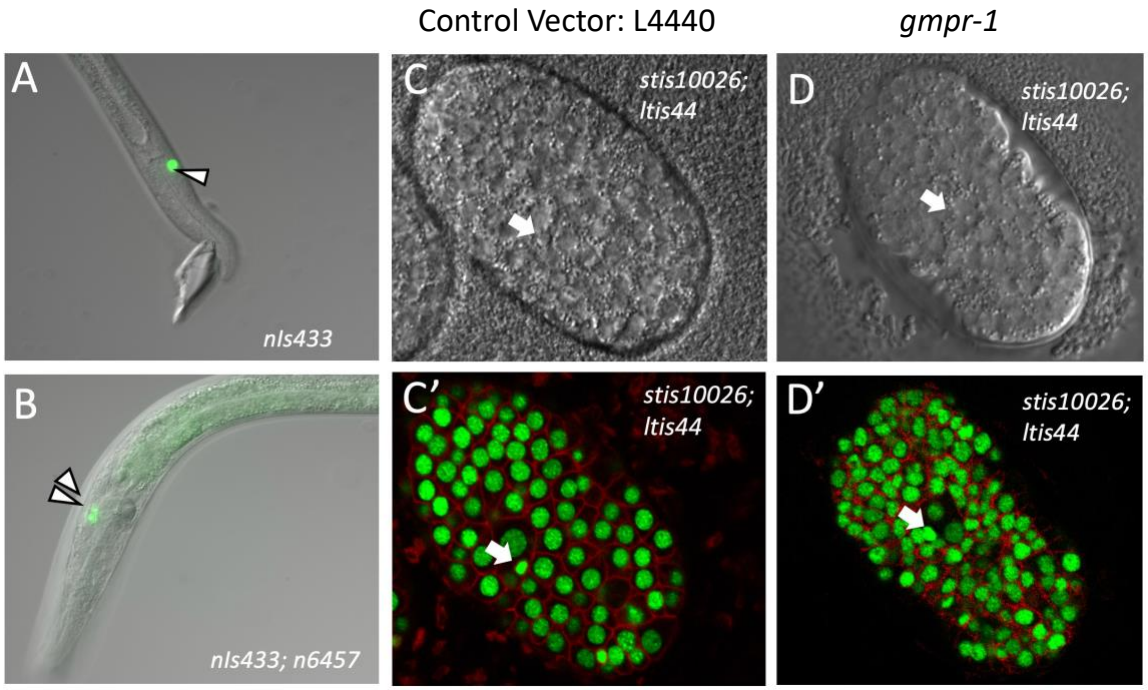
Control Vector: L4440
gmpr-1
A
nIs433
B
nIs433; n6457
C
stis10026;
ltis44
D
stis10026;
ltis44
C'
stis10026;
ltis44
D'
stis10026;
ltis44

Table 1. % Survival of ABplpappap observed by the presence of two or more cells expressing the excretory cell reporter *nIs433[$P_{pgp\text{-}12}$::GFP]* in a wild-type or *gmrp-1(lf)* ground. Human homolog in parentheses.

RNAi	Function	Likely effect on nucleotide pool	***nIs433; gmpr-1(n6457)***	***nIs433***
L4440	Control	None	36% n=350	0% n=350
F32D1.5	GMP reductase (GMPR1/GMPR2)	Decrease in IMP/AMP increase in GMP	37% n=350	12% n=350
pyr-1	*De novo* pyrimidine synthesis (CAD)	Decrease in pyrimidines	6% n=200	9% n=100
adss-1	Adenlyosuccinate synthesis (ADSS1/ADSS2)	Decrease in AMP increase in IMP	22% n=50	5% n=100
R151.2	Phosphoribosyl pyrophosphate synthesis (PRPS1)	Decrease in purines and pyrimidines	8% n=100	0% n=100

Figure 4. A simplified pathway of *de novo* purine and pyrimidine biosynthesis.

Genes of interest are shown in red with human homologs in parenthesis.

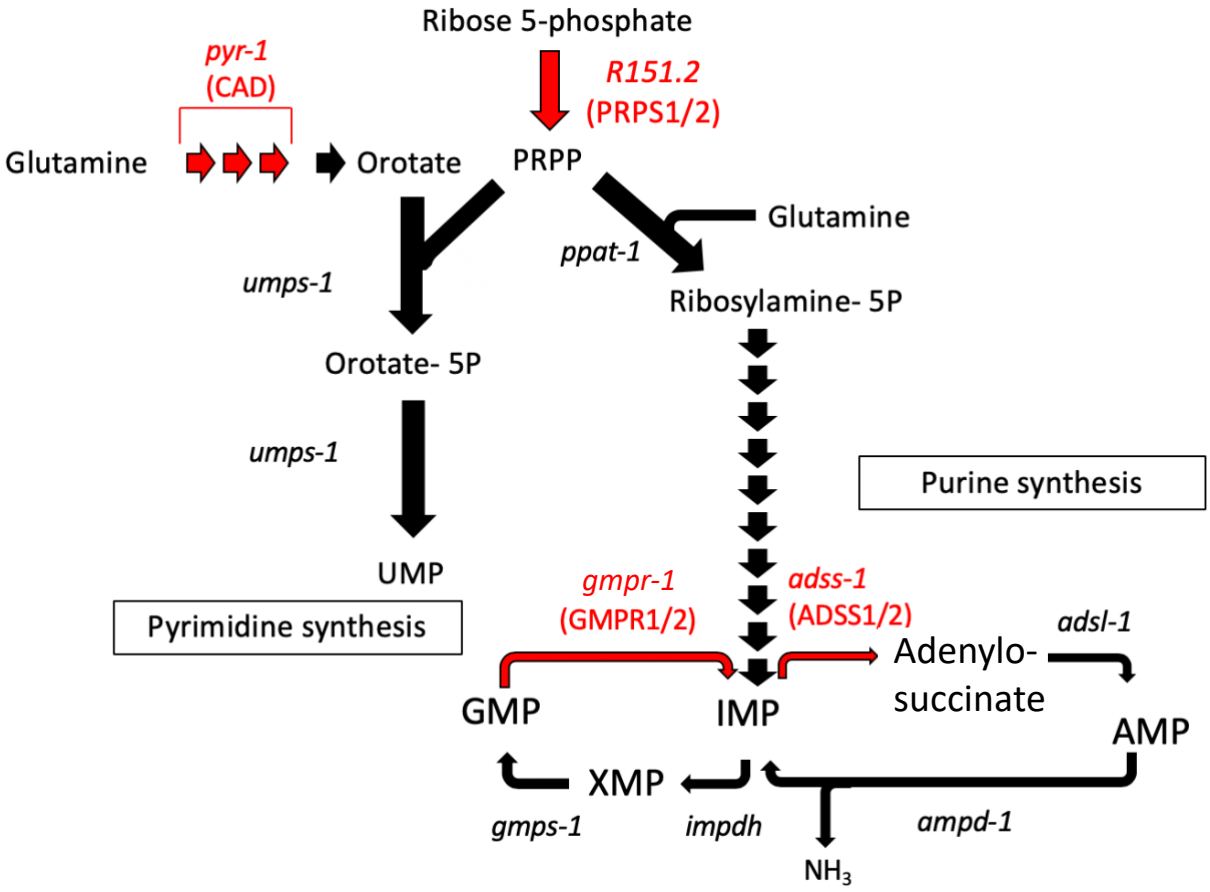
Ribose 5-phosphate
pyr-1
(CAD)
R151.2
(PRPS1/2)
Glutamine
Orotate
PRPP
Glutamine
ppat-1
umps-1
Ribosylamine- 5P
Orotate- 5P
umps-1
Purine synthesis
UMP
Pyrimidine synthesis
gmpr-1
(GMPR1/2)
adss-1
(ADSS1/2)
adsl-1
Adenylo-
succinate
GMP
IMP
AMP
XMP
gmps-1
impdh
ampd-1
NH3

References

Boxem, M., and Van Den Heuvel, S. (2001). *lin-35* Rb and *cki-1* Cip/ Kip Cooperate in Developmental Regulation of G1 Progression in *C. elegans*. *Development* **128**, 4349–4359. https://doi.org/10.1242/dev.128.21.4349

Boxem, M., and Van Den Heuvel, S. (2002). *C. elegans* Class B Synthetic Multivulva Genes act in G1 regulation. *Curr. Biol.* **12**, 906–911. https://doi.org/10.1016/S0960-9822(02)00844-8

Chen, F., Hersh, B.M., Conradt, B., Zhou, Z., Riemer, D., Gruenbaum, Y., and Horvitz, H.R. (2000). Translocation of *C. elegans* CED-4 to Nuclear Membranes during Programmed Cell Death. *Science* **287**, 1485–89. https://doi.org/10.1126/science.287.5457.1485.

Church, D.L., Guan, K.L. and Lambie, E.J. (1995). Three Genes of the MAP Kinase Cascade, *mek-2*, *mpk-1/sur-1* and *let-60* ras, are Required for Meiotic Cell Cycle Progression in *Caenorhabditis elegans*. Development **121**, 2525–2535. https://doi.org/10.1242/dev.121.8.2525

Gumienny, T.L., Lambie, E., Hartwieg, E., Horvitz, H.R., Hengartner, M.O. (1999) Genetic Control of Programmed Cell Death in the *Caenorhabditis* elegans Hermaphrodite Germline. *Development* **126**, 1011–1022. doi: https://doi.org/10.1242/dev.126.5.1011

Harrison, M.M., Ceol, C.J., Lu, X., and Horvitz, H.R. (2006) Some *C. elegans* Class B Synthetic Multivulva Proteins Encode a Conserved LIN-35 Rb-Containing Complex Distinct From a NuRD-like Complex. *Proc. Natl. Acad. Sci.,* **103**, 16782-16787. https://doi.org/10.1073/pnas.0608461103

Lewis, P.W., Beall, E.L., Fleischer, T.C., Georlette, D., Link, A.J., Botchan, M.R. (2004) Identification of a Drosophila Myb-E2F2/RBF Transcriptional Repressor Complex. *Genes Dev.* **18**, 2929–2940. doi:10.1101/gad.1255204

Li, P., Nijhawan, D., Budihardjo, I., Srinivasula, S.M., Ahmad, M., Alnemri, E.S., Wang, X. (1997). Cytochrome c and dATP-dependent formation of Apaf-1/caspase-9 complex initiates an apoptotic protease cascade. *Cell* **91**: 479-489. https://doi.org/10.1016/s0092-8674(00)80434-1

Litovchick, L., Sadasivam, S., Florens, L., Zhu, X., Swanson, S.K., Velmurugan, S., Chen, R., Washburn, M.P., Liu, X.S., DeCaprio, J.A (2007). Evolutionarily Conserved Multisubunit RBL2/p130 and E2F4 Protein Complex Represses Human Cell Cycle-Dependent Genes in Quiescence. *Mol Cell* **25**, 539-551. doi: 10.1016/j.molcel.2007.04.015.

Liu, X., Kim, C. N., Yang, J., Jemmerson, R., Wang, X. (1996**).** Induction of apoptotic program in cell-free extracts: Requirement for dATP and cytochrome c**.** *Cell* **86**: 147-157. https://doi.org/10.1016/s0092-8674(00)80085-9

Kluck, R.M., Bossy-Wetzel, E., Green, D.R. and Newmeyer, D.D. (1997). The release of cytochrome c from mitochondria: A primary site for Bcl- 2 regulation of apoptosis. *Science* **275**: 1132–1136. https://doi.org/10.1126/science.275.5303.1132

Korenjak, M., Taylor-Harding B., Binné, U.K., Satterlee, J.S., Stevaux, O., Aasland, R., White-Cooper, H., Dyson, N., Brehm, A., (2004). Native E2F/RBF Complexes Contain Myb-Interacting Proteins and Repress Transcription of Developmentally Controlled E2F Target Genes. *Cell* **119**, 181–193. doi: 10.1016/j.cell.2004.09.034

Pourkarimi, E., Greiss, S. & Gartner, A. (2012). Evidence that CED-9/Bcl2 and CED-4/Apaf-1 localization is not consistent with the current model for *C. elegans* apoptosis induction. *Cell Death Differ* **19**, 406–415 (2012). https://doi.org/10.1038/cdd.2011.104

Muller, H., Bracken, A.P., Vernell, R., Moroni, M.C., Christians, F., Grassilli, E., Prosperimi, E., Vigo, E., Oliner, J., and Helin, K. (2001) E2Fs regulate the expression of genes involved in differentiation, development, proliferation, and apoptosis. *Genes Dev*. **15**, 267–285. doi:10.1101/gad.864201

Reddien, P.W., Andersen, E.C., Huang, M.C., and Horvitz, H.R. (2007). DPL-1 DP, LIN-35 Rb and EFL-1 E2F act with the MCD-1 zinc-finger protein to promote programmed cell death in Caenorhabditis elegans. *Genetics* **175**, 1719–1733. https://doi.org/10.1534/genetics.106.068148

Schmit, F., Korenjak, M., Mannefeld, M., Schmitt, K., Franke, C., Von Eyss, B., Gagrica, S., Hänel, F., Brehm, A., Gaubatz, S. (2007). LINC, a Human Complex That is Related to pRB-Containing Complexes in Invertebrates Regulates the Expression of G2/M Genes. *Cell Cycle* **6**,1903–1913. https://doi.org/10.4161/cc.6.15.4512

Shaham, S. and Robert Horvitz, H. (1996) An Alternatively Spliced *C. elegans ced-4* RNA Encodes a Novel Cell Death Inhibitor. *Cell* **86**, 201-208. https://doi.org/10.1016/S0092-8674(00)80092-6

Hershko, T., Korotayev, K., Polager, S., Ginsberg, D. (2006) E2F1 modulates p38 MAPK phosphorylation via transcriptional regulation of ASK1 and Wip1. *J Biol Chem* 281, 31309-16. doi: 10.1074/jbc.M601758200

Xue, D., and Horvitz, H.R. (1997). *Caenorhabditis elegans* CED-9 Protein Is a Bifunctional Cell-Death Inhibitor. *Nature* **390**, 305–8. https://doi.org/10.1038/36889.

Yan, N., Chai, J., Eui, S.L., Gu, L., Liu, Q., He, J., Wu, J.W., Kokel, D., Li, H., Hao, Q., Xue, D., and Shi, Y. (2005). Structure of the CED-4-CED-9 Complex Provides Insights into Programmed Cell Death in *Caenorhabditis elegans*. *Nature* **437**, 831–37.

https://doi.org/10.1038/nature04002.

Yang J., Liu X., Bhalla K., Kim C.N., Ibrado A.M., Cai J., Peng T.I., Jones D.P., Wang X. (1997). Prevention of apoptosis by Bcl-2: Release of cytochrome c from mitochondria blocked. *Science* **275**: 1129–1132. https://doi.org/10.1126/science.275.5303.1129

Zou, H., Henzel, W. J., Liu, X., Lutschg, A. & Wang, X. (1997). Apaf-1, a human protein homologous to *C. elegans* CED-4, participates in cytochrome c-dependent activation of caspase-3**.** *Cell* **90**: 405-413. https://doi.org/10.1016/s0092-8674(00)80501-2

Zou, H., Henzel, W.J., Liu, X., Lutschg, A., and Wang, X. (1997). Apaf-1, a Human Protein Homologous to *C. elegans* CED-4, Participates in Cytochrome c-Dependent Activation of Caspase-3. *Cell* **90**, 405-413. https://doi.org/10.1016/S0092-8674(00)80501-2.